National Library
of Canada

Acquisitions and
Bibliographic Services Branch

395 Wellington Street
Ottawa, Ontario
K1A 0N4

Bibliothèque nationale
du Canada

Direction des acquisitions et
des services bibliographiques

395, rue Wellington
Ottawa (Ontario)
K1A 0N4

Your file Votre référence

Our file Notre référence

NOTICE

The quality of this microform is heavily dependent upon the quality of the original thesis submitted for microfilming. Every effort has been made to ensure the highest quality of reproduction possible.

If pages are missing, contact the university which granted the degree.

Some pages may have indistinct print especially if the original pages were typed with a poor typewriter ribbon or if the university sent us an inferior photocopy.

Reproduction in full or in part of this microform is governed by the Canadian Copyright Act, R.S.C. 1970, c. C-30, and subsequent amendments.

AVIS

La qualité de cette microforme dépend grandement de la qualité de la thèse soumise au microfilmage. Nous avons tout fait pour assurer une qualité supérieure de reproduction.

S'il manque des pages, veuillez communiquer avec l'université qui a conféré le grade.

La qualité d'impression de certaines pages peut laisser à désirer, surtout si les pages originales ont été dactylographiées à l'aide d'un ruban usé ou si l'université nous a fait parvenir une photocopie de qualité inférieure.

La reproduction, même partielle, de cette microforme est soumise à la Loi canadienne sur le droit d'auteur, SRC 1970, c. C-30, et ses amendements subséquents.

Canada

UNIVERSITY OF ALBERTA

Catalysis of Amide Hydrolysis and Formation by a Model for the Cysteine Proteases

BY

Jeffrey Wayne Keillor

A thesis submitted to the Faculty of Graduate Studies and Research in partial fulfillment of the requirements for the degree of Doctor of Philosophy.

DEPARTMENT OF CHEMISTRY

Edmonton, Alberta

Spring 1993

National Library
of Canada

Acquisitions and
Bibliographic Services Branch

395 Wellington Street
Ottawa, Ontario
K1A 0N4

Bibliothèque nationale
du Canada

Direction des acquisitions et
des services bibliographiques

395, rue Wellington
Ottawa (Ontario)
K1A 0N4

Your file *Votre référence*

Our file *Notre référence*

The author has granted an irrevocable non-exclusive licence allowing the National Library of Canada to reproduce, loan, distribute or sell copies of his/her thesis by any means and in any form or format, making this thesis available to interested persons.

L'auteur a accordé une licence irrévocable et non exclusive permettant à la Bibliothèque nationale du Canada de reproduire, prêter, distribuer ou vendre des copies de sa thèse de quelque manière et sous quelque forme que ce soit pour mettre des exemplaires de cette thèse à la disposition des personnes intéressées.

The author retains ownership of the copyright in his/her thesis. Neither the thesis nor substantial extracts from it may be printed or otherwise reproduced without his/her permission.

L'auteur conserve la propriété du droit d'auteur qui protège sa thèse. Ni la thèse ni des extraits substantiels de celle-ci ne doivent être imprimés ou autrement reproduits sans son autorisation.

ISBN 0-315-82236-8

Canada

UNIVERSITY OF ALBERTA

RELEASE FORM

NAME OF AUTHOR: Jeffrey Wayne Keillor

TITLE OF THESIS: Catalysis of Amide Hydrolysis and Formation by a Model for the Cysteine Proteases

DEGREE: Doctor of Philosophy

YEAR THIS DEGREE GRANTED: Spring 1993

Permission is hereby granted to the University of Alberta Library to reproduce single copies of this thesis and to lend or sell such copies for private, scholarly or scientific research purposes only.

The author reserves all other publication and other rights in association with the copyright in the thesis, and except as hereinbefore provided neither the thesis nor any substantial portion thereof may be printed or otherwise reproduced in any material form whatever without the author's prior written permission.

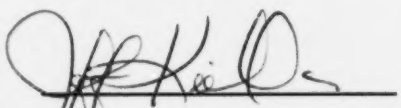

83 Brander Drive,

Edmonton, AB

T6H 4X5

23 April 1993

UNIVERSITY OF ALBERTA

FACULTY OF GRADUATE STUDIES AND RESEARCH

The undersigned certify that they have read, and recommend to the Faculty of Graduate Studies and Research for acceptance, a thesis entitled Catalysis of Amide Hydrolysis and Formation by Models of the Cysteine Proteases submitted by Jeffrey Wayne Keillor in partial fulfillment of the requirements for the degree of Doctor of Philosophy.

Supervisor
Dr. R.S. Brown

Dr. J.C. Vederas

Dr. J. Takats

Dr. K. Kopecky

Dr. G. Stemke

External Examiner
Dr. R. Pratt

23 April 1993

DEDICATION

To my father, K. Wayne Keillor:

Thank you for teaching me the opportunity in education

and for sharing with me the joy of learning.

ABSTRACT

A distorted anilide (**2**) has been shown to be remarkably susceptible to attack by zwitterions consisting of thiolates containing pendant N-H^+ groups. Thiolates alone are not reactive, nor are amines or ammonium ions. Attack of the zwitterionic form produces a thiolester, which is isolable in the case of N,N-dimethylcysteamine. If the pendant amine is primary, as in the case of cysteamine, the isolable product is the amide formed by intramolecular S to N acyl transfer. The kinetics of the reaction of 2-mercaptomethyl-N-methylimidazole (**7b**) with **2** show a bell-shaped pH vs log k_2 profile that results from attack of the zwitterionic form on the amide. The role of the pendant ammonium group is to serve as a general acid trapping agent of the unstable tetrahedral intermediate formed from $^+HR_2N$—S^- attack on the amide C=O.

Thiolesters **13b** and **17**, formed from the reaction of amide **2** with thiolamines dimethylaminoethanethiol (**10b**) and **7b** respectively, were prepared by an independent route. The rate of hydrolysis of these thiolesters was found to be dependent on the state of ionization of the pendant amino group in a manner suggestive of a general base role. The thiolesters were also found to be susceptible to intramolecular aniline aminolysis resulting in the re-closure to form amide **2**. These results indicate the reaction of **2** with **7b** to form the thiolester is reversible; hydrolysis of the latter generates **7b** as a true turnover catalyst.

This catalyst was then used to hydrolyze a series of non-activated substituted formamides, (formamide, DMF, and N-formylmorpholine, **20a-c**) in D_2O at near neutral pD values. N-formylmorpholine, **20c**, was also formed from its constituent acid and amine under the same experimental conditions using **7b** as a catalyst. The hydrolysis and formation of **20c** were allowed to proceed to completion, in order to approach the equilibrium position of the hydrolysis of **20c** from two independent directions. The endpoint of this reaction was used to calculate the equilibrium constant for the reversible hydrolysis of **20c** and the partitioning ratio of the common intermediate thiolester.

ACKNOWLEDGEMENTS

I gratefully acknowledge the friendship, supervision and enthusiastic guidance of Dr. R.S. Brown.

My thanks also to Dr. A.J. Bennet for his helpful suggestions during the early portion of this work.

Finally, I would like to thank my wife Jody for her constant encouragement and support. Her unfailing love and cheerful perspective have helped make all of this possible.

TABLE OF CONTENTS

INTRODUCTION.....1

A) Non-Enzymatic Amide Hydrolysis.....1

B) Enzymatic Amide (Peptide) Hydrolysis.....8

C) Models for Enzymatic Amide Hydrolysis.....19

D) Proposed Cysteine Protease Model.....33

CHAPTER 1.....34

A) Introduction.....34

B) Experimental.....35

C) Results.....39

D) Discussion.....48

E) Conclusions and Relevance to the Cysteine Proteases.....58

CHAPTER 2.....60

A) Introduction.....60

B) Experimental.....61

C) Results.....65

D) Discussion.....68

E) Conclusions.....76

CHAPTER 3.....78

A) Introduction.....78

B) Experimental.....79

C) Results and Discussion.....81

E) Conclusions.....88

CONCLUSION.....89

A) Relevance to the Cysteine Proteases.....89

B) Future Considerations.....91

REFERENCES.....94

APPENDIX 1.....110

APPENDIX 2.....124

APPENDIX 3.....128

LIST OF TABLES

Table 1.....41

Kinetic Second Order Rate Constants (k_2) and pKa^{SH} Values for the Reactions of Thiols **10a-d**, **11a-d** with **2** (T = 25 °C, μ = 1.0 (KCl)).

Table 2.....46

Kinetic Second Order Rate Constants (k_2) and pKa Values for Attack of **7b** on **2** (T = 25.0 ± 0.1 °C, μ = 1.0 (KCl)).

Table 3.....67

Kinetic pKa^{NH+} Values and Pseudo-First Order Background and Upper Limit Rate Constants for the Reactions of Thiolester **13b** and **17** in H_2O (T = 25 °C, μ = 1.0 (KCl)).

Table 4.....82

Rate Constants for the Hydrolysis (and Formation) of Various Formamides Mediated by Thiolimidazole **7b** in D_2O Solution (T = 98 °C, μ = 1.0 (KCl)).

Table 1S.....111

Second Order Rate Constants at Various pH Values for the Reaction of Cysteamine (**10a**) with Distorted Amide **2** (T = 25 °C, μ = 1.0 (KCl)).

Table 2S.....112

Second Order Rate Constants at Various pH Values for the Reaction of N,N-Dimethylaminoethanethiol (**10b**) with Distorted Amide **2** (T = 25 °C, μ = 1.0 (KCl)).

Table 3S.....112

Second Order Rate Constants at Various pH Values for the Reaction of 4-(2-Mercaptoethyl)morpholine (**10c**) with Distorted Amide **2** (T = 25 °C, μ = 1.0 (KCl)).

Table 4S.....113

Second Order Rate Constants at Various pH Values for the Reaction of 2-Mercaptomethyl-N-methylimidazole (**7b**) with Distorted Amide **2** (T = 25 °C, μ = 1.0 (KCl)).

Table 5S.....114

Second Order Rate Constants at Various pH Values for the Reaction of 3-Mercaptopropylamine (**10d**) with Distorted Amide **2** (T = 25 °C, μ = 1.0 (KCl)).

Table 6S.....114

Second Order Rate Constants at Various pH Values for the Reaction of 3-Mercaptopropylamine (**10d**) with Distorted Amide **2** in D_2O (T = 25 °C, μ = 1.0 (KCl)).

Table 7S.....115

Second Order Rate Constants at Various Concentrations of N-Methylimidazole Buffer for the Reaction of 4-(2-Mercaptoethyl)morpholine (**10c**) with Distorted Amide **2** (pH 7.4, T = 25 °C, μ = 1.0 (KCl)).

Table 8S.....116

Second Order Rate Constants at Various Concentrations of N-Methylimidazole Buffer for the Reaction of 4-(2-Mercaptoethyl)morpholine (**10c**) with Distorted Amide **2** (pH 8.4, T = 25 °C, μ = 1.0 (KCl)).

Table 9S.....117

Second Order Rate Constants at Various Concentrations of N-Methylimidazole Buffer for the Reaction of 4-(2-Mercaptoethyl)morpholine (**10c**) with Distorted Amide **2** in D_2O (pD 7.9, T = 25 °C, μ = 1.0 (KCl)).

Table 10S.....118

Second-order Rate Constants at Various Concentrations of N-Methylimidazole Buffer for the Reaction of 2-Mercaptomethyl-N-methylimidazole (**7b**) with Distorted Amide **2** (pH 7.3, T = 25 °C, μ = 1.0 (KCl)).

Table 11S.....119

Second-order Rate Constants at Various Concentrations of N-Methylimidazole Buffer for the Reaction of Cysteamine (**10a**) with Distorted Amide **2** (pH 7.8, T = 25 °C, μ = 1.0 (KCl)).

Table 12S.....124

Observed Pseudo-First Order Rate Constants vs pH for the Disappearance of **13b** (μ = 1.0 (KCl), T = 25 °C).

Table 13S.....125

Observed Pseudo-First Order Rate Constants vs pH for the Disappearance of **17** (μ = 1.0 (KCl), T = 25 °C).

Table 14S.....127

Observed Pseudo-First Order Rate Constants vs Equivalents of Added Dimethylamioethanethiol (**10b**) for the Disappearance of **13b**[a] (pH 10.10,[b] μ = 1.0 (KCl), T = 25 °C).

Table 15S.....128

Observed Pseudo-First Order Rate Constants for the Reaction of **7b** with 100 mM DMF (pD 8.0, T = 98 °C, μ = 1.0 (KCl)).

Table 16S.....129

Observed Pseudo-First Order Rate Constants for the Reaction of **7b** with 100 mM Formamide (pD 7.8, T = 98 °C, μ = 1.0 (KCl)).

Table 17S.....129

Observed Pseudo-First Order Rate Constants for the Reaction of **7b** with 200 mM N-Formylmorpholine (pD 8.0, T = 98 °C, μ = 1.0 (KCl)).

Table 18S.....130

Observed Pseudo-First Order Rate Constants for the Formation of NFM by the Reaction of **7b** with Formic Acid and Morpholine (T = 98 °C, μ = 1.0 (KCl)).

LIST OF FIGURES

Figure 1.....40

Plot of the log k_2^{obsd} vs pH profile for the reaction of **10a-d** with **2**; T = 25 °C, μ = 1.0 (KCl).

Figure 2.....43

Plot of the log k_2^{obsd} vs pH profile for the reaction of **7b** with **2** (T = 25 °C, μ = 1.0 (KCl)) and with **9a** (T = 37 °C, μ = 0.3 (KCl)).

Figure 3.....52

Plot of the maximal second order rate constant (k_2) for attack of amino thiols **7b**, **10a-d** on **2** vs the pKa^{SH} values in H_2O and D_2O; T = 25 °C, μ = 1.0 (KCl).

Figure 4.....56

Plots of log k_2^{obsd} for attack of **7b** and **10c** on **2** as a function of added N-methylimidazole (NMI); T = 25 °C, μ = 1.0 (KCl).

Figure 5.....66

Plot of the log k^{obsd} vs pH profile for the decomposition of thiolesters **13b** and **17** (T = 25 °C, μ = 1.0 (KCl)) and thiolester **6b** (T = 37 °C, μ = 0.3 (KCl)).

Figure 6.....73

Plots of the rate of disappearance of thiolester **13b** as a function of added dimethylaminoethanethiol (**10b**); pH 10.10, T = 25 °C, μ = 1.0 (KCl).

Figure 7.....87

Establishment of equilibrium endpoint between NFM hydrolysis and formation in D_2O; T = 98 °C, pD 7.6, μ=1.0 (KCl), [phosphate] = 200 mM.

LIST OF SCHEMES

Scheme 1.....2

Mechanism for H_3O^+-catalyzed amide hydrolysis.

Scheme 2.....5

Mechanism for ^-OH-catalyzed amide hydrolysis.

Scheme 3.....9

Stylized mechanism for acylation of SPases by amide substrates.

Scheme 4.....11

Stylized mechanism for deacylation of SPases.

Scheme 5.....12

Stylized mechanism for hydrolysis of amides mediated by APases.

Scheme 6.....15

Stylized mechanism for hydrolysis of amides mediated by APases.

Scheme 7.....16

Stylized mechanism for hydrolysis of amides mediated by cysteine proteases.

Scheme 8.....20

Cleavage of p-*tert*-butylphenyl acetate by a modified cyclodextrin as a model for serine proteases.

Scheme 9.....21

Cleavage of strained anilide by a modified imidazole as a model for serine proteases.

Scheme 10.....23

Intramolecular hydrolysis of maleamic acid as a model for APases.

Scheme 11.....24

Hydrolysis of strained anilide by dicarboxylic acid as a model for APases.

Scheme 12.....26

Intramolecular thiolester hydrolysis as a model for deacylation step of cysteine proteases.

Scheme 13.....27

Intramolecular thiolester hydrolysis as a model for deacylation step of cysteine proteases.

Scheme 14.....29

Intramolecular general base assisted thiolester hydrolysis as a model for deacylation step of cysteine proteases.

Scheme 15.....30

Cleavage of pNPA by thiolimidazole as a model for acylation step of cysteine proteases.

Scheme 16.....31

Imidazole catalyzed intramolecular thiolactonization as a model for acylation step of cysteine proteases.

Scheme 17.....44

Ionization equilibria of thiolimidazole **7b** in solution.

Scheme 18.....49

Mechanism of reaction of amide **2** with thiolamines **10a-d**.

Scheme 19.....51

Mechanism of acylation of thiolate with pNPA.

Scheme 20.....57

Mechanism of reaction of amide **2** with thiolamine **10c** with imidazolium general acid catalysis.

Scheme 21.....65

Hydrolysis of basic form of thiolamine esters.

Scheme 22.....69

Scavenging of free thiolate with Ellman's reagent.

Scheme 23.....71

Simplified hydrolysis and aminolysis reactions of thiolesters **13b** and **17**.

Scheme 23a.....75

Hydrolysis and aminolysis reactions of thiolesters **13b** and **17**, showing complexity of pH dependencies.

Scheme 24.....77

Catalysis of amide hydrolysis and formation by ammonium thiolates.

Scheme 25.....83

Mechanism of reaction of thiolimidazole **7b** with formic acid, and subsequent aminolysis of thiolester **21** to form amide **20c**.

Scheme 26.....84

Equilibria between formic acid and morpholine, amide **20c**, and thiolester **21**.

Scheme 27.....92

Stylized representation of thiolimidazole mounted on polystyrene bead solid support.

Scheme 28.....93

Possible mechanism of bifunctional phosphate catalysis of amide hydrolysis and formation.

LIST OF ABBREVIATIONS

APases	aspartate proteases
β	slope from Brønsted plot
CD	cyclodextrin
CPases	cysteine proteases
DMF	dimethylformamide
DSS	sodium 3-trimethylsilylpropanesulfonate
DTNB	5,5'-dithiobis(2-nitrobenzoic acid)
Ellman's reagent	5,5'-dithiobis(2-nitrobenzoic acid)
HIm^+	imidazolium
Im	imidazole
NFM	N-formylmorpholine
NLLSQ	non-linear least squares
NMI	N-methylimidazole
pNPA	p-nitrophenyl acetate
ρ	slope from Hammett plot
skie	solvent kinetic isotope effect
SPases	serine proteases
T^0	neutral tetrahedral intermediate
TE	thiolester
TI	tetrahedral intermediate
T_{N^+}	N-protonated tetrahedral intermediate
T_{O^-}	oxyanionic tetrahedral intermediate
$T_{O^{2-}}$	dioxyanionic tetrahedral intermediate
TS	transition state
ZW	zwitterionic species

INTRODUCTION

A) Non-Enzymatic Amide Hydrolysis

Peptides are found in all living cells. The stability of the peptide (amide) bond which joins together amino acids in the construction of proteins is therefore of extreme biological importance to all forms of life. Likewise, the acyl transfer reactions (including hydrolysis) of the amidic unit are of significant importance in organic chemistry.

There exist in nature many enzymes capable of facilitating the rapid cleavage of the peptide bond under mild physiological conditions. However, the non-enzymatic reaction of unactivated amides, due to the high stability of the N-C(O) linkage, is extremely slow under all but the most severe conditions of pH and temperature. Although a complete understanding of the non-enzymatic hydrolysis reaction would be very useful in the understanding of the enzymatic process and the design of enzyme mimics, the slowness of this reaction has discouraged the study of it, so that up until recently, the process has been rather ill-defined.[1]

The currently favoured mechanisms for the non-enzymatic hydrolysis of amides in acidic and basic aqueous media will be described, and an attempt will be made to define the general requirements for the hydrolysis of an amide. Recent experiments[2] have contributed significantly to the mechanistic analysis of amide hydrolysis. These experiments include: the measurement of the kinetics of hydrolysis versus the concentration of hydronium or hydroxide ions, from which the stoichiometry of the reaction can be determined; the measurement of carbonyl ^{18}O exchange vs $[H_3O^+]$ or $[OH^-]$, from which the reversibility of the tetrahedral intermediate can be determined and; the measurement of solvent kinetic isotope effects (skie) on the rate of hydrolysis and exchange, from which the degree of transfer of a proton in a rate-determining transition state can be ascertained. The relevance of these recent results to the simplified mechanism of the hydrolysis of amides in acidic and basic media will be discussed.

Acid-Catalyzed Hydrolysis

The generally accepted[1] mechanism for H_3O^+-catalyzed amide hydrolysis is shown in **Scheme 1**. Water-assisted H_2O attack on the O-protonated amide gives T^o and a molecule of H_3O^+. Plots of log k_{hyd} vs -log $[H_3O^+]$ have slopes of -1 and are characterized by a plateau region at high $[H_3O^+]$, followed by a reduction of rate at very high $[H_3O^+]$. This is consistent with the increase of the rate of reaction of water with amide as the amide becomes fully O-protonated, with an equilibrium pKa of ~0 to -2.

Scheme 1

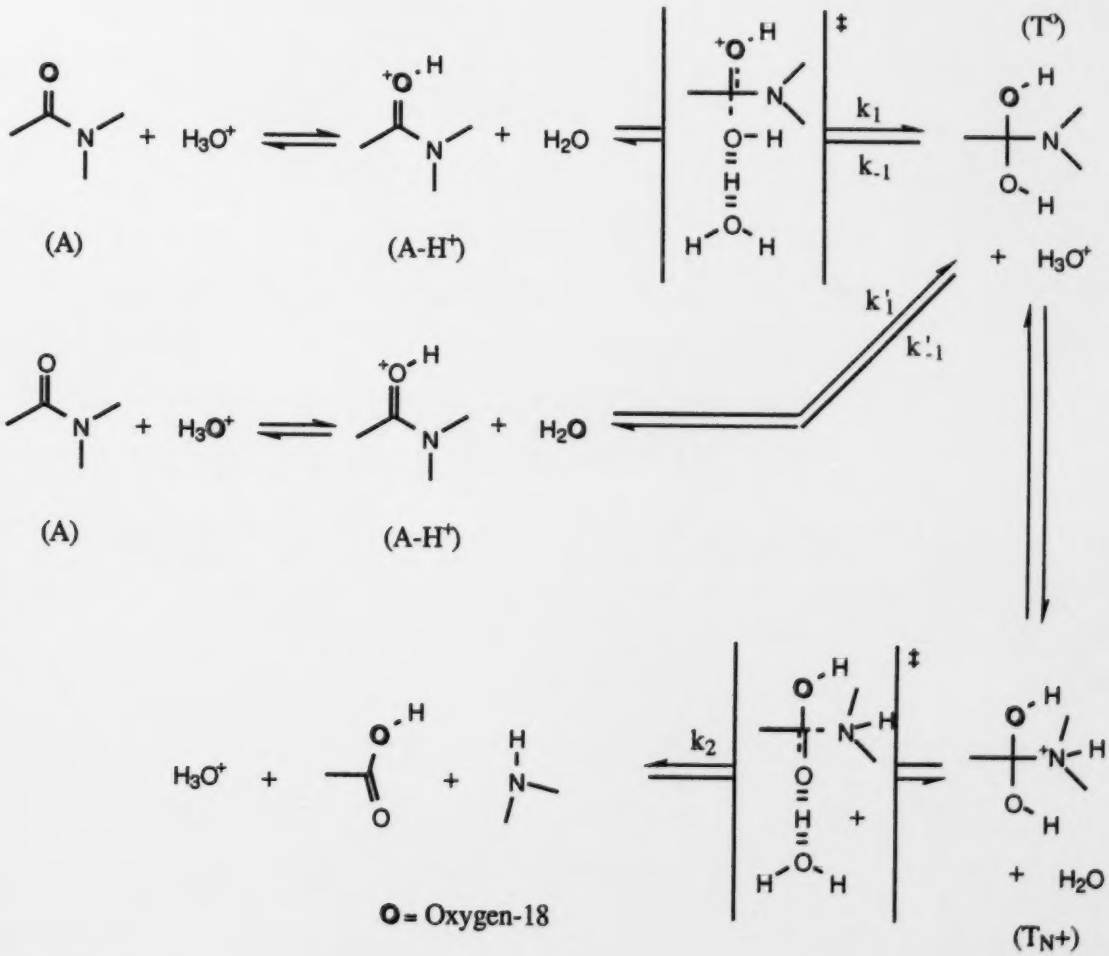

The reversible formation of intermediates during H_3O^+-catalyzed amide hydrolysis can be studied using ^{18}O=C labelled amides. From **Scheme 1**, tetrahedral intermediate T^o can reverse to eject either ^{16}OH or ^{18}OH, the latter of which leads to the exchange of carbonyl ^{18}O. The rate constants for exchange and hydrolysis (k_{ex} and k_{hyd}) can be expressed in terms of k_1, k_{-1} and k_2 in order to give a ratio of exchange to hydrolysis. This ratio, $k_{ex}/k_{hyd} = k_{-1}/2k_2$ corresponds to the partitioning of the tetrahedral intermediate T^o (assuming that the oxygens are in protonic equilibrium and that only half of the reversal by k_{-1} leads to loss of ^{18}O).[3] Although in earlier work by Bender,[4] Bunton[5] and Yates[6] no loss of label was detected in recovered amide, McClelland later reported[7] a small but significant loss of label from ^{18}O-enriched benzamide recovered from the hydrolysis medium. In more recent studies, Brown and co-workers have reported[8] significant loss of ^{18}O in amides such as N,2,4-trimethylacetanilide recovered from acidic media, ($k_{ex}/k_{hyd} \approx$ 0.2) with both exchange and hydrolysis processes being first order in $[H_3O^+]$ and having solvent isotope effects of unity. These results confirm that there is an intermediate that partitions between hydrolysis and exchange (most likely intermediate T^o from **Scheme 1**) and that for the amides considered the predominantly rate determining step must be k_1, the formation of this intermediate, since hydrolysis is faster than exchange. Also, since both exchange and hydrolysis are first order in $[H_3O^+]$, the transition states leading from T^o on both the hydrolytic or exchange pathways must have one proton incorporated in them (see **Scheme 1**) ruling out the possibility of a neutral or zwitterionic TS. The structures of the transition states leading from T^o (i.e. for the k_{-1} and k_2 steps) are further constrained by the skie data, which were shown[8] to arise from an equilibrium isotope effect (i.e. $k_H/k_D < 1$) compensated by a normal isotope effect for one proton in flight. In each transition state of **Scheme 1**, water acts as a general base, removing a proton from another water molecule in the attack on protonated amide in the k_1 step and removing a proton from the oxygen of the tetrahedral intermediate in the breakdown of T_N+ concurrent with C-N cleavage to form products in the k_2 step. Note that this mechanism requires that a proton be fully installed on

the nitrogen of T_N+ prior to C-N cleavage so the only protons contributing to the skie are those associated with the H_2O-mediated deprotonation of the O-H accompanying C-N cleavage. Otherwise, if the departing nitrogen was also protonated concurrent with C-N cleavage, the expected skie would be larger (for two protons in flight in the transition state leading to products) than what is observed. Finally, the amount of ^{18}O exchange was found to vary from amide to amide as a function of amine leaving group basicity - more reversal from T^o takes place as it becomes increasingly difficult to install a proton on the amino nitrogen to form T_N+.[2]

Base-Catalyzed Hydrolysis

In unbuffered basic media, the hydrolysis of amides in general follows the pathway shown in **Scheme 2**.[2] The anionic intermediate T_O-, formed by attack of hydroxide on neutral amide, can revert back to starting materials or proceed to products with or without dependence on a second hydroxide molecule.

Terms second order in [OH^-] have been observed[9] for several different amides, and have been interpreted as arising from a mechanism where a second OH^- removes a proton from T_O- to yield the dianion T_O2-, which then ejects the amine as an amide ion, with or without general acid assistance by the solvent. At high [OH^-], this second order term dominates the process such that T_O- goes on to product every time it is formed, eliminating reversal and making the formation of T_O- (k_1) the rate determining step. However, many amides do not display second order behaviour,[10-13] so that T_O- breaks down to products without the assistance of a second OH^- (via k_2 in **Scheme 2**).

Scheme 2

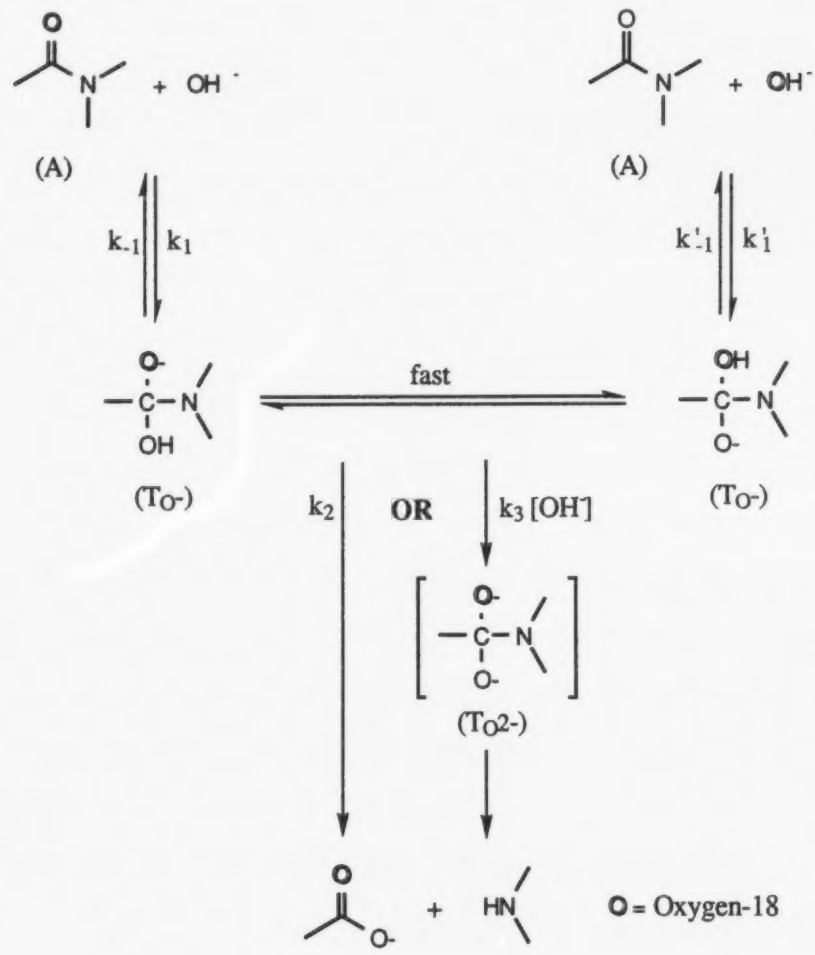

In early ^{18}O-exchange studies of a series of substituted benzamides, Bender and Bunton reported[10,11] k_{ex}/k_{hyd} ratios independent of [OH^-] (both exchange and hydrolytic processes being first order in [OH^-]) with no exchange detected for the tertiary dimethylbenzamide. This apparent inability of only the tertiary amide to exchange ^{18}O was originally attributed[11] to the requirement for at least one hydrogen on the amino nitrogen of T_O- to assist in protonic equilibration of the oxygens. Later, Deslongchamps[1e,14] re-interpreted this observation[11] in terms of the stereoelectronic control theory, claiming the

protonic equilibration of the oxygens was fast, but the lifetime of T_O^- was too short to allow sufficient conformational changes at N, through inversion or rotation, that would be required to assist in the ejection of the $^{18}OH^-$. However, this theory failed to consider the steric and leaving group effects on the C-N/C-O cleavage ratio. Subsequent studies of ^{18}O exchange and hydrolysis (both first order in $[OH^-]$) of a series of substituted toluamides later demonstrated[12] not only significant exchange in tertiary amides, but also the independence of ^{18}O exchange on the ability of the nitrogen to adapt the conformation supposedly required for breakdown of T_O^- with expulsion of $^{18}OH^-$. Importantly, it was demonstrated that the k_{ex}/k_{hyd} ratio was strongly dependent on amine basicity. Since both the exchange and hydrolytic processes are first order in $[OH^-]$, each transition state incorporates only one OH^-. This study also showed that in certain limiting cases where tertiary toluamides exhibited either much more or much less exchange than hydrolysis, a simple expression could be derived[15] for the exchange / hydrolysis ratio (i.e. $k_{ex} / k_{hyd} = k_{-1} / 2k_2$). When exchange is much faster than hydrolysis, k_{ex} is limited by the k_1 transition state, and k_{hyd} is limited by the k_2 transition state. The experimentally observed skie values on k_{ex} and k_{hyd} could then be interpreted as providing information regarding the nature of the attack step (k_1) and the breakdown step (k_2) respectively. Analysis of the skie data for the attack step led to the interpretation that the unit value for $(k_{ex})_{H/D}$ arises not from protons in flight, but from the reordering of solvent water molecules around the attacking OH^- and developing alkoxide anion in T_O^-. Likewise, interpretation of the observed skie data for the breakdown step $(k_{hyd})_{H/D}$ indicated that there are no protons in flight in the transition state leading to products; rather, the departing N has the requisite proton fully installed prior to C-N cleavage. Similar to the case for acid-catalyzed hydrolysis, reduction of amine basicity was found to increase the ratio of exchange to hydrolysis (until the amine basicity became so low that breakdown proceeded through ejection of amide ion.)

Generalized Mechanism

For the H_3O^+- or OH^--catalyzed hydrolysis of amides, it appears from all of the presently available experimental data that the path chosen for hydrolysis and the amount of ^{18}O exchange observed are dependent on the basicity of the departing amine, or rather the ability to fully install a proton on the nitrogen prior to C-N cleavage. The skie data also show that the oxygens of the tetrahedral intermediates formed are in protonic equilibrium, since there does not seem to be any significant slowing of ^{18}O exchange in D_2O over H_2O as would be expected if the transition state included a proton in flight as part of the rate-determining equilibration.

The hydrolysis of an amide appears to have two fundamental requirements. The first of these is the attack of a nucleophile on the amide carbonyl. If the nucleophile is weak, such as water is in acidic medium, this attack may be facilitated through O-protonation. It may also occur without general or specific acid assistance if the nucleophile is strong enough, such as hydroxide in basic medium. The second requirement is the protonation of the departing nitrogen. This protonation increases the leaving group ability of the amine, thereby assisting in the breakdown of the tetrahedral intermediate to form products, rather than its reversal resulting in the re-ejection of the nucleophile and regeneration of amide.

These requirements for amide hydrolysis should be satisfied regardless of whether the hydrolysis reaction is mediated by acid or base or proteolytic enzymes (*vide infra*). Synthetic catalysts for this reaction must therefore also be designed to incorporate functional groups capable of meeting the nucleophile / proton transfer requirements.

B) Enzymatic Amide (Peptide) Hydrolysis

In general, the requirements for acyl transfer from an amide are primarily the attack of a nucleophile on the carbonyl of the amide, and the protonation of the departing nitrogen concurrent with, if not prior to, C-N cleavage. There are three main classes of non-metallo proteolytic enzymes which accomplish these requirements in their cleavage of peptide bonds. These classes are the serine proteases, the aspartate proteases, and the cysteine proteases.

Serine Proteases

The serine proteases[16] (SPases) make up a large class of enzymes (of which the enzymes chymotrypsin and subtilisin are the best known) with active sites containing an Asp-CO_2^-, a His-imidazole, and a Ser-OH as a triad of amino acid side chains responsible for catalysis (see **Scheme 3**). The pH-activity optimum is near neutrality, suggesting an ionized Asp-CO_2^- and a neutral His-imidazole. It is the Ser-OH group which becomes temporarily acylated during the hydrolysis of all esters and amides. While this suggests there may be a mechanism common to ester and amide hydrolysis mediated by serine proteases, there are subtle but significant substrate-dependent differences in the mechanistic pathways employed by various species within this class. For example, the hydrolysis of some small "unnatural" ester substrates by chymotrypsin, a typical serine protease, proceeds via N-acylation of the His-57 imidazole, followed by acyl transfer to the Ser-195 oxygen.[17] Other reports[18] indicate that several SPases use mechanisms involving a different number of protons in flight for different substrates. Those substrates which are able to interact with binding subsites distant from the active site are able to activate the full catalytic effect of the catalytic triad, involving two protons in flight. Those substrates which are unable to do so are cleaved by a simpler mechanism which does not invoke the complete utilization of the triad and involves only one proton in flight, presumably between His-imidazole and Ser-OH. Another difference is that for amide substrates, the formation

of the acyl enzyme is rate limiting, but during the hydrolysis of esters, the acyl enzyme often accumulates and deacylation is the rate-determining step.[16]

Scheme 3

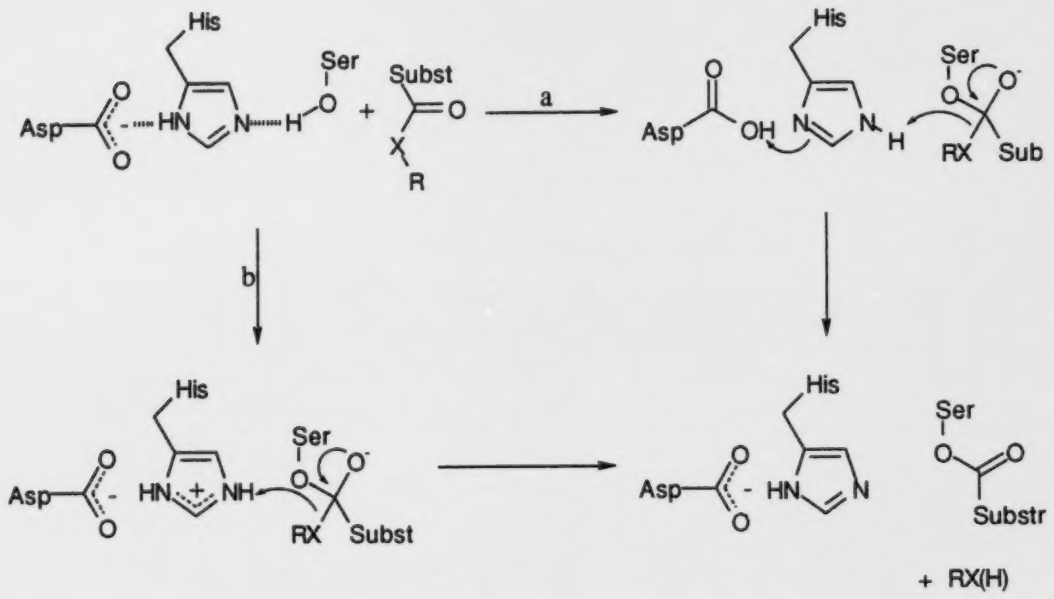

Recently, much of the discussion in the literature regarding the nature of the mechanism of action of the catalytic triad has been involved with the structure and reactivity of the hydrogen bond network in the active site. Although it is generally accepted that the histidine imidazole of the triad is able to act as a general base catalyst in increasing the nucleophilicity of the serine hydroxyl group toward the substrate carbonyl, some question remains as to the possibility of the presence of a hydrogen bond between the imidazole and hydroxyl groups in the triad. Early x-ray crystallographic studies[19a,b] of the active sites of a series of SPases showed that the "frozen" enzyme displayed interatomic distances between the histidine nitrogen and serine oxygen that were too large for the existence of a hydrogen bond. However, later evidence was provided through ^{15}N NMR which proved

the existence of a hydrogen bond to the imidazole nitrogen from the serine hydroxyl in the resting enzyme in solution.[19c]

The role of the aspartate residue in catalysis has also been questioned.[20] Represented in **Scheme 3** are the two main possible roles of the carboxylate in acylation of the enzyme, as either a general base (path a) or as an electrostatic enhancer of the imidazole basicity (path b). The earliest proposals[19a] of the role of the aspartate involved its becoming fully protonated (path a) in a complete "charge-relay" system, but it would appear from more recent evidence[19c] that this theory is incompatible with the unusually low pKa of the aspartate, and with ^{1}H NMR and neutron diffraction studies[19c] which indicate there is no proton transfer from the histidine to the aspartate in the active site. Rather, the aspartate serves (path b) to ensure the proper tautomeric form of the imidazole, properly orient the imidazole to accept the serine proton, and provide electrostatic stabilization of the developing imidazolium cation.[20]

The acylation of a serine protease by an amide can be visualized as involving binding of the substrate followed by attack of the serine hydroxyl on the carbonyl carbon of the substrate to form the tetrahedral intermediate. This nucleophilic attack is assisted by the removal of the serine proton by the adjacent histidine imidazole to form an imidazolium cation stabilized by a carboxylate anion (path b, **Scheme 3**). The tetrahedral intermediate is never observed to accumulate, but is thought to be stabilized in its oxyanionic form through hydrogen bonding within the active site. The nitrogen of the intermediate is protonated by the imidazolium cation as the intermediate collapses to form the acyl enzyme thereby expelling the amino leaving group.

Deacylation involves a mechanism that shows close similarities to that of acylation, in that the hydroxyl of a water molecule (as opposed to a serine hydroxyl) nucleophilically attacks the carbonyl carbon of the acyl-enzyme with general base assistance by the imidazole. The tetrahedral intermediate then breaks down to form product carboxylic acid through the ejection of serine hydroxyl, which is protonated in a general acid fashion by the

imidazolium as it departs to regenerate the enzyme in its active form. This deacylation process is summarized in **Scheme 4**.

Scheme 4

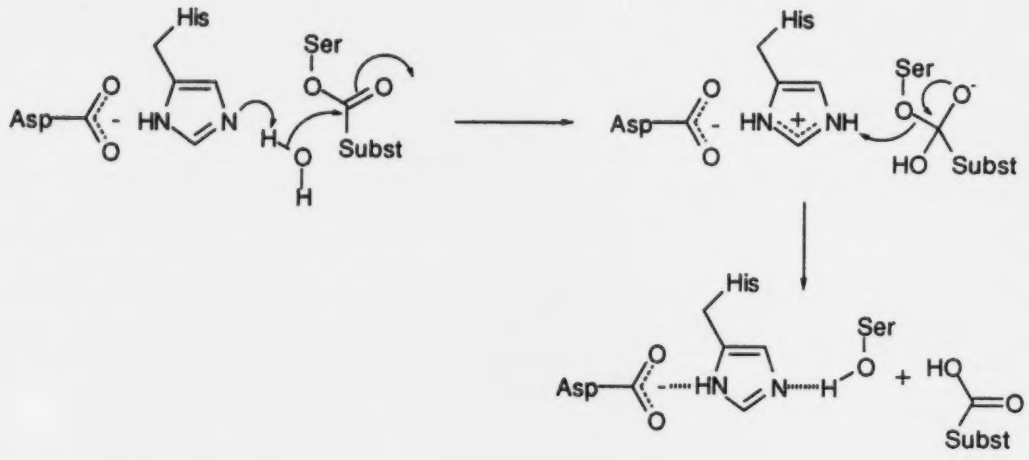

Aspartate Proteases

The aspartate proteases (APases) are widely occuring hydrolytic enzymes containing two catalytically essential aspartate residues in the active sites, linked to each other through a hydrogen bond.[21] The best known member of this family of enzymes is pepsin, a digestive enzyme present in mammalian gastric juice, where it functions to break down ingested protein. Because of the environment in which APases such as pepsin naturally function, it is not surprising that they are active at low pH, having pH-activity profiles with optima around pH 2 to 3. These profiles show dependence on the basic form of one carboxylic acid group of pKa ~1.1 and the acidic form of another carboxylate group of pKa ~4.5. The mechanism by which these aspartate residues cleave proteins, however, is still unknown.[22] Two different possibilities have been proposed for the acylation of APases, as depicted in **Scheme 5**. One possibility (path a) is a nucleophilic mechanism; the other (path b) is a general base / general acid mechanism.[21-26]

Scheme 5

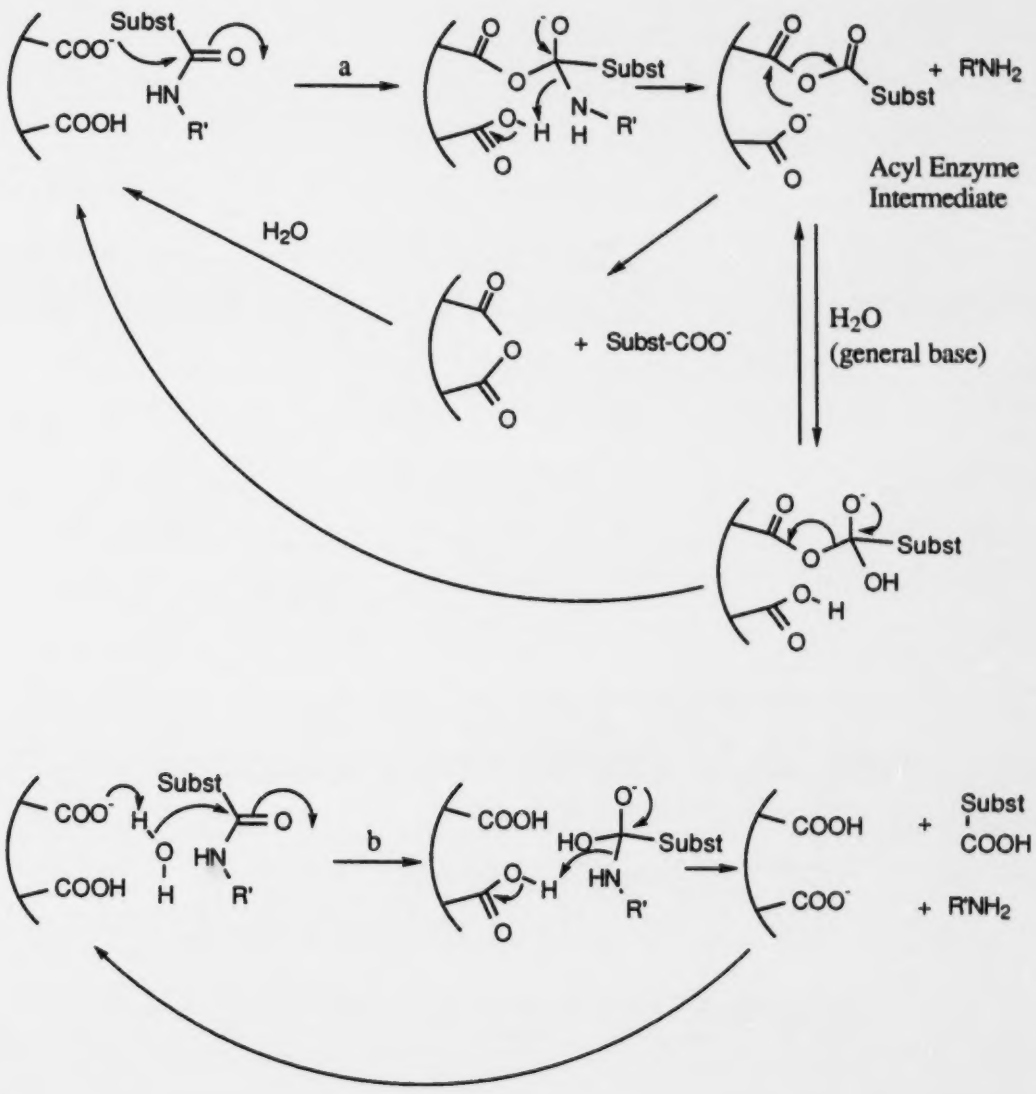

The primary reason for the initial favouring of a general base / general acid mechanism was the inability to detect covalent intermediates, (the most easily envisioned one of which is the acyl intermediate of **Scheme 5**) which are required in the nucleophilic route. However, it was pointed out[25] that peptide hydrolysis intermediates may indeed

exist and be bound by the enzyme but not necessarily linked to it *covalently*. Also some studies in which APases have promoted trans-peptidation, in which acyl transfer has ocurred from one peptide amine to another, were interpreted in terms of covalent intermediates being formed and held long enough for another substrate to be bound and for a different peptide to be re-formed.[27] On the other hand, the formation of trans-peptidation products was also explained[21b] without invoking an acyl-enzyme, simply by proposing the nucleophilic attack on the carbonyl of a peptide in its binding site on the enzyme by the amino group of another peptide.

Reported studies[28a,b] of the hydrolysis of substrates mediated by pepsin and penicillopepsin in $H_2{}^{18}O$ indicated the lack of incorporation of ^{18}O into the enzyme active site aspartates during the course of enzyme-mediated hydrolysis, contrary to what may be expected if the deacylation step was also to proceed by a nucleophilic mechanism. Another $H_2{}^{18}O$ study reported[28c] the incorporation of ^{18}O into trans-peptidation product. This was interpreted to arise from the general base catalyzed attack of $H_2{}^{18}O$ on substrate to form R-$CO^{18}OH$, which then reacts with the free amino end of another peptide to form trans-peptidation product with ^{18}O incorporated into the peptide bond. Together, these reports led to the conclusion that APase catalysis follows the general-base mechanism. However, these results were in turn re-interpreted in terms of a transient anhydride acyl-enzyme intermediate that is rapidly cleaved by $H_2{}^{18}O$ through general base catalyzed deacylation, also shown in **Scheme 5**, or by nucleophilic attack of another peptide in the trans-peptidation reaction.[29] According to this view, it is the reversible formation of the tetrahedral intermediate of $H_2{}^{18}O$ addition that accounts for the incorporation of ^{18}O into the carbonyl of the anhydride and thus the peptide bond of the trans-peptidation product. This re-interpretation[29] accounted for the observed lack of enzyme aspartate ^{18}O incorporation for APase-mediated hydrolysis in $H_2{}^{18}O$, the observed ^{18}O incorporation into trans-peptidation product, and the difficulty associated with the detection of such an

intermediate in the enzyme active site, since its decomposition is so much faster than its formation.

Recently, investigation[30] of the mechanism of action of the APases has been initiated in an attempt to determine the structural requirements of inhibitors of APases such as renin for antihypertensive therapy and the retroviral protease from human immunodeficiency virus (HIV) for the possible treatment of acquired immunodeficiency syndrome (AIDS).[30] These investigations have typically been conducted through the inhibition of various APases with ketone substrates which are similar to peptides but are unable to undergo hydrolysis. Structural analysis of the enzyme-inhibitor complexes thus formed has demonstrated the existence of a bound hydrate form of the substrate. With the assumption that "natural" peptide substrates similar in structure to the inhibitors undergo hydrolysis by a similar mechanism, these complexes have been taken as evidence for the formation of a tetrahedral intermediate through (general base catalyzed) water attack on the amidic carbonyl.

Although many aspects of the chemical mechanism of the APases remain unresolved, it is now widely believed that the active site aspartyl groups participate in general acid / general base catalysis. In this mechanism deprotonation of a bound water molecule is performed by the basic aspartate residue, and protonation (or at least polarization) of the carbonyl oxygen is achieved by the protonated aspartyl residue, as shown in **Scheme 6**. Importantly, breakdown of the so-formed tetrahedral intermediate can be facilitated by protonation of the amino nitrogen by COOH either concurrent with, or prior to C-N cleavage.

Scheme 6

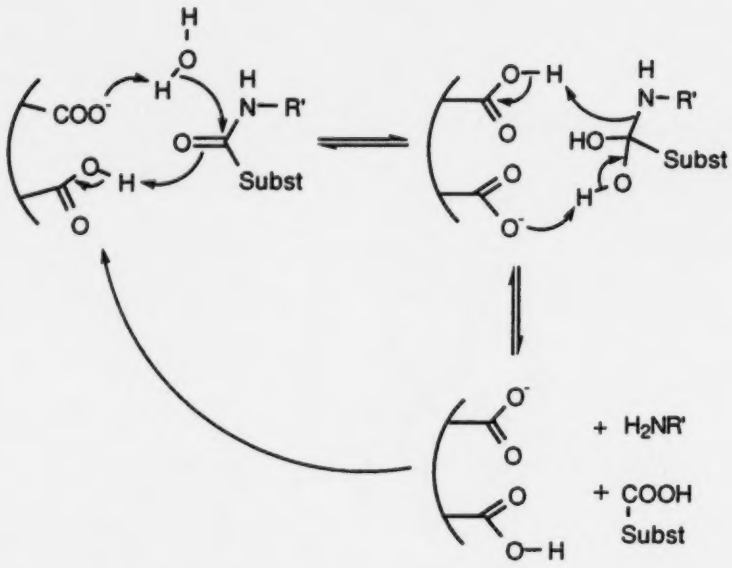

Cysteine Proteases

The cysteine proteases form a large class of enzymes from plant, animal and bacterial sources,[31] and contain essential cysteine thiol and histidine imidazole units.[32] Papain is the best known cysteine protease, and is found in large quantities in the latex or fruit of the papaya. Although its natural function in the plant is unknown, it functions as a robust proteolytic enzyme. The catalytic pathway for the hydrolysis of both amides and esters involves the acylation of the cysteine sulfhydryl to form a transient S-acyl enzyme.[31,33] For ester substrates, the deacylation is predominantly rate-limiting, whereas for amides the acylation step is.[34] The acylation process follows bell-shaped pH/rate profiles for typical amide substrates and depends upon two active site residues having pKa values of ~ 3.9 - 4.3 and 8.2 - 8.5.[35] These ionizations have been attributed to the imidazolium and thiol residues.[36,37] Although there was some early ambiguity about which group had the lower pKa, and at one point a general base role was proposed for the

imidazole during the nucleophilic attack of the thiol,[36] it is now generally accepted[31h,37] that in the cysteine proteases, the active site cysteine side chain has the unusually low pKa of 3 - 4, while the histidine imidazolium ion has the pKa of ~8.5. Thus, it is proposed[38a] that at physiological pH, 90% of the enzyme exists in a form wherein the active site consists of a kinetically competent[37,38] imidazolium thiolate zwitterionic pair. In **Scheme 7**, a representation of the pathway for acyl transfer from amides mediated by the cysteine proteases is presented.

Scheme 7

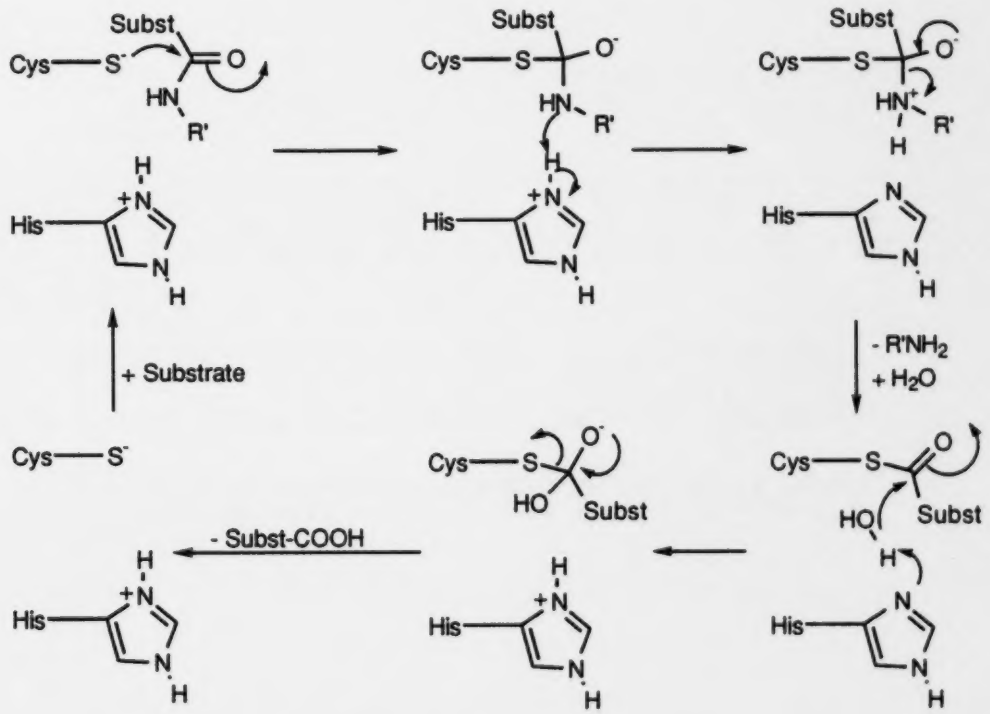

The acyl enzyme, once formed, is hydrolyzed with the assistance of an active site residue having an apparent pKa of 3.3 - 4.7,[31a,35a] and with a D_2O skie from 2.75 to 3.35,[35a,39] depending on the substrate. This apparent pKa of deacylation has been

found[36b,40d] to decrease on moving from H_2O to dioxane-H_2O mixtures. These observations are consistent with a general-base role for an imidazole in a hydrophobic[33i,40] environment, also shown in **Scheme 7**. (It should be noted however, that the data do not require a general-base role for the imidazole, and could be accommodated by a nucleophilic pathway whereby S→N acyl transfer occurs from the thiolester to the histidine imidazole unit with subsequent hydrolysis.[41])

Generalized Mechanism

In spite of the uncertainty surrounding some of the mechanistic details of the hydrolysis of amides promoted by the non-metallo proteases, there are striking similarities between the pathways chosen for this reaction by the serine, aspartate and cysteine proteases. In each case, the first step is the nucleophilic attack of the enzyme on the carbonyl of the bound substrate. In SPases, this nucleophilic attack is assisted through general base removal of the hydroxyl proton by a nearby imidazole. In cysteine proteases, the active site sulfhydryl exists predominantly as an ion pair consisting of a nucleophilic thiolate anion with an adjacent imidazolium cation. In APases, the general acid / general base - nucleophilic mechanistic controversy currently favours a general base assisted nucleophilic attack of a water molecule as the first step. However, it also seems at least possible that the nucleophile is the ionized carboxylate moiety. In either case the nucleophile, whether a water molecule or carboxylate, is adjacent to a protonated carboxylic acid. The groups adjacent to the nucleophile (imidazolium for SPases and Cysteine proteases, carboxylic acid for APases) also play an important role, as they are then able to act as general acid traps of the anionic tetrahedral intermediates, protonating the nitrogen of the departing amine, assisting in breakdown of the TI to an acyl enzyme intermediate. These groups, now in their basic form, are able to act as general base catalysts for the hydrolysis of the acyl enzyme (if one is formed) to form carboxylic acid products, and to regenerate the respective enzymes in their active form, completing the catalytic turnover.

Certainly the elegance and catalytic efficiency of the hydrolysis of amides mediated by these enzymes lies in the fact that the active form of the enzyme necessary for each successive transformation is the form resulting from the previous transformation. That is, after each step along the hydrolytic pathway, the form of the intermediate enzyme produced is such that the essential active site constituents are correctly poised and in the appropriate state of protonation to carry out the next step.

C) Models for Enzymatic Amide Hydrolysis

As the preceding section has made clear, certain ambiguities in the mechanism of action of proteolytic enzymatic pathways remain in spite of intense effort by many research groups. Certainly working with the enzymes themselves, even those whose isolation is simple and whose structure is known, can present complications. Enzymes are generally very large proteins with relatively small active sites, so while the bulk of the protein may serve to offer substrate specificity or to structurally predispose the substrate to nucleophilic attack, the sheer size of it may obscure detection of the detailed mechanism of action within the active site itself. Primarily because of the complexity of detailed mechanistic investigations of enzymatic reactions, many studies have been undertaken with the reactions of small molecules as enzyme models.[42] Perhaps our future comprehension of enzymatic mechanisms lies in the basic understanding of the mechanisms of simple non-enzymatic reactions of small molecules containing approximations for the functional groups found in the active sites of enzymes.

The following is a brief summary of some of the model systems studied with the objective of shedding light on the enzymatic mechanisms they model. Although many model systems have been proposed, this cursory review is concerned primarily with those in which small molecules were used as analogues of the active sites of the three classes of proteases discussed above.

Serine Protease Models

Although the catalytic triad employed by the serine proteases offers a considerable mechanistic advantage and an obvious rate acceleration in the hydrolysis of peptides, surprisingly few studies have used the triad to facilitate the O-acylation of a small molecule. Some studies have dealt with the reaction of amino alcohols with esters[43] or reactive amides,[44] as models of the acylation of the serine proteases. Fewer studies have dealt with the interaction of imidazole and carboxylate during acyl transfer from esters to water[45] as a

model of the deacylation of SPases, and fewer still have used the complete triad in the modeling of the O-acylation of SPases.[44c,44d,46]

Scheme 8

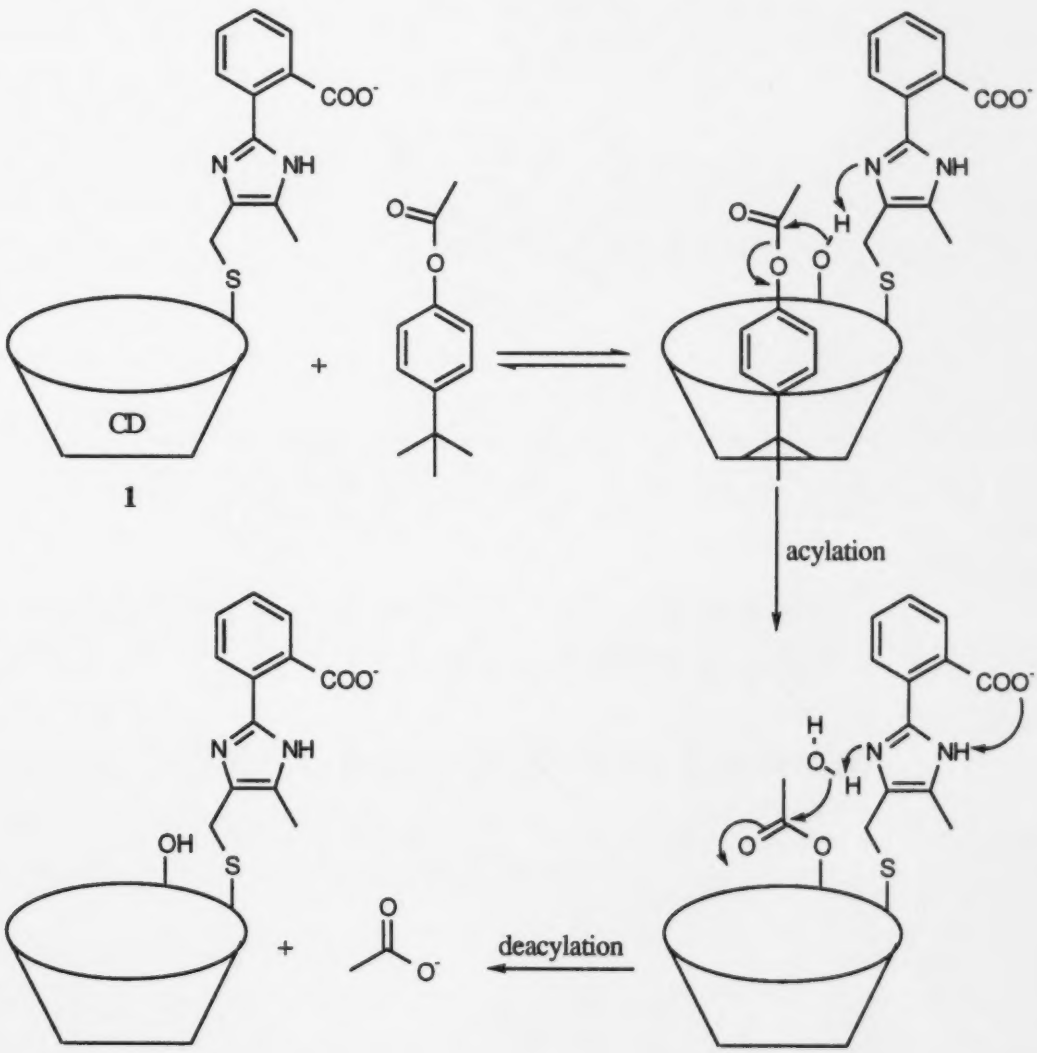

1

To study a complete triad, Bender reported[46a,b] the synthetic modification of a cyclodextrin to include an imidazole group and a carboxylate (**1** in **Scheme 8**). These

groups, together with a hydroxyl group on the rim of the cyclodextrin cavity, comprise the essential moieties of the catalytic triad, whereas the cyclodextrin portion of the molecule provides a kind of "binding site" for a hydrophobic ester such as p-*tert*-butylphenyl acetate. In fact, the efficiency of **1** as an "artificial enzyme" for the catalytic hydrolysis of p-*tert*-butylphenyl acetate ($k_{cat}/K_m = 210\ M^{-1}s^{-1}$ at its optimum pH) compared favourably to that of chymotrypsin for the catalytic hydrolysis of pNPA ($k_{cat}/K_m = 275\ M^{-1}s^{-1}$ at its optimum pH). No mention was made of the nature of the role of the carboxylate, but a large skie of 3 was reported in support of the reaction being catalyzed by a general basic mechanism, as opposed to a nucleophilic attack by imidazole. Unfortunately, the hydrolysis of amides mediated by this "artificial enzyme" was not reported.

A study more concerned with the role of the carboxylate, and the detailed mechanism of the catalysis of amide hydrolysis by an SPase model was reported by Brown and co-workers.[44c,d]

Scheme 9

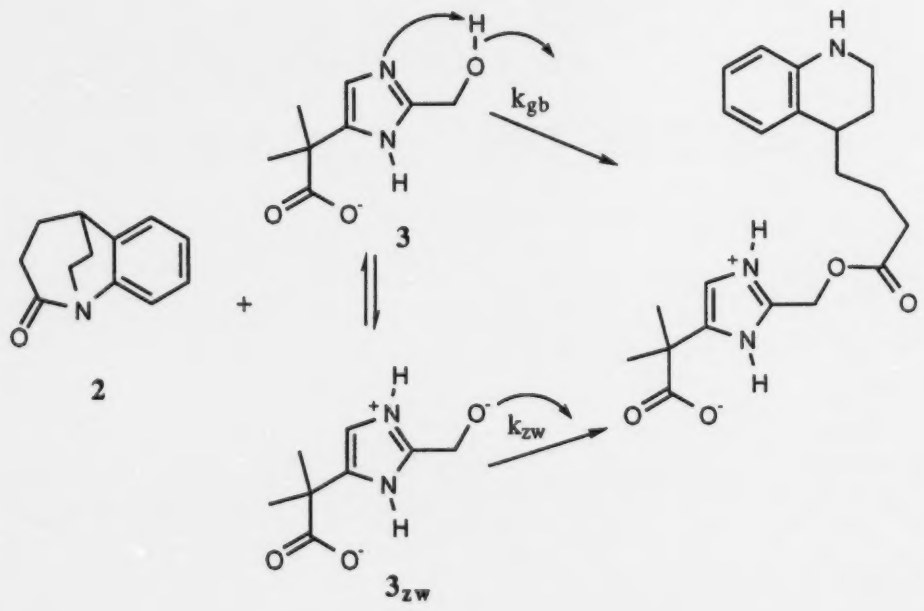

This study revealed that a series of imidazole and amino alcohols reacted with distorted amide **2** to give the initial O-acylation product esters, as shown in **Scheme 9**. The reactivity of the various amino alcohols increased with the pKa of the amino group in a Brønsted relationship and was dependent on the basic form of the amine. When a pendant carboxylic acid was added to an imidazole alcohol to give model molecule **3**, the observed rate constant for O-acylation fit on the same Brønsted plot, indicating that the same mechanism dependent solely on amine basicity is in operation for **3**, as for the other amino alcohols used to define the Brønsted line. In this case, the role of the carboxylate is simply the enhancement of amine basicity through electrostatic or inductive means. This was found to be particularly effective in solvents of reduced polarity, since this effect tended to counteract the normal drop in amine pKa experienced by amino alcohols without a pendant COO^-. Solvent kinetic isotope effects of 1 to 2 were found, indicating that the mechanism operated through general base catalysis (k_{gb} in **Scheme 9**). The skie were found to decrease to 1 as the amine pKa increased, suggesting that the zwitterionic form of the model molecule ($\mathbf{3_{zw}}$) may play an increasingly important nucleophilic role (k_{zw} in **Scheme 9**) with increased amine basicity.

Aspartate Protease Models

The mechanism by which the APases cleave proteins is probably the most obscure of any protease. Part of the reason for this is the existence of very few satisfactory simple models to provide chemical precedence for the transformations achieved within the active site.[24,25,47]

A popular model for the acylation of APases by amide substrates is the hydrolysis of a series of maleamic acids. As shown in **Scheme 10**, these reactions proceed through the intramolecular nucleophilic attack of carboxylate to yield maleic anhydride. In most cases, the general acid catalyzed cleavage of the C-N bond is the rate determining step. However, in some cases[24] the proton transfer to form the zwitterionic tetrahedral

intermediate capable of breakdown ($T^{\pm}$) is rate limiting, and in other cases[25] diffusion of the amine away from the nascent carboxylic acid is rate limiting.

Scheme 10

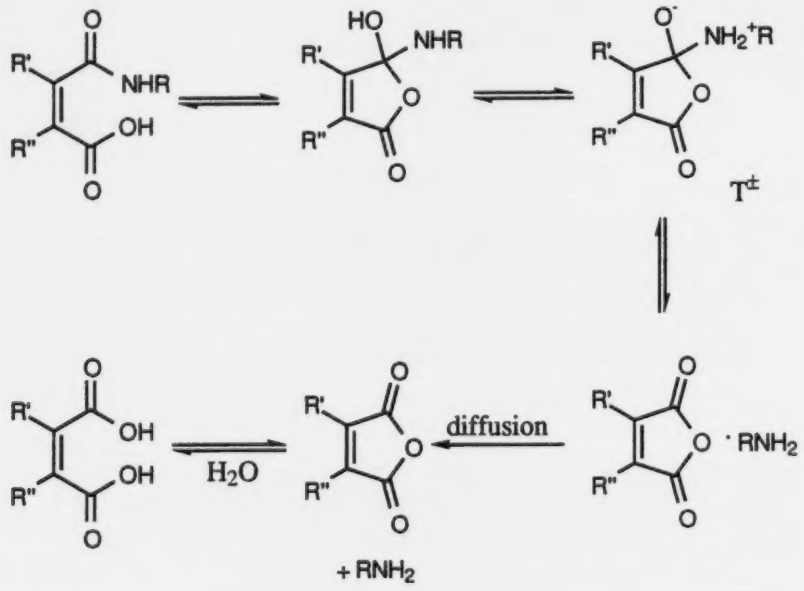

One of the few studies that models the intermolecular formation of the acylation product followed by intramolecular catalysis of deacylation was reported by Somayaji and Brown.[47,29a] In that study, certain dicarboxylic acids were reacted with activated amide **2** as a model of the acylation of the active site of APases containing two aspartate carboxylates.

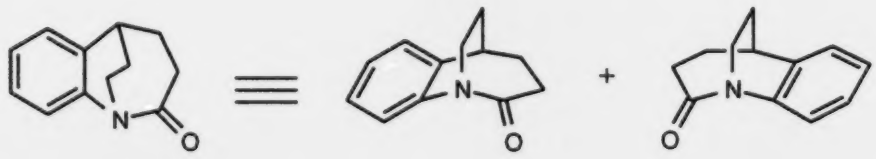

2

Like the maleamic acid studies, the cleavage of the amide bond was found to proceed through the nucleophilic attack of carboxylate on the amide (or the kinetically equivalent dicarboxylate on the protonated amide) to form a linear anhydride, shown in **Scheme 11**. However, this anhydride was never detected, as it was rapidly cleaved through intramolecular nucleophilic attack by the pendant second carboxylate group, forming the cyclic anhydride of the diacid. In the absence of such a suitably positioned second carboxylate the linear anhydride rapidly reversed to starting materials such that nucleophilic attack of carboxylate alone did not lead to enhanced hydrolysis.

Scheme 11

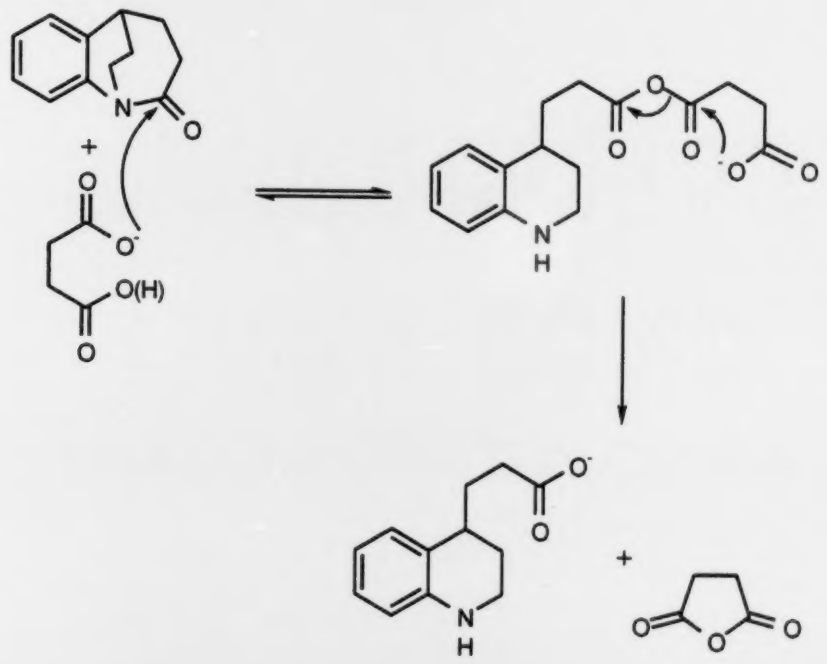

All of these studies attempted to explain some of the more complex features of APase peptide hydrolysis, such as transpeptidation products and isotope exchange, in light of the mechanism of the respective model reactions. Literature precedence for the role of

carboxylate as a nucleophile in the formation of an anhydride and as a general base in the catalysis of anhydride hydrolysis was also cited,[48] but the detailed mechanism of peptide hydrolysis promoted by APases remains in question.

Cysteine Protease Models

As a model for the deacylation of cysteine proteases, several imidazole-containing thiolesters have been investigated[41a-c] in an effort to ascertain the role of the intramolecular imidazole in facilitating the breakdown of the normally hydrolysis resistant[41,49] thiol ester. In these studies, only S→N acyl transfer was observed. For example, Bruice reported[41b] reversible lactam formation (followed by slow aqueous hydrolysis) through the intramolecular nucleophilic attack of a pendant imidazole on the carbonyl of *S*-*n*-propyl γ-(4-imidazolyl)thiobutyrate (**Scheme 12**). Later, Fife and DeMark reported[41a] a similar reaction for *S*-*n*-propyl o-(2-imidazolyl)-thiolbenzoate. Although general base catalysis was observed in this reaction, it was shown to arise from the rate-limiting breakdown of the tetrahedral intermediate formed by nucleophilic attack of imidazole, also shown in **Scheme 12**. In both cases, no evidence was obtained which would support a general-base role for the imidazole unit although such is believed to be the case in the deacylation of papain.[33i,35a,36b,40]

The principle drawback with respect to comparing these systems to the enzymatic deacylation reaction is that with both thiolesters studied, the thiol unit is expelled upon ring closure, while in the enzyme the imidazole and thiol units are retained in the same active site. Bruice[41b] was aware of this problem and noted that the hydrolysis of *S*-*n*-propyl γ-(4-imidazolyl)thiobutyrate was completely inhibited by the addition of free thiol, with reformation of thiolester, demonstrating the reversibility of the formation of N-acyl product. This observation also indicates that for this thiolester, the intramolecular imidazole acts entirely in a nucleophilic capacity to promote thiolester decomposition. Since the suppression of this nucleophilic role through the addition of free thiol completely inhibits

the hydrolysis reaction, the imidazole is apparently incapable of acting effectively as a general base in promoting thiolester hydrolysis.

Scheme 12

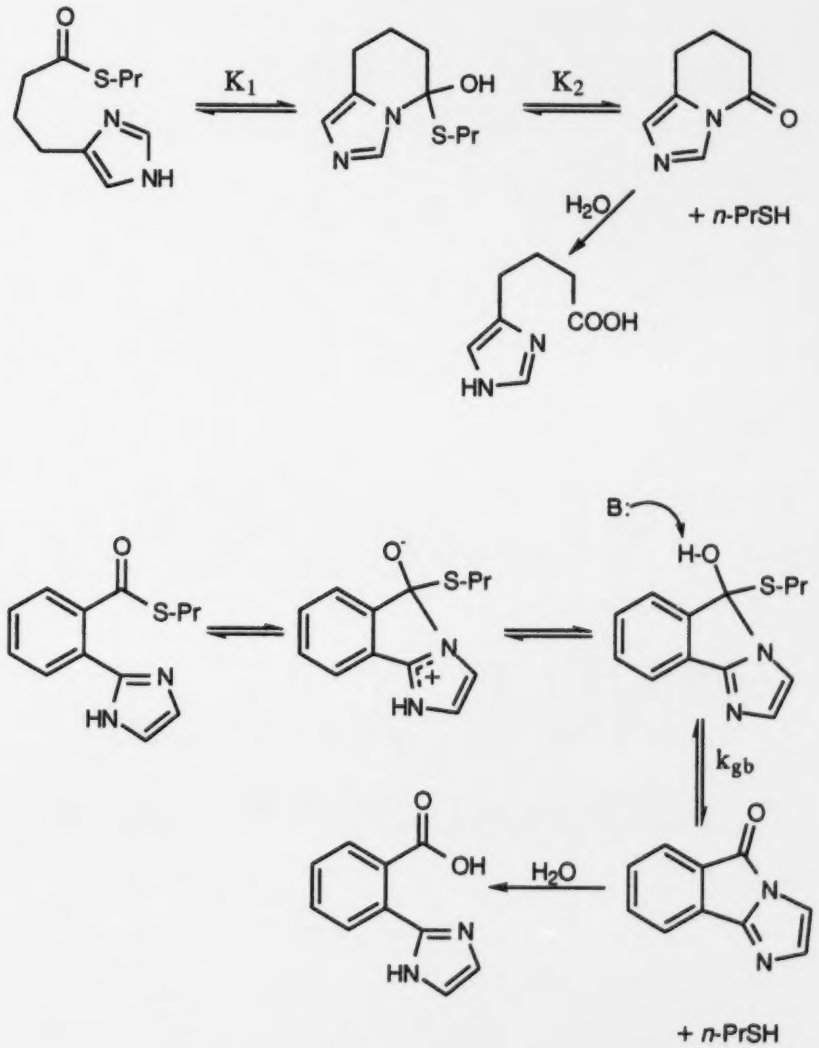

However, more recently there have been reported[50] studies by Brown and co-workers in which the departing thiol and imidazole were retained intramolecularly,

phenomenologically more similar to the S-acyl enzyme thiolester hydrolysis which occurs in the enzyme active site. In these studies, the kinetics of the hydrolysis of thiolesters **4**, **5** and **6a-b**, including solvent isotope effect studies and thiolate trapping experiments, were analyzed in detail.

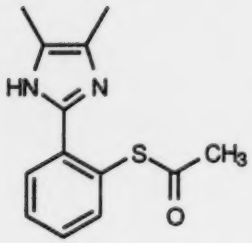

4

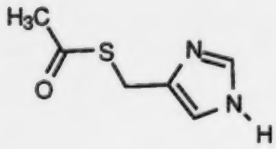

5

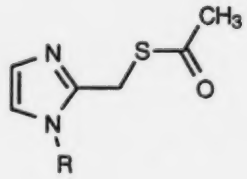

6a R = H

b R = CH_3

It was demonstrated for all of the species studied that the main pathway, at physiological pH, involves a general base delivery of H_2O to the thiolester by the pendant imidazole. This is represented in **Scheme 13**, using thiolester **6b** as an example.

Scheme 13

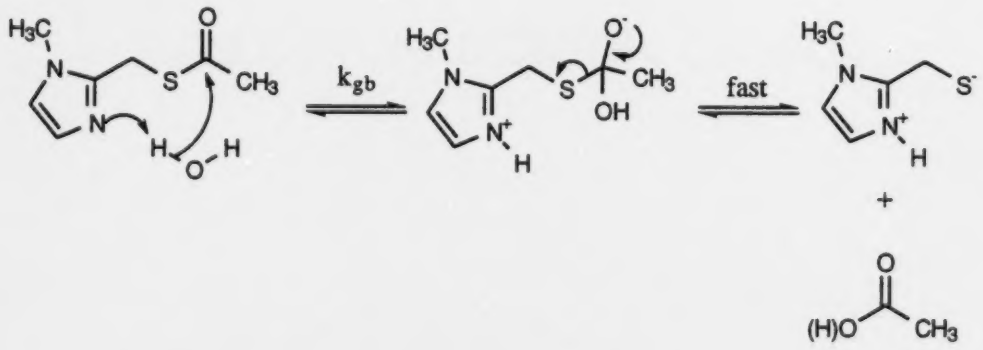

As models for the acylation of papain with esters, the reactions of a number of substituted thiols with esters such as pNPA have been investigated.[49a,51] In all cases, the thiols were found to react as their respective thiolates, without the requirement of general base assistance in their rate-limiting nucleophilic attack on the ester carbonyl units. Some of the small molecules studied have also contained imidazole units,[51a-g] but for the most part, these models showed little or no cooperative effect of the imidazole in S-acylation such as is believed to occur in the cysteine proteases. For example, Klotz and co-workers have investigated[41c] the reaction of some phenyl acetates with various peptides containing both histidine and cysteine amino acids, but no cooperative effect of the adjacent histidine imidazole was found for these peptides in the acylation of the cysteine sulfhydryl.

However, in their study of the reactions of several benzimidazolethiols with p-nitrophenyl esters as enzyme model reactions, Lochon and co-workers have reported[51f,g] enhanced activity of 2-mercaptomethyl benzimidazoles over simple thiols and other benzimidazole thiols in their reaction with pNPA. On a plot of the rate constants for the reaction of *thiolate* (derived from the observed rates) with pNPA vs pK^{SH}, the points for the 2-mercaptomethyl benzimidazoles studied fell slightly above the Brønsted line defined by the data observed for many other simple alkyl thiols and other benzimidazole thiols. In the narrow pH range of 7.2 - 8.2 over which these compounds were studied, the authors proposed that any zwitterionic form of the benzimidazole thiols would be practically non-existent, since the reported pKa values of the imidazole (~5.0) and the thiol functionalities (~8.5) are so far from each other. The pathway shown in **Scheme 14** therefore represents the mechanism suggested[51f] for the reaction of neutral benzimidazole thiols with pNPA. Although the slight rate enhancement over thiols with similar thiol acidities is explained in terms of a general base role for the adjacent benzimidazole, no evidence was given for this proposal.

Scheme 14

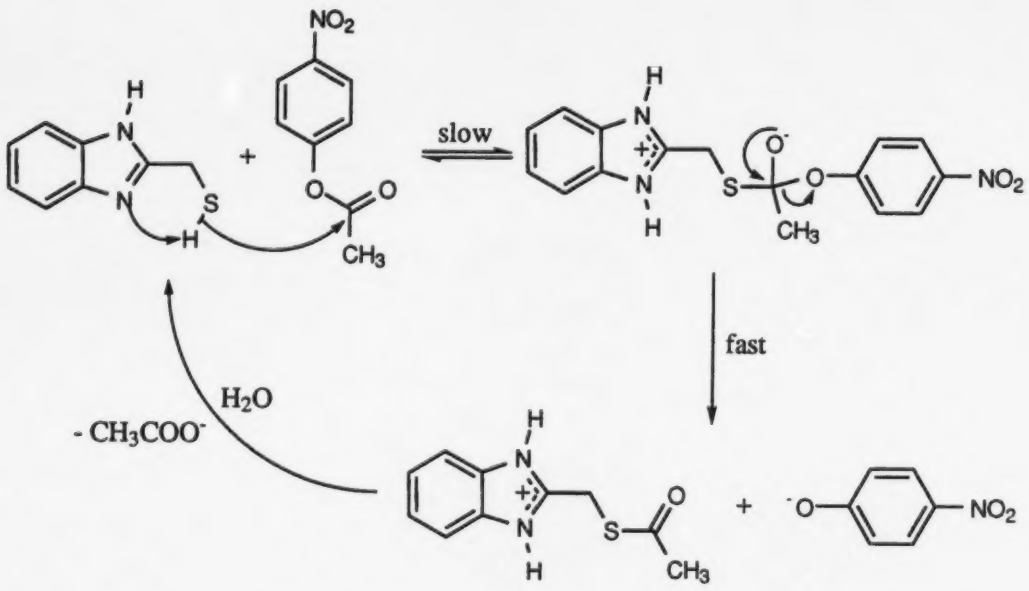

More recent reports[52] by Brown and co-workers have shown that imidazole-thiols **7** and **8** react rapidly as their zwitterionic and anionic forms with the activated esters p-nitrophenyl acetate (pNPA, **9a**) and 2,4-dinitrophenyl acetate (**9b**).

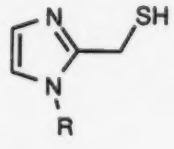

7a R = H

b R = CH_3

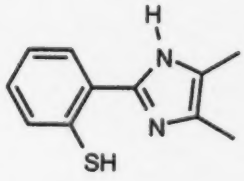

8

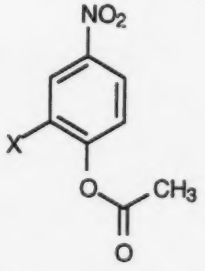

9a X = H

b X = NO_2

In those cases there is no sign of a bell-shaped pH rate profile, and throughout the pH range from 5 - 10, the rate limiting step involves nucleophilic thiolate attack (either as the zwitterion or anion) on the ester, as shown in **Scheme 15** for the reaction of **7b** with **9a**. The imidazolium unit plays the passive role of electrostatically reducing the SH pKa so that large concentrations of nucleophilic thiolate are present at neutral pH.

Scheme 15

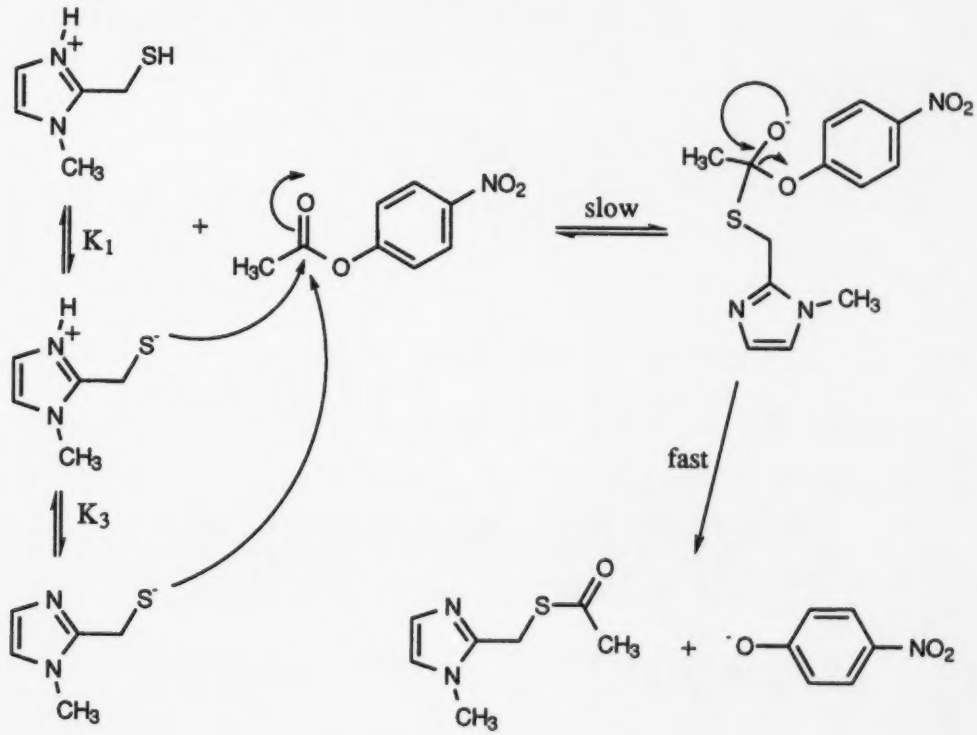

Few studies have been reported where amino thiols have been used to facilitate cleavage of the amide bond.[53] Carriuolo and Jencks have reported[53c] the bimolecular attack of 2-mercaptoethanol on the activated amide, N-acetylimidazole. At neutral pH this reaction was found to proceed through nucleophilic attack of thiolate catalyzed by free imidazolium

cation. Other studies reported by both Koshland[53d] and McDonald[53a,b] involved intramolecular thiolactonization of unactivated amides.

Scheme 16

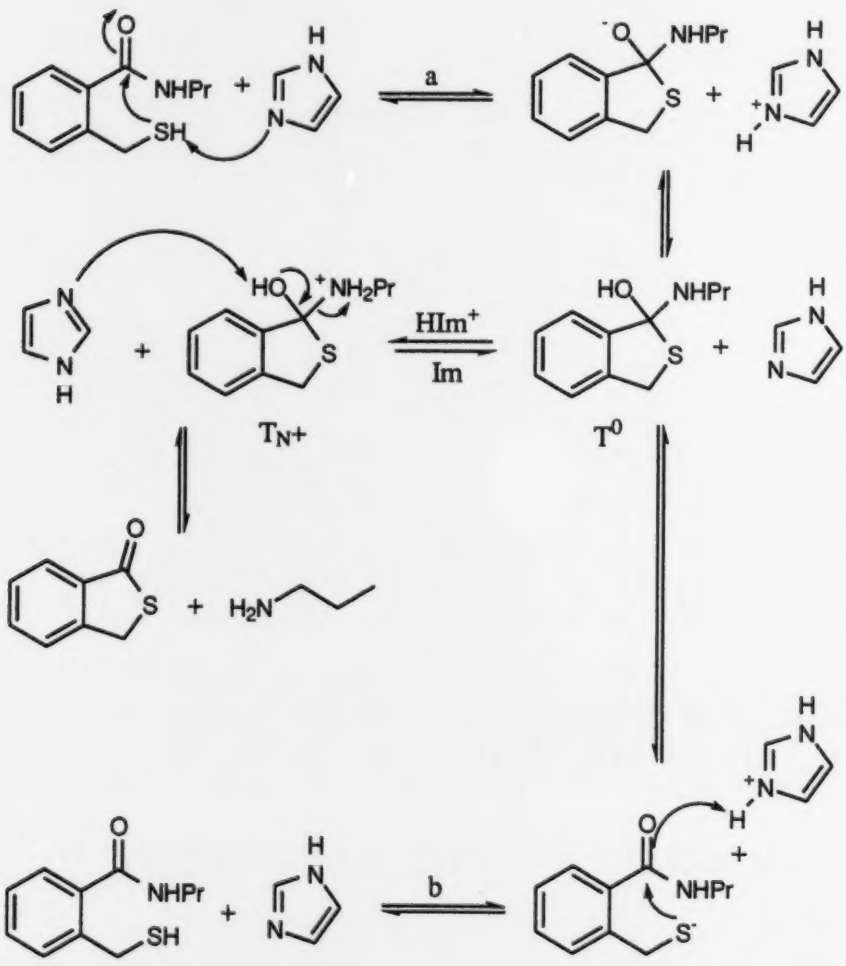

In the study reported by McDonald, it was found that half-protonated imidazole buffer was a uniquely efficient catalyst. The observed bell-shaped pH rate profile was accounted for through the suggestion of a mechanism involving stepwise imidazole general base catalysis of the formation of an intermediate (T^0), followed by imidazolium general

acid catalyzed breakdown of that intermediate to give product thiolactone. This mechanism is shown in **Scheme 16**, with the general acid catalyzed breakdown of the neutral intermediate T^0 represented by the kinetically equivalent general base catalyzed breakdown of N-protonated tetrahedral intermediate T_N+. It was noted that while recent evidence seems to indicate an imidazolium thiolate ion pair in the active site of papain, in the model study it was impossible to distinguish kinetically between true general base catalysis by imidazole of thiol attack on the amide carbonyl (path a), and the formation of the ion pair followed by acid-assisted thiolate attack on the amide (path b).

It is surprising that bimolecular attack of thiolamines on amides has not been studied extensively as a model for the chemistry believed to be operative in the cysteine proteases. Undoubtedly, this is due not to lack of interest in the subject, but to the resistance of the unactivated N-C(O) unit toward nucleophilic attack which precludes such studies under all but the most vigorous conditions.

D) Proposed Cysteine Protease Model

The reaction of esters with small molecule analogues of the cysteine proteases is convenient and has offered much insight into the mechanism of hydrolysis mediated by these enzymes. However, there are obvious differences between esters and amides, and the information gleaned for ester hydrolysis may or may not be applicable to the mechanism of the enzymatic hydrolysis of a "natural" peptide (amide) substrate. Unfortunately, as mentioned earlier, the resistance of the unactivated amidic N-C(O) unit toward nucleophilic attack precludes the study of the bimolecular attack of thiols on amides under all but the most vigorous conditions. However, presented herein are the results of several studies of a simple model system for (1) the acylation by amides of the active site SH in the cysteine proteases,[54] (2) the deacylation of the intermediate S-acyl enzyme, and (3) the catalytic hydrolysis and re-formation of non-activated amides at neutral pH.[55]

CHAPTER 1

A) Introduction

It was shown earlier by this research group that 2,3,4,5-tetrahydro-2-oxo-1,5-ethanobenzazepine,[56] distorted anilide **2**, is remarkably susceptible towards nucleophilic attack by bifunctional nucleophiles such as β-amino alcohols[44c,d] or certain dicarboxylic acids[47] in ways that are reminiscent of reactions promoted by the serine proteases and aspartate proteases. Described in this chapter are the reactions of **2** with certain amino thiols (**7b**, **10a-d**) as a simple model for the acylation of the active site sulfhydryl group in cysteine proteases by amides.[54] These studies reveal (1) that the zwitterionic forms are responsible for nucleophilic attack, (2) the origin of a bell-shaped pH/rate profile for reaction of **7b** with **2**, and (3) significant differences in the catalytic requirements for the S-acylation of aminothiols by the amide, **2**, and the activated ester, pNPA, **9a**.

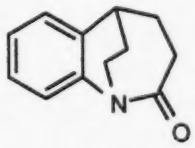

2

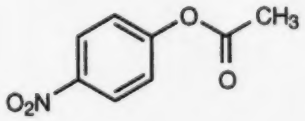

9a

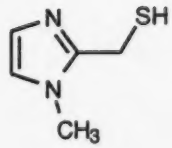

7b

10a X = NH_2

b X = $N(CH_3)_2$

c X =

d X = CH_2NH_2

11a R = H; X = CH_3

b R = H; X = CO_2Et

c R = H; X = CH_2CN

d R = Et; X = CH_2NH_2

B) Experimental

a) General: Routine IR and ^1H NMR and mass spectra were recorded on a Nicolet 7199-FTIR spectrophotometer, a Bruker WP-80 (80 MHz) spectrometer, and an AEI MS-50 mass spectrometer respectively. High field NMR spectra (^1H and ^{13}C) were recorded on a Bruker AM-300 (300 MHz) spectrometer.

b) Materials: 2-Mercaptoethylamine (cysteamine, **10a**), N,N-(dimethylamino)-ethanethiol (dimethylcysteamine, **10b**), ethyl mercaptoacetate (**11b**), ethanethiol (**11a**) and 2-ethylthioethylamine (**11d**) were commercially available (Aldrich) and were used as supplied if solid or after distillation if liquid. Buffers (MES, morpholinoethanesulfonic acid; MOPS, morpholinopropanesulfonic acid; EPPS, N-(2-hydroxyethyl)-piperazine-N'-3-propanesulfonic acid; TAPS, tris(hydroxymethyl)-methylaminopropanesulfonic acid; CHES, cyclohexylaminoethanesulfonic acid; and CAPS, cyclohexylaminopropanesulfonic acid) were reagent grade (Sigma) and used as supplied. Acetonitrile was dried over 3Å molecular sieves, and then distilled and stored under Ar. Amide **2** (2,3,4,5-tetrahydro-2-oxo-1,5-ethanobenzazepine) was prepared as reported.[56] 2-Mercaptomethyl-1-methylimidazole (**10b**) was prepared as reported.[50b] 4-(2-Mercaptoethyl)morpholine (**10c**) and 3-mercaptopropionitrile (**11c**) were prepared from the corresponding commercially available alkyl chlorides by displacement with thiourea according to methods analogous to a published procedure.[57]

4-(2-Mercaptoethyl)morpholine•HCl (**10c**•HCl): from 2-(4-morpholino)ethyl carbamimidothioate dihydrochloride in 80% yield; mp 156-156.5 °C; ^1H NMR (D_2O) δ 4.60 (s, >2H), 3.98 (t, 4H), 3.40 (m, 6H), 2.89 (t, 2H); FTIR (KBr, cm^{-1}) 3400 (br), 3000-2900 (s), 2800-2000 (s, br), 1460. Anal. Calcd for $C_6H_{13}NOS$•HCl: C, 39.23; H, 7.63; N, 7.63; S, 17.45. Found: C, 39.21; H, 7.60; N, 7.43; S, 17.36.

3-Mercaptopropionitrile•HCl (**11c**•HCl): from 3-isothioureidopropionitrile in 84% yield; bp 59-60 °C (4 Torr); ^1H NMR ($CDCl_3$) δ 2.72 (m, 4H), 1.82 (t, 1H); FTIR (film)

2947, 2566, 2250, 1418, 1291 cm^{-1}. Anal. Calcd for $C_3H_5NS \bullet HCl$: C, 41.35; H, 5.78; N, 16.07. Found: C, 40.89; H, 5.62; N, 15.77.

3-Mercaptopropylamine•HCl (**10d**•HCl): This was prepared by $Na/NH_{3(l)}$ reduction of the corresponding S-benzylthiopropylamine according to the method already published:[50b] yield 50%; mp 68 °C [lit.[58] 69 °C]; ^1H NMR (D_2O) δ 4.64 (s, > 4H), 3.15 (t, 2H), 2.65 (t, 2H), 2.00 (m, 2H); FTIR (KBr, cm^{-1}) 3400, 2980, 2000, 1600, 1400, 1260; mass spectrum, m/z (rel. intensity) 91 (M^+-HCl, 100), 74 (53.1), 58 (49.6).

c) Kinetics: Buffers (50 mM, μ = 1.0 (KCl)) were used to control the pH; MES (pH 5.4 - 6.3); MOPS (pH 6.9 - 7.9); EPPS (pH 8.0 - 8.3); TAPS (pH 8.4 - 8.7); CHES (pH 8.6 - 9.7); CAPS (pH 10.3 - 11.0). Distilled water was further purified and deoxygenated with an Osmonics Aries water purification system. Buffers were prepared and stored under Ar using the above deoxygenated water.

Kinetics of the ring opening of **2** by excess **7b**, **10a-d**, ethanethiol, ethyl mercaptoacetate, and 3-mercaptopropionitrile were followed at 25.0 ± 0.1 °C by observing the rate of production of the substituted aniline chromophore at 291 nm using a Cary 210 uv-vis spectrophotometer interfaced to a microcomputer as previously described.[59] Deoxygenated aqueous buffers (3.0 mL) were transferred by syringe to an Ar-flushed septum-sealed 1.0 cm quartz cuvette. Varying concentrations of the thiols were introduced by injection of 50 - 200 μL aliquots of deoxygenated buffer solutions containing 60 - 65 mM thiol. Runs were initiated (after thermal equilibration of the cell in the spectrophotometer cell holder for ~ 10 min) by injection of 10 - 15 μL of a 20 - 25 mM stock solution of **2** in CH_3CN into the cell. To ensure pseudo-first order conditions, [thiol] was kept to a 10 - 40 fold excess over [**2**]. No evidence for the build up of transient intermediates such as biphasic or saturation kinetics was observed in any case. The pH of the solutions was measured after the kinetic runs to ensure there were no changes (Radiometer TTT2 titrator equipped with a GK2321C combination electrode standardized

by Fisher Certified pH 4.00, 7.00, and 10.00 buffers). Reactions displayed excellent first order kinetics to up to 5 half-times. Rate constants (k_{obsd}) were obtained by fitting the absorbance vs time data to a standard exponential model. Runs with each [thiol] were performed in duplicate or triplicate. Second order rate constants for the reaction of thiol with **2** (k_2^{obsd}) were obtained from the slopes of the plots of k_{obsd} vs $[thiol]_{total}$ (4 - 6 concentrations). For the amino thiols **10a-d**, plots of k_2^{obsd} vs pH showed evidence of a plateau above pKa^{SH}. For thiols not containing an amine, the k_2^{obsd} was obtained by determining k_{obsd} at the pKa of the thiol, and then dividing this value by $[RS^-]$. In some cases (**11a,c**) no detectable rate acceleration was observed in the presence of thiol so the k_2^{obsd} values are given as upper limits in **Table 1**.

d) D_2O studies: The buffers and stock solutions were prepared under Ar in the way described above, using D_2O which had been purged of O_2 by passing a stream of Ar through it for several hours. pD was determined by adding 0.4 units to the pH meter reading.[60]

e) Product Studies: Large scale reactions of **2** and cysteamine (**10a**) or dimethylcysteamine (**10b**) were performed under standard kinetic conditions for ~ 10 $t_{1/2}$. The reaction mixtures were extracted and worked up as below to identify the final product.

Into 25 mL of 1 M KCl solution was placed ~ 3 mL of a 62 mM cysteamine solution (in Ar-purged H_2O) and 0.83 mL of a 22 mM solution of **2** in CH_3CN. The pH was kept constant at ~ 8.6 for 30 min by the addition of small amounts of dilute NaOH, after which the mixture was extracted with 3 × 20 mL aliquots of distilled CH_2Cl_2. The organic extracts were combined, dried ($MgSO_4$), and then stripped of solvent. The residue was shown by ^1H and ^{13}C NMR to contain a predominant species having peak positions identical to the ring opened amide product (**14a**) synthesized independently by an unambiguous route. (See Appendix 1 for preparation and spectral characterization of **14a**).

For the reaction of amide **2** with dimethyl cysteamine (**10b**) the kinetic extraction procedure used for cysteamine (**10a**) was repeated using dimethylaminoethanethiol (**10b**) to give reaction product thiolester **13b**: ^{1}H NMR (300 MHz, $CDCl_3$) δ 6.98 (m, 2H), 6.61 (d of t, 1H), 6.47 (d of d, 1H), 3.65 (br s, 1H), 3.29 (m, 2H), 3.03 (t, 2H), 3.01 (br s, 1H), 2.86 (m, 2H), 2.69 (m, 2H), 2.52 (t, 2H), 2.31 (s, 6H), 1.79 (m, 2H). ^{13}C NMR (75 MHz, $CDCl_3$) δ 199.43, 144.17, 129.16, 127.56, 123.85, 116.78, 114.21, 45.27 (2 C), 41.62, 38.13, 36.83, 34.79, 31.85, 26.71, 26.16 ppm. FTIR ($CDCl_3$, cm^{-1}) 3320, 2930, 2860, 2820, 2760, 1688, 1645, 1605, 1581, 1497, 1456.

The product of the reaction of **2** with **7b** was determined in an NMR experiment wherein the spectrum of a solution consisting of 17.6 mg of **7b**, 100 μL of 1.06 N KOD, 600 μL of CD_3CN and 20.2 mg of **2** was monitored periodically. The thiol ester was formed within ~10 min: ^{13}C NMR (75 MHz) δ 199.5, 145.8, 144.5, 129.9, 127.9, 126.5, 124.8, 123.7, 123.3, 117.1, 115.2, 41.9, 38.4, 35.6, 32.7, 26.5, 24.7 ppm. The volatiles were removed and a FTIR spectrum of a CH_2Cl_2 cast was taken: 3360, 3280, 2920, 1689, 1648, 1605, 1581, 1491 cm^{-1}. By the characteristic ^{13}C resonance at δ 199.5, the product was identified as the corresponding thiol ester.[61]

C) Results

a) Kinetics: The kinetics of the reactions of the various thiols with **2** were followed at 25 °C and μ = 1.0 (KCl), under pseudo first order conditions of excess thiol to give k_{obsd}. The observed second order rate constants (k_2^{obsd}) were evaluated from the slopes of the plots of k_{obsd} vs $[thiol]_{total}$ at several pH values. (See Appendix 1 for tables of these observed second order rate constants vs pH for the attack of thiols **7b**, **10a-d**, and **11a-d** on amide **2**). As can be seen in **Figure 1**, for aminothiols **10a-d**, the k_2^{obsd} values plateau above the pKa value for the thiol which indicates that the neutral or, more probably, the kinetically equivalent zwitterionic form is the active one. Overall, the data support the process in equation (**1**) for which can be derived the kinetic expression given in equation (**2**).

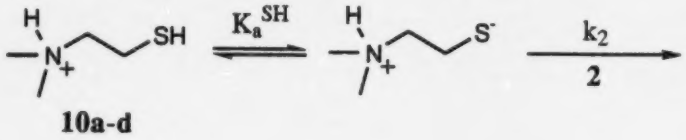

10a-d

(**1**)

$$k_2^{obsd} = k_2 \, Ka^{SH} / (Ka^{SH} + [H_3O^+]) \qquad (2)$$

Given in **Table 1** are the various maximal second order rate (k_2) and kinetic acidity (pKa^{SH}) constants derived for **10a-d** on the basis of the fit of the k_2^{obsd} vs $[H_3O^+]$ data to equation (**2**) by non linear least squares techniques. Also in the Table are the thermodynamic macroscopic pKa values for the SH and $^+$NH groups from literature sources.

Figure 1 : Plot of the log k_2^{obsd} vs pH profile for the reaction of **10a-d** with **2**; T = 25 °C, μ = 1.0 (KCl). Line through the data computed on the basis of NLLSQ fit to equation **(2)**. (**10a**, circles; **10b**, diamonds; **10c**, squares; **10d**, triangles)

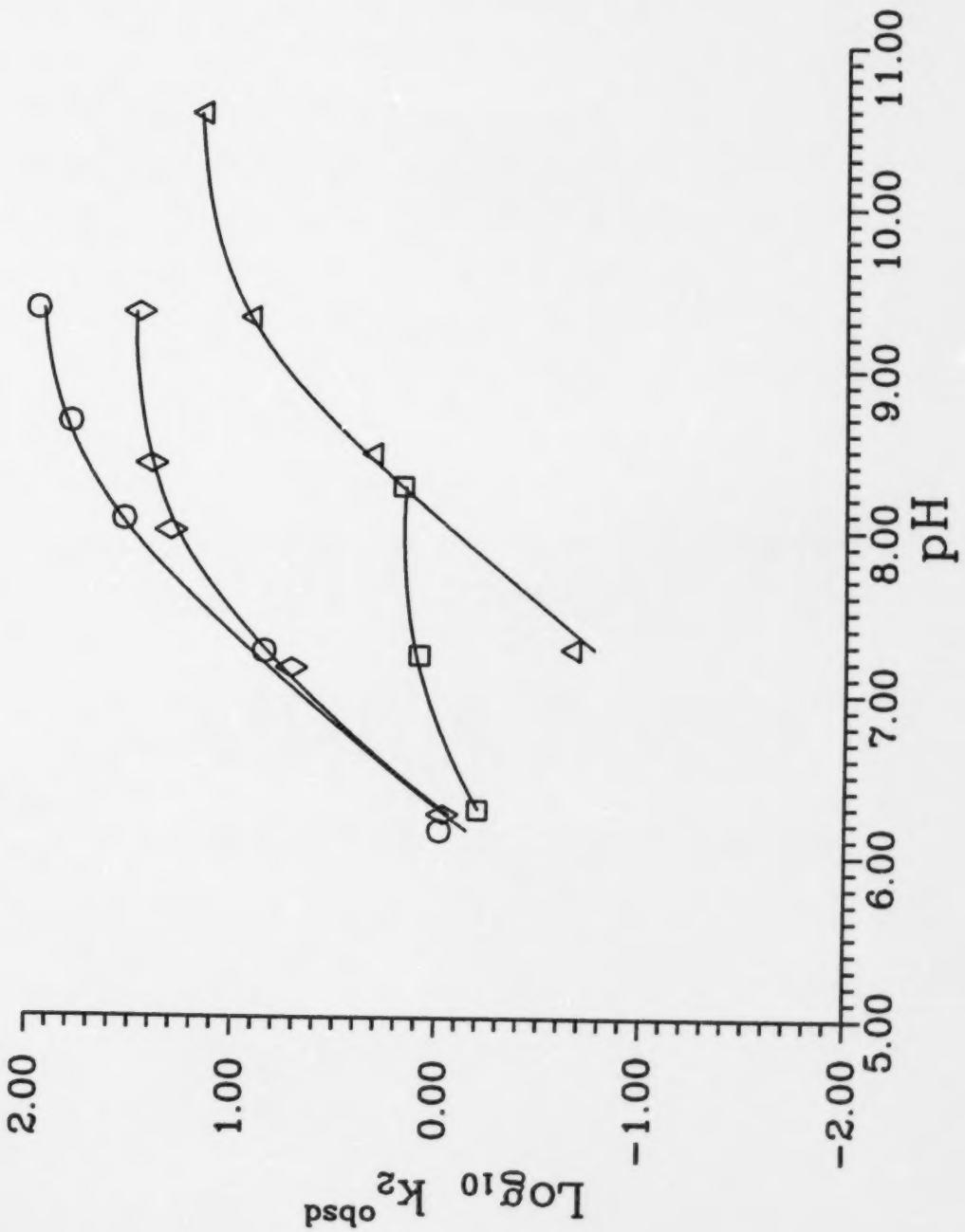

Table 1 : Kinetic Second Order Rate Constants (k_2) and pKa^{SH} Values for the Reactions of Thiols **10a-d, 11a-d** with **2** (T = 25 °C, μ = 1.0 (KCl))

Thiol	k_2 (M^{-1} s^{-1}) [a]	kinetic pKa^{SH} [b]	lit. pKa^{SH}	lit. pKa^{NH+}
10a	99.2 (100)[d,e]	8.37	8.35[c] (8.74)[d,f]	10.86[c]
10b	30.5	7.73	7.74[g]	10.89[g]
10c	1.47 (1.74)[d,i]	6.44	6.57[h] (6.78)[d,j]	9.55[h]
10d	15.5 (15.7)[d,l]	9.23 (9.59)[d,l]	9.26[k] (9.60)[d,j]	10.84[k]
11a	<0.05[m]	-	10.55[n]	
11b	0.36	-	8.03[g]	
11c	<0.02[m]	-	8.74[g]	
11d	nil	-	-	

a. Relative standard error (from standard deviation of fits of k_2^{obsd} vs $[H_3O^+]$) is less than 5%.

b. Standard error is less than 0.05 pK units as determined from fits of k_2^{obsd} vs $[H_3O^+]$.

c. Reference 62.

d. Determined in D_2O.

e. Value of k_2 calculated from k_2^{obsd} determined at pD = 9.08 and pKa^{SD} (D_2O) of 8.74.

f. Reference 37e.

g. Reference 63.

h. Reference 64.

i. Value of k_2 calculated from k_2^{obsd} determined at pD = 8.85 and pKa^{SD} (D_2O) of 6.78.

j. Calculated as $\Delta pKa\ (H \rightarrow D) = 0.26 + 0.012\ pKa^{SH}$. See reference 65.

k. Reference 66.

l. Computed from k_2^{obsd} values at pD 9.08, 9.75, 10.9 and fixed pKa^{SD} of 9.60.

m. An upper value estimated from detection limit due to slowness of reaction in presence of thiol relative to blank reaction. See Experimental.

n. Reference 67.

Thiols **11a-c** are far less reactive toward **2** than the aminothiols. This suggests a pendant amino (ammonium) functionality is necessary for activity. Also, the blocked S derivative of cysteamine, namely 2-ethylthioethyl amine (**11d**) does not react with **2** at all in the studied pH range of 7-9. Thus, the ammonium (amine) functionality is insufficient alone to generate activity. The k_2^{obsd} values for thiols **11a-c** were evaluated at the pH equivalent to the pKa^{SH}; the maximal k_2 values given in **Table 1** are twice the k_2^{obsd}. In fact, **11a** and **11c** exhibited no activity toward **2** under the conditions investigated so that the values given in the Table are upper limits.

Figure 2 : Plot of the log k_2^{obsd} vs pH profile for the reaction of **7b** with **2**; T = 25 °C, μ = 1.0 (KCl). Line through the data computed on the basis of NLLSQ fit to equation (**4**). Dashed line represents reaction of **7b** with **9a**; T = 37 °C, μ = 0.3 (KCl), from reference 50b.

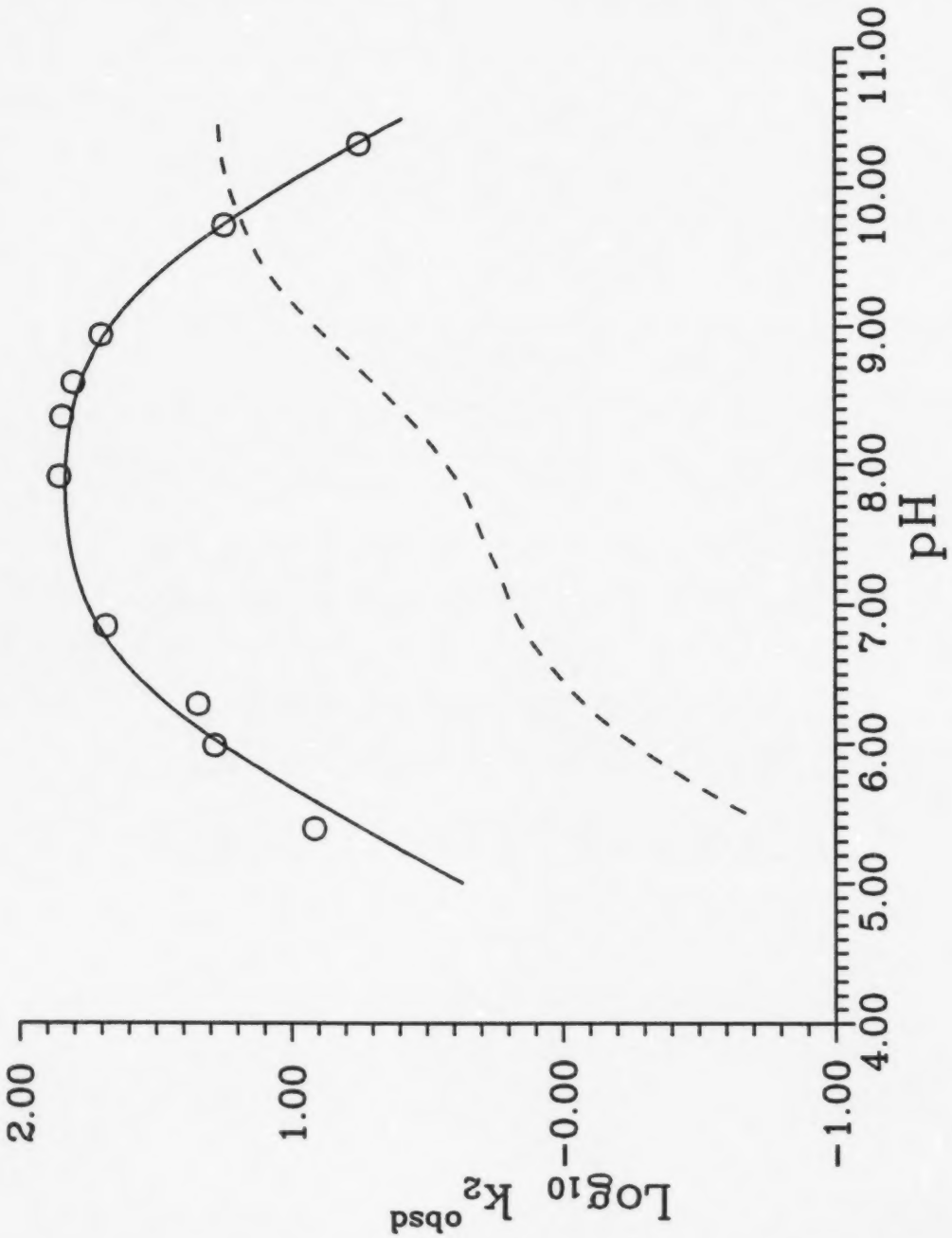

The log k_2^{obsd} vs pH profile for the reaction of **7b** with **2** is presented in **Figure 2**, along with a previously determined[50b] profile for the reaction of **7b** with p-nitrophenyl acetate (pNPA, **9a**). The striking aspect is the bell-shaped appearance of the former profile which indicates that the activity toward the amide depends upon the state of ionization of both the SH and Im-H^+ residues. The profile is clearly different from that presented for pNPA which suggests the mechanisms operative for the two cases are different. Previously,[50b] it has been shown that **7b** exists in solution as the four microscopic pH dependent forms given in **Scheme 17**.

Scheme 17

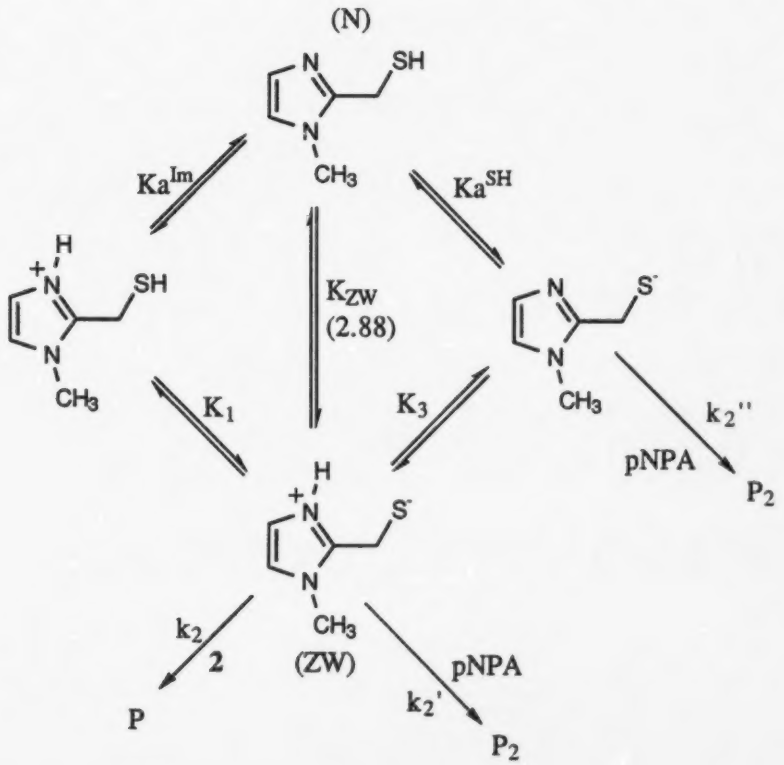

It has also been shown previously[50b] that both thiolate forms of **7b** are reactive toward pNPA, as shown in **Scheme 17** by rate constants k_2' and k_2''. For this process the kinetic expression given in equation **(3)** was reported[50b] (see Appendix 1 for derivation).

$$k_2^{obsd} = \frac{(k_2' \, Ka^{Im} \, K_{ZW}) \, [H_3O^+] + k_2'' \, Ka^{Im} \, Ka^{SH}}{[H_3O^+]^2 + (Ka^{Im} + Ka^{Im} \, K_{ZW}) \, [H_3O^+] + Ka^{Im} \, Ka^{SH}} \qquad (3)$$

In **Scheme 17** are defined the microscopic pKa values[68] and the value $K_{ZW} = K_1/Ka^{Im} = [ZW]/[N] = 2.88$ which indicates that at neutrality, ~ 70% of the formally neutral species in solution are zwitterionic. From the various species and constants shown in **Scheme 17** can be derived kinetic expression **(4)** (see Appendix 1) in which it is assumed that only the zwitterionic form of **7b** reacts with **2**.

$$k_2^{obsd} = \frac{(k_2 \, Ka^{Im} \, K_{ZW}) \, [H_3O^+]}{[H_3O^+]^2 + (Ka^{Im} + Ka^{Im} \, K_{ZW}) \, [H_3O^+] + Ka^{Im} \, Ka^{SH}} \qquad (4)$$

Non-linear least squares (NLLSQ) fitting of the k_2^{obsd} vs $[H_3O^+]$ data for attack of **7b** on **2** to equation **(4)** [69] yields the kinetic constants given in **Table 2** from which is calculated the line through the data in **Figure 2**. The fitting requires setting K_{ZW} to the value (2.88) determined previously by titration and UV-visible spectrophotometry,[68,50b] and generates the maximal rate constant, k_2, and the two kinetic microscopic dissociation constants, pKa^{Im} and pKa^{SH}. From these can be determined all of the microscopic pKa values, as well as the macroscopic ones[70] which are presented in **Table 2** along with the literature values.[68]

Table 2 : Kinetic Second Order Rate Constants (k_2) and pKa Values for Attack of **7b** on **2** (T = 25.0 °C, μ = 1.0 (KCl))[a]

Parameter	Kinetic Value	Literature Value[b]
k_2 (M^{-1} s^{-1})	99 ± 11	-
	(83 ± 7)[c]	-
pKa^{Im}	7.07 ± 0.10	6.96
pKa^{SH}	8.66 ± 0.10	8.67
pKa^{1}	6.48[d]	6.37
pKa^{2}	9.25[d]	9.26

a. Constants defined as in **Scheme 17**.

b. References 50b,68.

c. Determined in D_2O at pD = 7.95, the crest of the pD vs log k_2^{obsd} profile.

d.Macroscopic pKa values computed from K_{ZW} = 2.88 and equations given in reference 70.

b) D_2O Studies: Solvent kinetic isotope effects (skie) for the reactions of **7b**, **10a,c,d** with **2** were determined and the maximal k_2 values are presented in **Tables 1** and **2**. In the case of **10d**, the complete pD vs log k_2^{obsd} profile (see Appendix 1) was determined and fit to equation (**2**) by NLLSQ techniques to yield both k_2 and Ka^{SD}.

For **10a,c**, the pKa^{SD} values were computed according to the equation presented by Jencks and Salvesen.[65] This value and k_2^{obsd} at the pD equivalent to the pKa^{SD} of the aminothiol were used to calculate the k_2 presented in **Table 1**. For **7b**, the k_2 (D_2O) was determined at the crest of the bell-shaped profile of pL vs k_2^{obsd} shown in **Figure 2**. $(pK_1)_D$ (**Scheme 17**) was calculated by the method of Jencks and Salvesen,[65] while $(pKa^{Im})_D$ was assumed to increase by 0.4 units from the value in H_2O, as a consequence of the increased acidity of D_3O^+ relative to H_3O^+.[71] From these values the percentage of ZW can be estimated which, when normalized to 100% allows calculation of the $(k_2)_D$ given in **Table 2**.

D) Discussion

a) Mechanism: For the aminothiols **10a-d** and comparison species **11**, the available evidence for the reaction with **2** supports the process given in **Scheme 18**. The facts that require reconciliation are:

1. The aminothiols show maximum activity at pH values above the pKa^{SH} and below the pKa^{NH+}. This implies that the zwitterion, or far less likely, the neutral aminothiol is the kinetically competent form. Thiols **11a-c** which contain no pendant amino group show little or no activity. Also the S-blocked derivative CH_3CH_2–$SCH_2CH_2NH_2$ (**11d**) shows no activity indicating that the presence of an amino group alone is insufficient to bring about reaction with **2**.

2. The product of the reaction of **2** with the N-blocked derivative **10b** is thiolester **13b**. In the case of cysteamine (**10a**, R = H) the isolated product is the corresponding amide, **14a**. Given that the thiolate is required for activity (compare **10a**, **11d**), amide **14a** is likely formed by an intramolecular S→N acyl transfer from **13a**. Reaction of **2** with **7b** in CH_3CN generates the corresponding thiolester.

Scheme 18 predicts that the role of the ammonium group is to trap the initially produced tetrahedral intermediate (**12**) by intramolecular proton transfer to produce $\mathbf{12}^{N}$ or $\mathbf{12}^{\pm}$, the latter being poised for breakdown to the observed thiolester **13**. Such intramolecular trapping drives the reaction forward by preventing the expulsion of thiolate to reform **2** and ammonium thiolate. Probably, thiolate anion alone can attack **2**, but the reaction is reversible and unproductive unless the unstable tetrahedral intermediate can be trapped. In the scheme, we cannot tell whether the intramolecular trapping protonation proceeds to N (to yield $\mathbf{12}^{\pm}$) or O (to yield $\mathbf{12}^{N}$). Protonation of the latter to yield $\mathbf{12}^{N}$ would be thermodynamically preferred,[72] but at some point the proton must be transferred to N to give $\mathbf{12}^{\pm}$ which is almost certainly the form required for breakdown.

Scheme 18

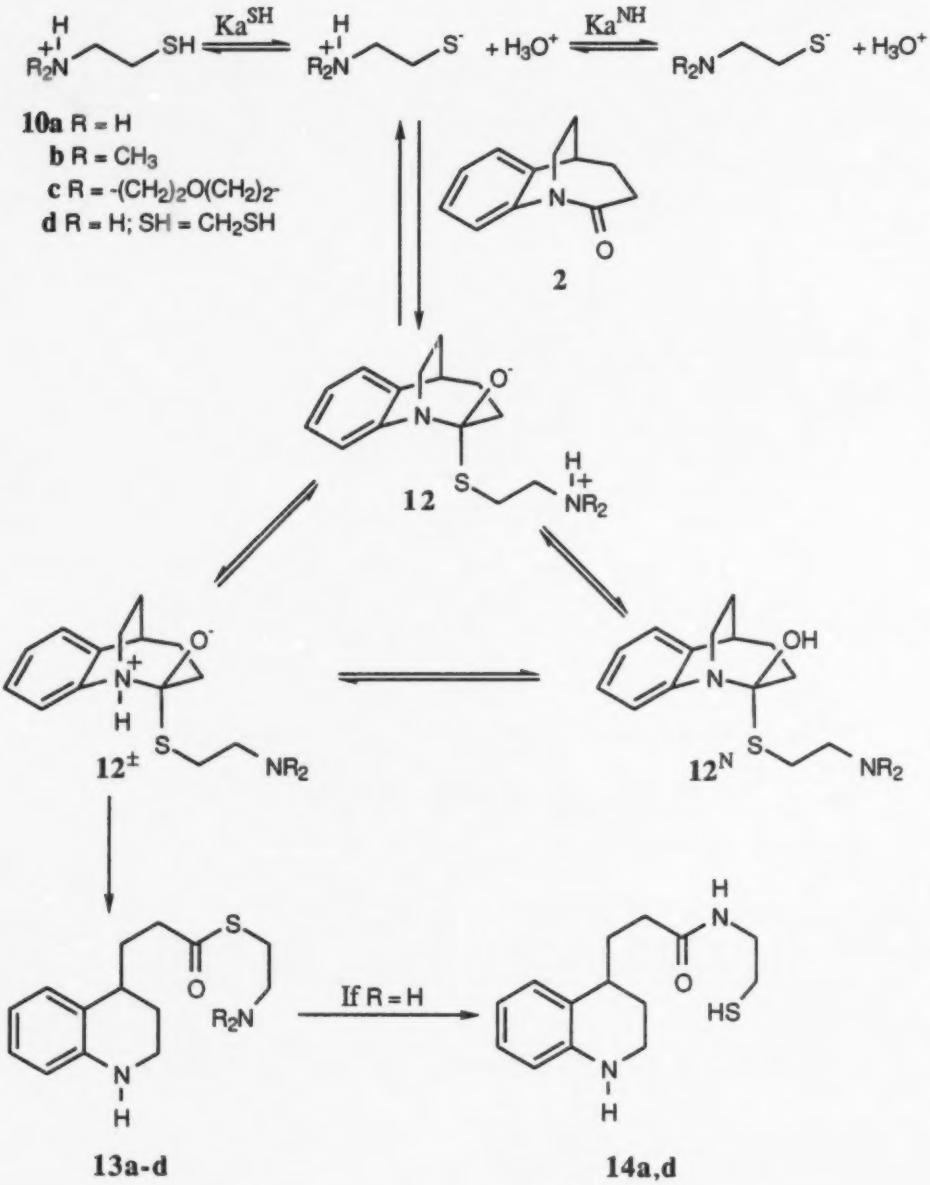

Several pieces of evidence support the above. First, Jencks and Barnett[73] have shown that the microscopic reverse reaction, intramolecular aminolysis of a thiolester, is subject to general base catalysis. This has been proposed to result from rate-limiting

deprotonation of the ammonium ion in the tetrahedral intermediate analogous to **12**$^{\pm}$, causing expulsion of the thiolate anion to be favoured. Second, although the alkyl thiols **11a-c** showed little activity alone toward **2**, the thiolysis reaction is subject to catalysis by such buffering agents as CAPS, CHES, and EPPS.[74] Thiolysis of **2** by **10c** is also subject to buffer catalysis by N-methylimidazole but we have been unable to detect buffer catalysis of the reaction of **2** with **7b** (*vide infra*). In the case of **10c**, catalysis by N-methylimidazole buffers is larger at pH 7.4 than at pH 8.4 by a factor of 3 signifying that the acidic form of the buffer is the catalytically active one.

3. The process given in **Scheme 18** requires for ammonium thiolates in which the pKa of SH and NH^+ both fall in the range of neutrality, that the k_2^{obsd} vs pH profile should be bell-shaped. It should reach a maximum at the pH where the zwitterionic form is optimized, and fall with further increases in pH that titrate the essential $N\text{-}H^+$. This is not observable for aminothiols **10a-d** because the pKa^{NH} is >10, and we cannot follow the reaction at larger pH values because the background hydrolysis is too fast. However, for **7b**, exactly the predicted situation occurs, the observed profile being presented in **Figure 2**. Also in that figure is the NLLSQ best fit line calculated on the basis of equation (3) which in turn is derived from the process shown in **Scheme 17** under the assumption that only the zwitterionic form is the active one.

b) Different Catalytic Requirements for Attack of Ammonium Thiolates on p-Nitrophenyl Acetate and Amide **2**: Also shown in **Figure 2** is the pH/rate profile for attack of **7b** on pNPA at T = 37 °C, μ = 0.3 (KCl).[50b] The plot fits the kinetic expression in equation (3) which is derived (see Appendix 1) for the process in **Scheme 17** wherein both the zwitterionic and anionic thiolate are active.[50b]

Hupe and Jencks[75] have shown that the attack of basic thiolates on substituted phenyl acetates shows a small dependence on thiol basicity (β_{NUC} = 0.27) and a break near ΔpKa = 0 to a slope of β_{NUC} = 0.84 as the pKa of the thiol is decreased and phenolate

expulsion becomes rate limiting. This is the expected situation for a two step process in which the rate determining step changes from attack (k_1) to uncatalyzed breakdown of the intermediate (k_2, **Scheme 19**). For the attack of **7b** on pNPA, the more basic thiolate form (the anionic one) is more active than the less basic zwitterionic one. Here, the rate determining step is simply S^- attack and p-nitrophenoxide expulsion is fast and requires no following general acid catalysis. The presence of the imidazole is passive, serving only to modify the SH pKa depending upon its existence as Im-H^+, or Im.

Scheme 19

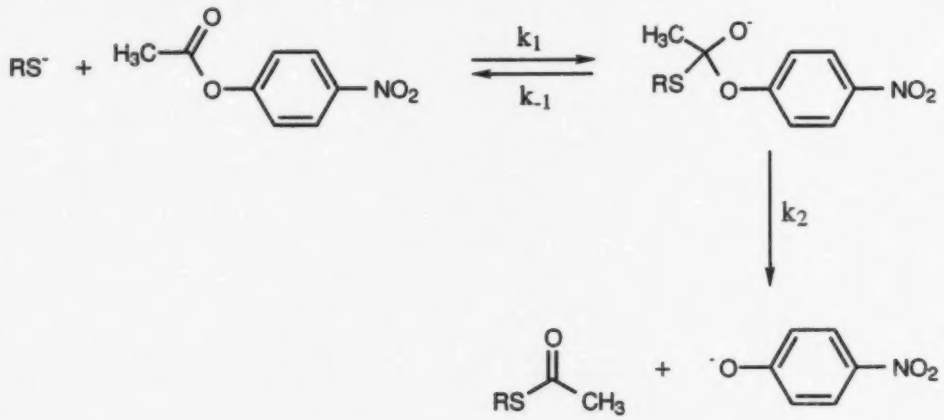

On the other hand, the bulk of the evidence we have presented for amino thiol attack on amide **2** suggests that thiolate attack is followed by N-H^+ trapping of the unstable intermediate (**12, Scheme 18**). Shown in **Figure 3** is a plot of the maximal k_2 values for attack of the various thiols (**7b, 10a-d**) on **2** vs their pKa^{SH} values in H_2O and D_2O.

Figure 3 : Plot of the maximal second order rate constant (k_2) for attack of amino thiols **7b**, **10a-d** on **2** vs the pKa^{SH} values in H_2O (open symbols) and D_2O (closed symbols); T = 25 °C, μ = 1.0 (KCl). (**7b**, circles; **10a** inverted triangles; **10b**, diamond; **10c**, squares; **10d**, triangles)

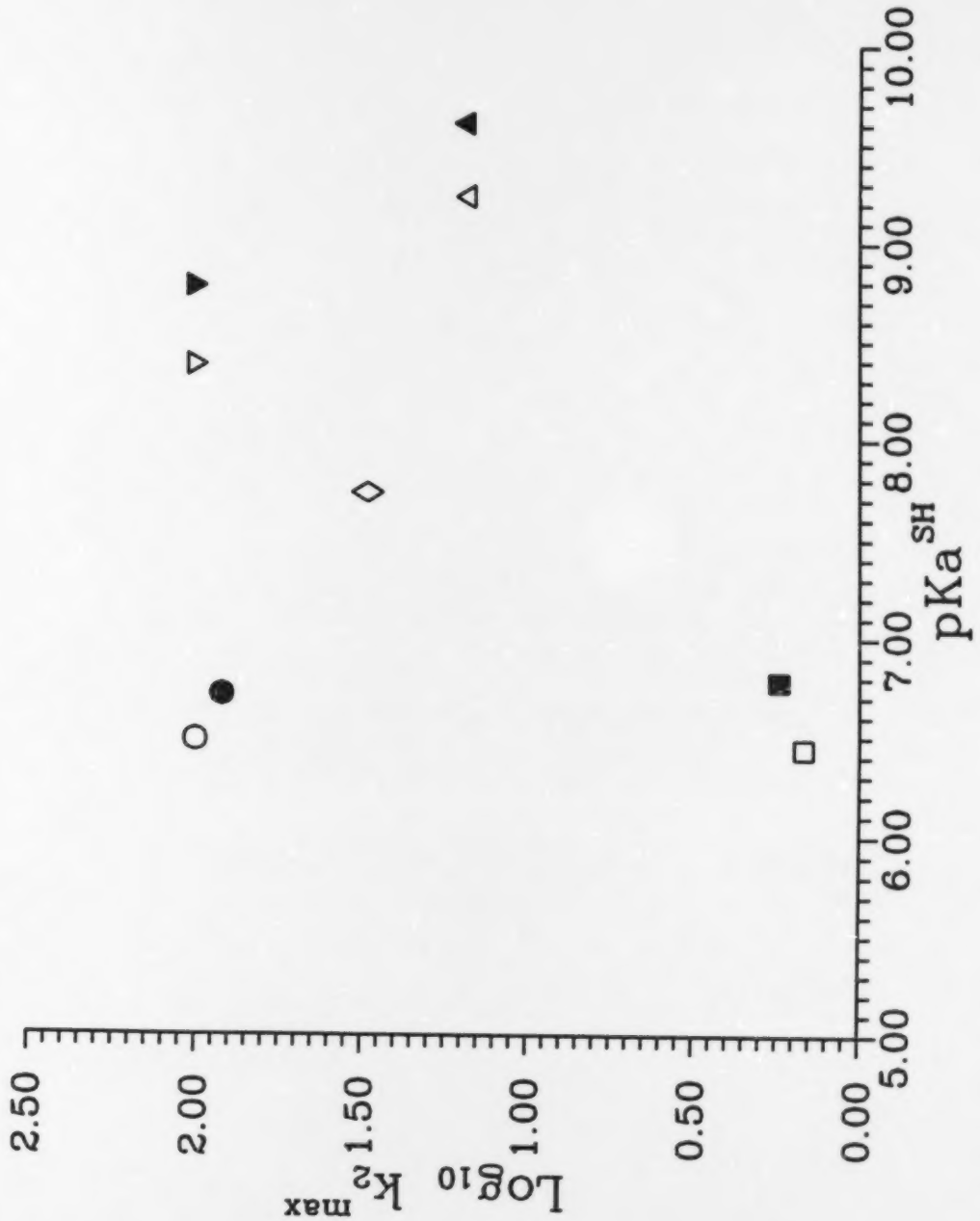

From **Figure 3** two main points are evident. First, the data cannot be reconciled by any simple Brønsted relationship, which implies that the rate constants are not simply dependent upon the thiolate basicity (nucleophilicity). Admittedly, **7b**, **10a-c**, and **10d** could be members of three sets of aminothiols, each adhering to its own Brønsted line. Second, although there is a small solvent isotope effect of ~ 0.4 units[65] on the pKa^{SH} values, the $(k_2)_{H/D}$ ratios are, in all cases, indistinguishable from unity (actually 1.0 ± 0.1). Since the preferred mechanism involves the essential steps of S^- attack and $N\text{-}H^+$ trapping, it might be supposed that amino thiols whose structure impedes the following trapping should be less reactive than expected on the basis of the thiol pKa. For example, the 3-aminopropane thiol derivative (**10d**) has the highest pKa^{SH} of the series, but contains a three carbon link with more rotational degrees of freedom that would have to be restricted in transferring the NH^+ proton to the tetrahedral intermediate. Consistent with this, its k_2 value is far lower than the value for cysteamine. In this, and related cases, the requisite proton transfer might be anticipated to become part of the rate-limiting step and therefore subject to a solvent kinetic isotope effect, but this is not observed. Although the observed values of unity are lower than what is customarily expected for a rate-limiting general catalyst mediated proton transfer,[76] they do not rule out our preferred mechanism. Analysis of solvent isotope effects is complex[76,77] and small values have been explained by invoking non-linear N---H—X geometries, asymmetric transition states, and solvation effects, any of which could be operative in the reactions in question. Furthermore, there has been a long-standing debate whether the proton transferred by a general catalyst would show a primary isotope effect of unity (solvation rule[78]) or a more normal effect with a potential maximum value based in the usual way on the vibrational frequency of the bond from H to catalyst.[77b,79] Kresge[80] and Jencks[81] have demonstrated very narrow isotope maxima for general-base-catalyzed reactions, and these were for trapping of an unstable intermediate by the catalyst with the actual proton transfer being rate limiting only for a narrow range around $\Delta pKa = 0$. Outside this range, when the proton transfer is

thermodynamically very uphill or downhill, the primary isotope effect would be small. This would be the expected case for uphill proton transfer from the not very acidic ammonium ions of **10a-d** to the anilino N of **12**, where the pKa of its corresponding ammonium is roughly 5-6.[72] Even if, as mentioned before, trapping involved a more thermodynamically neutral N-H^+---O transfer to generate $\mathbf{12}^N$, a large skie would not be observed if the proton transfer is fast, and some other step were rate limiting. Based on arguments presented above, $\mathbf{12}^{\pm}$ is probably the form required for breakdown to product so that if $\mathbf{12}^N$ were formed, the intramolecular catalyst could be envisioned as the base that assists in transferring the proton from the oxygen to the anilino N. In effect, the overall process is equivalent to attack of the zwitterion on **2** followed by proton transfer to yield $\mathbf{12}^{\pm}$.

A comparison of the attack of **7b** and **10c** is instructive since both have similar pKa values for the ionization of the SH to form the zwitterion (e.g., 6.48 (**Table 2**) and 6.44 (**Table 1**) respectively). However, as shown in **Figure 3**, the maximal k_2 values differ by nearly two orders of magnitude with the imidazole derivative having a k_2^{max} of ~ 100 M^{-1} s^{-1}. For the two tetrahedral intermediates (**12**, **Scheme 18**) produced from attack of the zwitterions of **10c** and **7b** on **2**, proton transfer from the morpholine-H^+ to the aniline is more thermodynamically uphill than is the case for **7b**. Furthermore, inspection of molecular models for **12** reveals that for the morpholino derivative the following proton transfer to create $\mathbf{12}^{\pm}$ may be sterically inhibited because the N-H^+ proton must be transferred perpendicular to the 6-membered morpholine ring. This introduces severe steric compression between that ring and the bicyclic anilide portion, as can be seen from representative structure **15**. However, for the corresponding tetrahedral intermediate generated from attack of **7b** (e.g. **16**), the N-H^+ proton is transferred in the plane of the imidazole ring, which avoids the steric buttressing apparent in **15**.

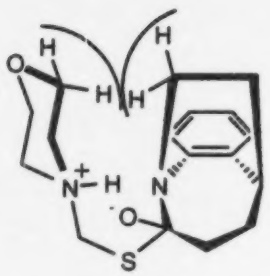

15

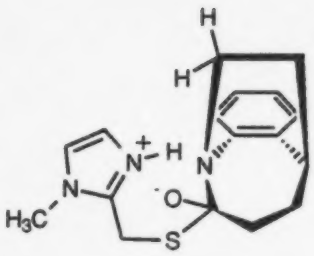

16

If proton transfer is hindered in the case of the morpholine derivative, the reaction may show evidence of catalysis by added general acids. Shown in **Figure 4** is a plot of the observed second order rate constant for attack of **10c** on **2** at pH 7.4 and 8.4 as a function of added N-methylimidazole (NMI). Also in the plot is shown the effect of [NMI] on the rate of attack of **7b** at pH 7.3 (see Appendix 1). Two things are apparent. First, with **7b**, added NMI, up to a concentration of 0.5 M, does not change k_2. This rules out any general acid catalytic effect on initial attack of RS^- and suggests that external buffers cannot compete with an already efficient following intramolecular catalysis. Second, in the case of **10c**, increasing [NMI] up to 2 M accelerates the reaction markedly. We had hoped that eventually, when the following proton transfer was no longer rate limiting, that saturation kinetics would be observed, and further increases in [NMI] would produce no acceleration. Unfortunately, we were limited to [NMI] $\leq$ 2 M which is apparently less than is required to change the rate limiting step. Finally, that the slope of the line at pH 8.4 is less than that at pH 7.4, indicates that the following catalysis is of a general acid nature. Overall, the process consistent with these observations is shown in **Scheme 20**.

Figure 4 : Plots of log k_2^{obsd} for attack of **7b** (squares, pH 7.3) and **10c** (open circles, pH 7.4; closed circles, pH 8.4) on **2** as a function of added N-methylimidazole (NMI); T = 25 °C, μ = 1.0 (KCl).

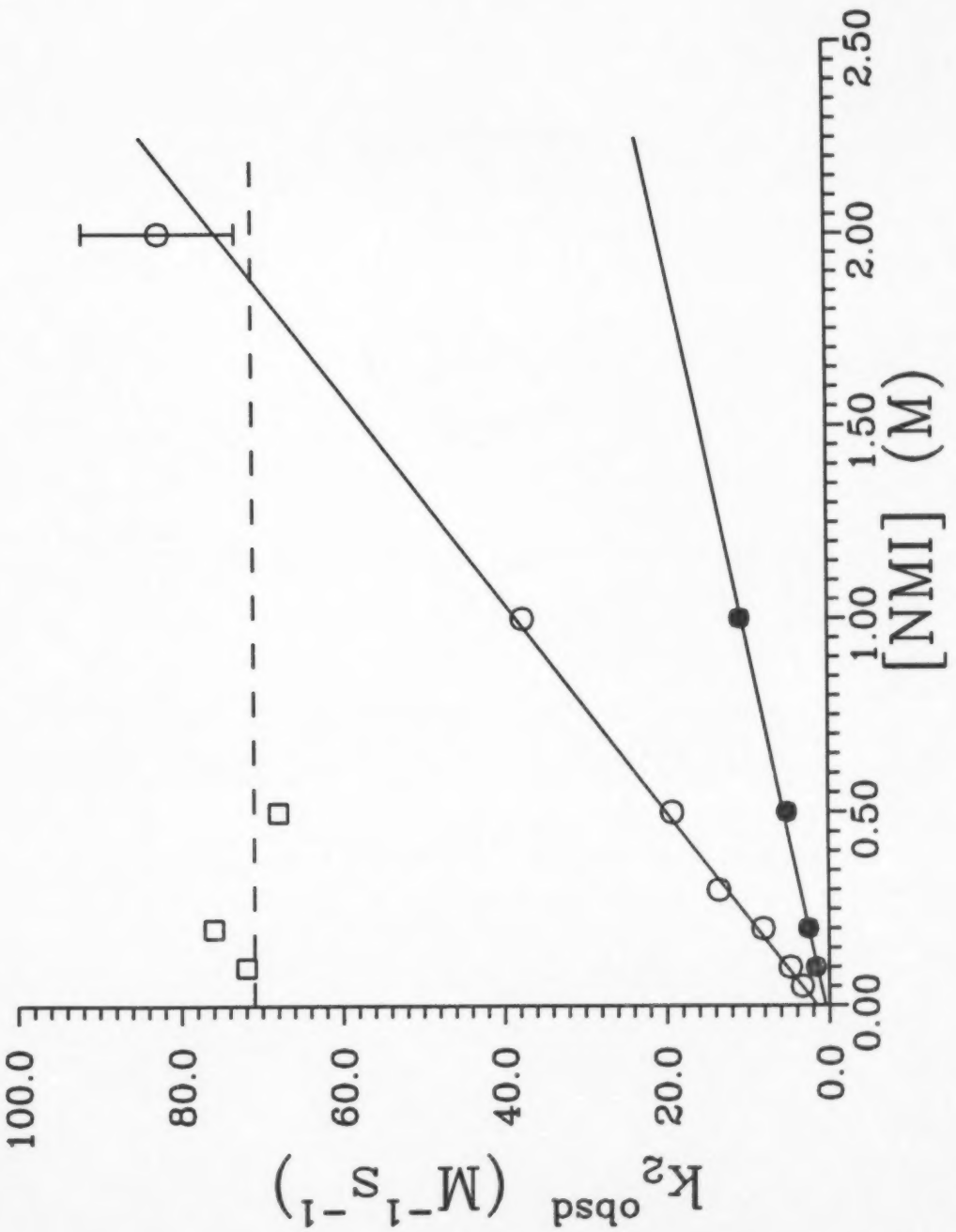

Scheme 20

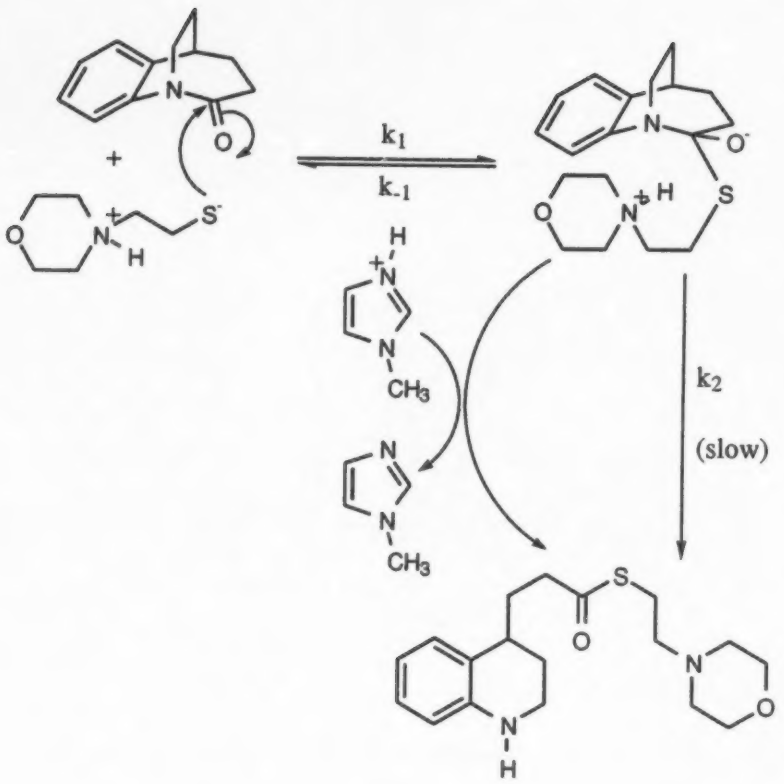

E) Conclusions and Relevance to the Cysteine Proteases

The general features of the model system of relevance to the acylation of papain by p-nitrophenyl esters or by anilides are the pH vs log k_2^{obsd} profiles shown in **Figure 2.** Based on the kinetics of acylation of the enzyme by a series of p-substituted phenyl esters of hippuric acid, a Hammett ρ of +1.2 was observed.[33b] Since the phenoxides are relatively good leaving groups, the positive ρ suggested that formation of the tetrahedral intermediate was rate limiting,[33b,33i] and expulsion of the leaving group was fast in all cases and required no general acid catalysis. However, when the leaving group becomes poorer, as in the case of the p-substituted anilides of hippuric acid, a Hammett ρ of -1.04 is obtained for the papain mediated hydrolyzes.[35c] This change in ρ is consistent with the breakdown of the intermediate being rate-limiting for anilide hydrolyses and suggests that general acid catalysis of these leaving groups is necessary.

The model system of acylation of **7b** by pNPA or **2** shows similar trends. For the ester, the plot in **Figure 2** shows that the thiolate nucleophilicity alone dictates the reaction rate, and that the state of ionization of the pendant imidazolium is only important insofar as it modifies pKa^{SH}. For attack on **2**, the available evidence suggests that both thiolate nucleophilicity and subsequent general acid trapping of the unstable tetrahedral intermediate are important in the two step process. The bell-shaped dependence of the rate constant on pH is readily accommodated in the high pH range by titration of the essential imidazolium $N\text{-}H^+$.

The data for acylation of **7b** or **10c** by **2** also reveal special features about the imidazole that make it ideally suited for enzymatic catalysis. The first, which is often cited, is that because its conjugate acid form has a pKa of 7, or close to it depending upon the environment, the imidazole is an ideal mediator of biological proton transfers because it can act as an acid or a base at physiological pH. Moreover, for proton transfer from a catalytically essential histidine imidazolium to the unstable tetrahedral intermediates produced from thiolate attack on amides where the substituents on the N is are aliphatic, the

proton transfer is thermodynamically favourable, and in the case of anilides is either thermodynamically neutral or only slightly uphill.

The second and less obvious feature of imidazole which makes it unusually suitable for general acid or base catalysis relative to an aliphatic amine (ammonium) has to do with the molecular shape. Because the proton transfer from imidazole occurs at the sp^2 N, and in the plane of the ring, there is minimal steric hindrance in transfer to sterically congested tetrahedral intermediates.

CHAPTER 2

A) Introduction

Previous work from this laboratory has shown[50] that acetic thiolesters **4**, **5**, and **6a,b** hydrolyze through a pathway in which the imidazole groups provide intramolecular general base assistance, as mentioned in the Introduction. Chapter 1 describes the formation of thiolesters **17** and **13b** from the reaction of thiolamines **7b** and **10b** with amide **2** as a model for the acylation of cysteine proteases with amides. Described in this chapter are the reactions of these thiolesters in water as a simple model for the deacylation of cysteine protease acyl-enzymes. The results from this study demonstrate (1) the hydrolysis of thiolesters **17** and **13b** in aqueous solution, (2) a plateau region of the pH/rate profile of this hydrolysis consistent with the involvement of the neutral form of the pendant amino group, and (3) the susceptibility of these thiolesters to an intramolecular aminolysis reaction resulting in re-closure of the amide.

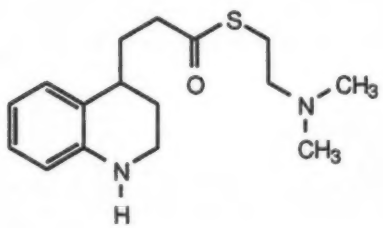

13b

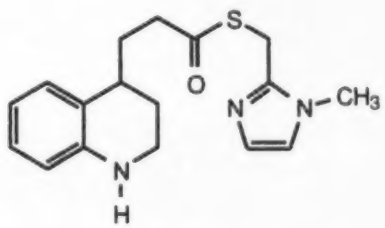

17

B) Experimental

a) General: Routine IR and ^1H NMR and mass spectra were recorded on a Nicolet 7199-FTIR spectrophotometer, a Bruker WP-80 (80 MHz) spectrometer, and an AEI MS-50 mass spectrometer respectively. High field NMR spectra (^1H and ^{13}C) were recorded on a Bruker AM-300 (300 MHz) machine.

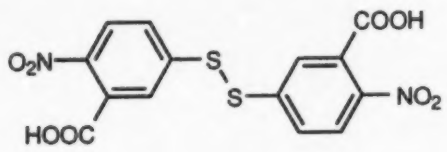

18

b) Materials: Buffers used were reagent grade (Aldrich, Sigma) and were used without further purification. 5,5'-Dithiobis(2-nitrobenzoic acid) (Ellman's reagent, DTNB, **18**) was used without further purification, as supplied by Sigma. Acetonitrile (BDH) was freshly distilled from P_2O_5 (BDH) under argon. Triethylamine (Fisher) was opened and used immediately without further purification. Dimethylaminoethanethiol hydrochloride (Aldrich) was used without further purification. 2-Mercaptomethyl-1-methylimidazole was prepared as previously described.[50b] Thiolesters **13b** and **17** were prepared as follows :

Thiolester **13b**: To a solution of 36 mg (0.25 mmol) of dimethylcysteamine hydrochloride (**10a**•HCl) with 1 equivalent of triethylamine in 1 mL (freshly distilled dry) acetonitrile was added by syringe (under argon, with stirring) a solution of 47 mg (0.25 mmol, 1 equivalent) of amide **2** in 5 mL acetonitrile. The solution was stirred under argon overnight at room temperature. After 20 hours, the solvent was reduced *in vacuo* to ~1 mL in volume, resulting in precipitation of white solid salts from the pale yellow supernatant. The precipitate was filtered off and the pale yellow solution applied to a 20 cm alumina preparative TLC plate. The plate was developed with 50/50 EtOAc/petroleum ether to give two major bands - one on the origin, the other with Rf 0.66. The latter band was scraped

off the glass plate, and the alumina extracted with 3 × 150 mL boiling 90/10 EtOAc/MeOH. This solvent was then removed under reduced pressure and the residue characterized (~48 mg, 66% yield). ^{1}H NMR (200 MHz, $CDCl_3$) δ 6.90 (d of t, 2H), 6.54 (d of t, 1H), 6.39 (d, 1H), 4.05 (br s, 1H), 3.22 (m, 2H), 2.96 (t, 2H), 2.71 (m, 1H), 2.59 (m, 2H), 2.44 (t, 2H), 2.22 (s, 6H), 2.06 - 1.65 (m, 4H); FTIR (cm^{-1}) 3400, 2940, 2857, 2820, 2775, 1687, 1607, 1500, 1460, 1315, 1041, 747; ^{13}C NMR (75 MHz, $CDCl_3$) δ 199.35 (4° C), 144.21 (4° C), 129.16 (3° C), 127.17 (3° C), 123.78 (4° C), 116.73 (3° C), 114.22 (3° C), 58.44 (2° C), 45.05 (1° C, 2 C's), 41.62 (2° C), 38.24 (2° C), 34.81 (3° C), 31.83 (2° C), 26.59 (2° C), 26.17 (2° C); mass spectrum, m/z (relative intensity) 292 (M^+, 0.73), 221 (2.86), 187 (16.47), 160 (2.54), 147 (1.28), 146 (1.93), 132 (23.60), 130 (17.94), 77 (2.96), 58 (100); Exact mass calculated for $C_{16}H_{24}N_2OS$: 292.16094. Found : 292.16049.

Thiolester 17: Prepared by an analogous procedure in 50 % yield; ^{1}H NMR (300 MHz, $CDCl_3$) δ 6.88 (m, 3H), 6.76 (s, 1H), 6.52 (d of t, 1H), 6.39 (d of d, 1H), 5.20 (br s, 1H), 3.58 (s, 2H), 3.57 (s, 3H), 3.20 (m, 2H), 2.70 (m, 1H), 2.61 (m, 2H), 2.06-1.65 (m, 4H); FTIR (cm^{-1}) 3400, 3280, 3015, 2927, 1690, 2606, 1498, 1316, 1282, 750; ^{13}C NMR (75 MHz, $CDCl_3$) δ 198.22 (4° C), 144.19 (4° C), 143.44 (4° C), 129.09 (3° C), 127.25 (3° C), 123.53 (4° C), 122.14 (3° C), 121.64 (3° C), 116.74 (3° C), 114.27 (3° C), 41.27 (2° C), 38.19 (2° C), 34.82 (3° C), 33.11 (1° C), 31.72 (2° C), 26.15 (2° C), 24.20 (2° C); mass spectrum, m/z (relative intensity) 316 ($M-H^+$, 1.00), 315 (M^+, 1.04), 220 (1.87), 187 (18.39), 183 (18.20), 144 (11.54), 132 (66.92), 130 (65.60), 127 (10.97), 96 (100), 91 (5.24), 77 (12.53); Exact mass calculated for $C_{17}H_{21}N_3OS$: 315.14053. Found : 315.13958.

c) Kinetics: Buffers (100 mM, μ = 1.0 (KCl)) were used to control the pH; KH_2PO_4 / K_2HPO_4 (phosphate, pH 6.21, 7.38), $NaHCO_3$ / Na_2CO_3 (carbonate, pH 9.25, 9.50, 10.10, 10.93), NaOH (pH 12.39). All buffers were prepared under Ar with

distilled water which was further purified and deoxygenated by passage through an Osmonics water purifier. A typical kinetic run was carried out as follows : Into a septum-sealed, argon-flushed UV cuvette was injected 3 mL of buffer solution. The cell was allowed to equilibrate to 25 °C (maintained by a Neslab RTE-110 water bath) in the cell holder of an Olis-17 UV-vis. spectrophotometer for about 10 minutes. Kinetic runs were initiated by injecting 20 μL of a 65 mM stock solution of thiolester in acetonitrile into the cell, inverting quickly a couple of times, and replacing the cell in the cell holder. The disappearance of **13b** was followed at 260 nm. At lower pH values, the disappearance of **17** was followed at 275 nm. However, at higher pH the tailing of the large UV absorbance of the 2-mercaptomethyl-1-methylimidazole (**7b**) produced during the reactions of **17** perturbed the first order decay curves, so the reactions were followed instead at 412 nm using 1 mm cells, and 10 equivalents of Ellman's reagent (DTNB). Control experiments were done to ensure Ellman's reagent did not react with **17** by itself, and that the rate of appearance of free thiol determined by this method corresponded to the rate of disappearance of **17** measured at 275 nm. All runs were performed in duplicate or triplicate, and pseudo-first order rate constants were determined from non-linear least squares analysis of the exponential curves. These k^{obsd} values were then plotted against the pH at which they were determined in order to construct pH rate profiles.

e) D_2O Studies: Stock solutions and a carbonate buffer solution (100 mM, μ = 1.0 (KCl), pD 10.6) were prepared under argon in the way described above, using 99.9 % D_2O which had been purged of O_2 by passing a stream of Ar through it for several hours. pD was determined by adding 0.4 units to the pH meter reading.[60]

e) Product Studies: Several reactions of **17** under standard kinetic conditions were performed for ~ 10 $t_{1/2}$. The solutions were combined, acidified to pH 4.75 and extracted with 3 × 10 mL $CHCl_3$. The chloroform layers were dried over $MgSO_4$ and stripped of

solvent. The remaining residue was characterized and shown to be identical to the corresponding carboxylic acid,[56] **19** (see **Scheme 23**): ^{1}H NMR (300 MHz, $CDCl_3$) δ 7.02 (br s, 2H), 7.00 (m, 2H), 6.62 (d of t, 1H), 6.49 (d of d, 1H), 3.29 (m, 2H), 2.80 (p, 1H), 2.46 (m, 2H), 2.11-1-73 (m, 4H). ^{13}C NMR (75 MHz, $CDCl_3$) δ 179.75 (4 °C), 129.91 (3° C), 127.19 (3° C), 124.03 (4° C), 116.97 (3° C), 114.42 (3° C), 38.28 (2° C), 34.81 (3° C), 31.61 (2° C), 31.05 (2° C), 26.18 (2° C). FTIR ($CHCl_3$, cm^{-1}) 3400-2200 (br), 2936, 1708, 1606, 1500, 1314, 750.

C) Results

Pseudo-first order rate constants for the disappearance of **13b** and **17** were determined at various pH levels (see Appendix 2) and used to construct the pH/rate profiles shown in **Figure 5**. Product studies (see Experimental) demonstrated that the final products of these reactions are the corresponding carboxylic acid and free thiols. The pH/rate profiles each display a plateau region at low pH, a sharp rise at intermediate pH, and an upper plateau at high pH. Consistent with these features is the acceleration of the rate of hydrolysis due to the involvement of the basic form of an intramolecular group such as the pendant amine (see **Scheme 21**). This pH/rate dependence is expressed in equation **(5)** (see Appendix 2 for derivation).

Scheme 21

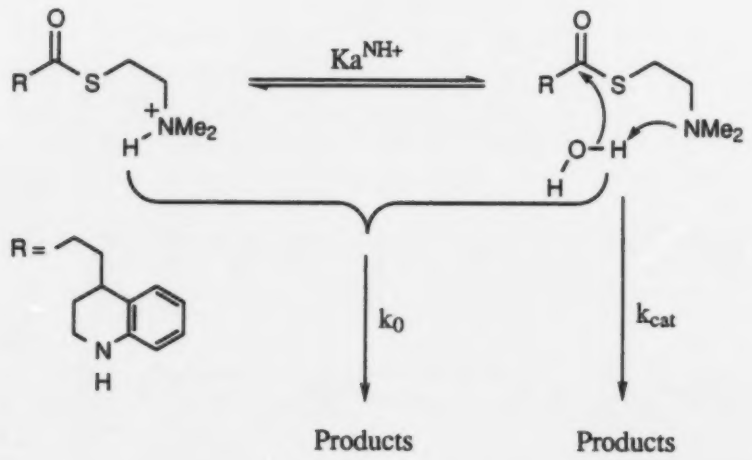

$$k^{obsd} = k_0 + k_{cat} / (1 + [H^+] / Ka^{NH+}) \qquad (5)$$

Figure 5 : Plot of the log k^{obsd} vs pH profile for the decomposition of thiolesters **13b** (circles) and **17** (squares); T = 25 °C, μ = 1.0 (KCl). Line through the data computed on the basis of NLLSQ fit to equation (**5**). Dashed line represents reaction of thiolester **6b**; T = 37 °C, μ = 0.3 (KCl), from reference 50b.

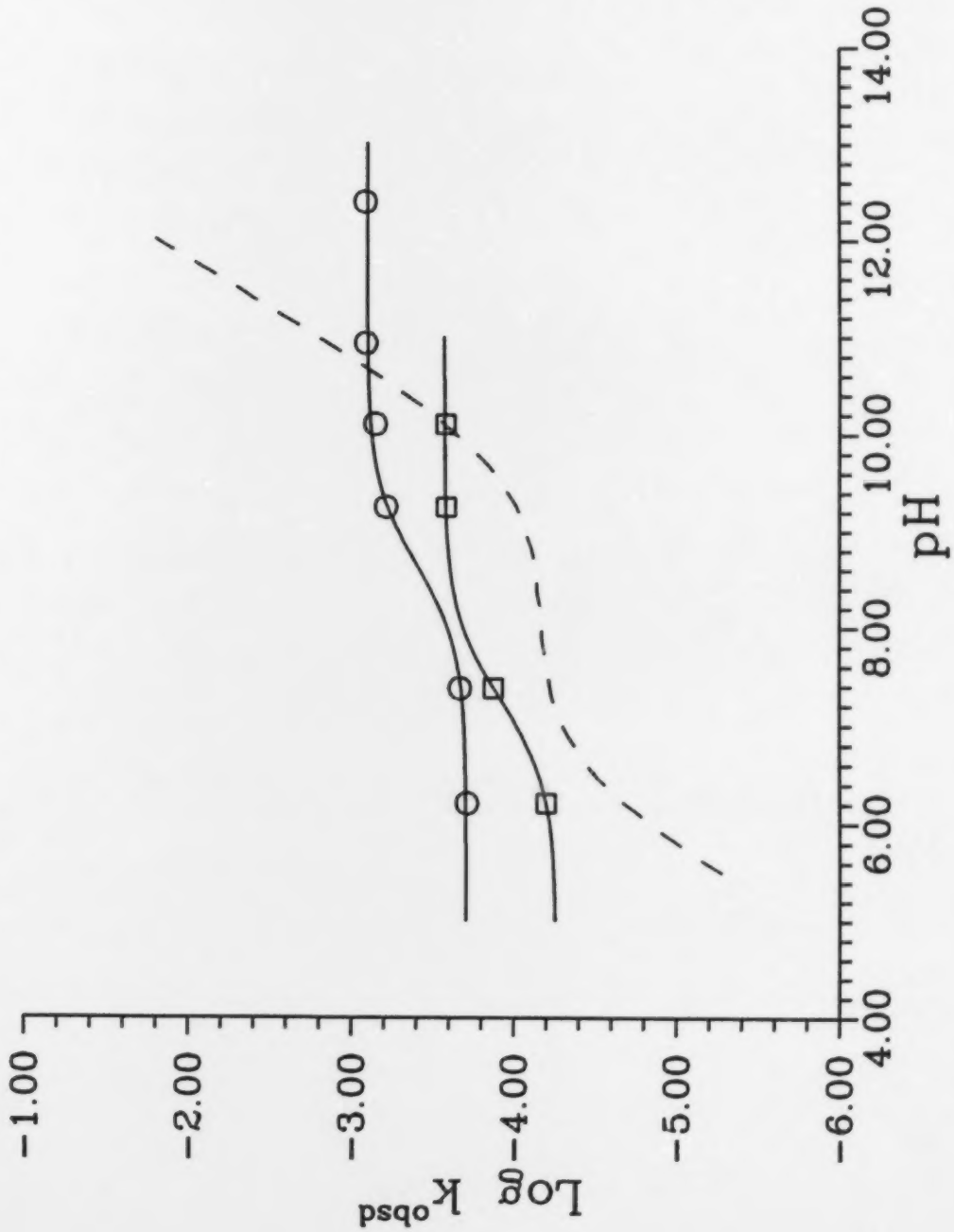

Control experiments indicated that the rate of reaction was independent of buffer concentration (50 - 100 mM) and first order in thiolester (0 - 0.4 mM). Values for the kinetic pKa^{NH+} of the pendant ammonium groups, the rate constant of the "background" reaction (k_0), and the upper limit rate constant (k_{cat}) were determined from the NLLSQ fit of the observed rate constants to equation (**5**) for the disappearance of thiolesters **13b** and **17**. These values are compiled in **Table 3**.

Table 3 : Kinetic pKa^{NH+} Values[a] and Pseudo-First Order Background and Upper Limit Rate Constants[a] for the Reactions of Thiolester **13b** and **17** in H_2O (T = 25 °C, μ = 1.0 (KCl))

Thiolester	$k_0 \times 10^4$ (s^{-1})	$k_{cat} \times 10^4$ (s^{-1})	Kinetic pKa^{NH+}
13b	1.96 ± 0.26	6.07 ± 0.23	8.95 ± 0.14[b]
17	0.55 ± 0.04	2.13 ± 0.10	7.61 ± 0.20

[a] Relative errors shown are based on the standard deviations from the NLLSQ fit of the observed kinetic data to equation (**5**).

[b] This kinetic value compares favourably to the thermodynamic pKa values measured for similar thiolesters. Reference 82 reports a pKa of 8.30 ± 0.05 for a series of dimethyl-aminoethanethiol esters.

D) Discussion

The hydrolysis of thiolesters **4**, **5**, and **6a,b** using methods analogous to those employed here has been reported.[50] The structures of these thiolesters are also very similar to those studied here, particularly the structures of **6b** and **17**. A detailed discussion of the previously determined[50] hydrolysis reaction mechanism would therefore be instructive, since the thiolesters studied herein may hydrolyze by a similar mechanism. Plots of log k^{obsd} vs pH for thiolesters **4**, **5**, and **6a,b** all displayed a broad plateau region between pH 6.5 and 9. On the basis of the significant skie (k_H / k_D = 1.9 - 2.3 at pH 8.0), the plateau region was accounted for on the basis of a general base delivery of H_2O by the pendant imidazole to the thiolester.

Since a dominant process for hydrolysis of previously reported[41a-c] thiolesters of similar structure is S→N acyl transfer, trapping experiments using Ellman's reagent (**18**) were performed[50b] in order to establish in more detail the nature of the species produced in solution during the hydrolysis of **6a,b**. Ellman's reagent was used to scavenge of any free thiolate as it was formed (from both hydrolytic and S→N acyl transfer pathways) to determine the observed pseudo-first order rate of production of thiolate, as shown for **6a** in **Scheme 22**. This sum of the rate constants for production of thiol from normal hydrolysis and S→N acyl transfer, k_{obsd} from **Scheme 22**, was found to increase with added Ellman's reagent until ~4 equivalents (~ 4 mM) of **18** were added. At this point, the observed rate constant did not increase with further additions of **18**, and the limiting value (~ 1.8×10^{-3} s^{-1} for **6a**) was taken as the rate constant for S→N acyl transfer. Since (from **Scheme 22**) $k_{-1} = k_2$ [**18**] at one-half the limiting value for k_1 (i.e. ~ 9×10^{-4} s^{-1}), k_{-1} can be calculated from a knowledge of k_2 (~ 10^5 $M^{-1}s^{-1}$)[50b] and [**18**] (1.5 mM), yielding a value of 1.5×10^2 s^{-1}. Thus it was shown that $K_{eq} = k_1/k_{-1} \equiv 1.2 \times 10^{-5}$, suggesting the equilibrium between S-acyl and N-acyl material lies far to the side of the S-acyl thiolester, and that little N-acyl transfer material is present. Similar calculations were performed for thiolester **6b** to yield a value of ~ 1×10^{-7} for K_{eq}. Through comparison with the known

pseudo-first order rate constant for H_2O attack on N-acetylimidazole, the rate at which the small amount of N-acyl material would have to react if it was to contribute significantly to the observed hydrolysis rate was shown to be unreasonably high, ruling out the possibility of an S→N acyl transfer pathway.

Scheme 22

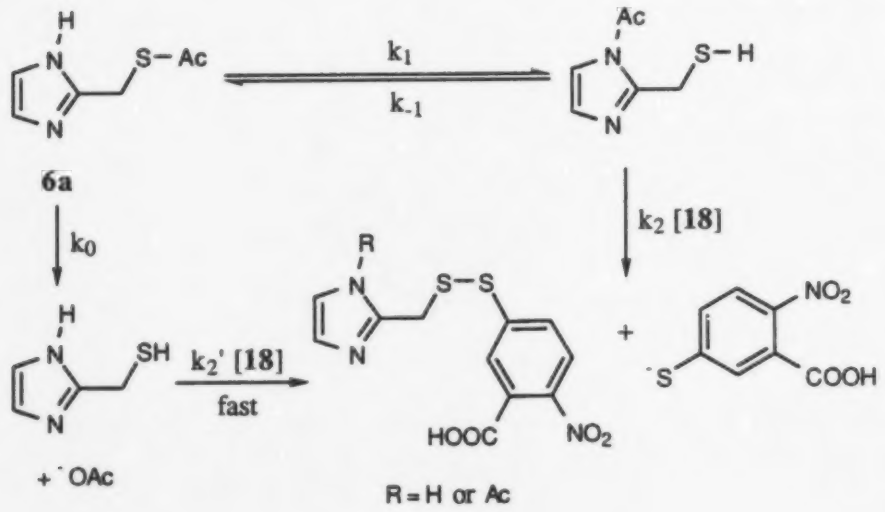

$$k_{obsd} = \frac{k_1 k_2 [18]}{k_{-1} + k_2 [18]} + k_0$$

Finally, the hydrolysis reactions of **5** and **6a** were not found[50b] to proceed appreciably faster than the hydrolysis of **6b**, giving further indication that the pendant imidazoles were participating in a manner dependent not on their nucleophilicity, but their basicity. For all of the above reasons, the hydrolysis of these thiolesters was concluded[50b] to proceed through a general base pathway. For the hydrolysis of **6b**, this pathway is shown in **Scheme 13**, and the pH/rate profile (T = 37 °C, μ = 0.3 (KCl)) is included in **Figure 5**.

As can be seen in **Figure 5**, thiolesters **6b**, **13b**, and **17** all display pH/rate profiles featuring a dependence on the neutralization of the pendant amino group, and a high pH plateau region suggestive of a common general base hydrolytic pathway. Generally, the mechanism of hydrolysis of thiolesters **13b** and **17** is expected to be identical to that outlined in the previous study (and depicted in **Scheme 13**) for thiolester **6b**. However, from **Figure 5** it is also obvious that the rate of reaction for the acetic thiolester **6b** is much slower than for anilino acid thiolesters **13b** and **17**. A comparison between the hydrolysis of **6b** and **17** is instructive, since both of these thiolesters have the same thiolimidazole leaving group, but very different carboxylic acid moieties. Both thiolesters show rises in their pH/rate profiles arising from the titration of imidazolium groups having kinetic pKa^{NH+} values ($pKa^{NH+} = 6.58 \pm 0.4$ for **6b**,[50b] $pKa^{NH+} = 7.61 \pm 0.20$ for **17** from **Table 3**) and plateau regions at higher pH. However, thiolester **6b** shows a sharp rise in its pH/rate profile at pH > 9 (accounted for[50b] by the attack of hydroxide) that thiolester **17** (up to pH 10.1) does not. This is perhaps not very surprising, since the steric bulk of the amino acid portion of **17** would make it more resistant to bimolecular nucleophilic attack than **6b**. But it is surprising that while the profile of **6b** shows a gradual decrease in rate at low pH values, the profile of **17** displays a distinct leveling at low pH to form a plateau. The presence of this lower plateau region, and the fact that the hydrolysis of **17** is more than 3 times faster than the hydrolysis of **6b** ($k_{cat} = (6.90 \pm 0.96) \times 10^{-5}$ s^{-1} at 37 °C for **6b**,[50b] $k_{cat} = (2.13 \pm 0.10) \times 10^{-4}$ s^{-1} at 25 °C for **17** from **Table 3**) indicate a kinetically significant background reaction is operative with the hydrolysis of **17** that is not present for **6b**.

Since the thiolimidazole portions of **6b** and **17** are identical, this background reaction must be related in some way to the difference in the structure of the carboxylic acid portion of these thiolesters. The most significant of these differences is the anilino nitrogen of **17**. Amide **2** was prepared through the intramolecular nucleophilic attack of this anilino nitrogen on the activated carbonyl.[56] Furthermore, the susceptibility of thiolesters to

nucleophilic attack by amines is well known[41] and has been demonstrated for thiolester **13a** in an intramolecular aminolysis reaction to form amide **14a** (see Chapter 1). It seems reasonable to propose that the rapid background reaction of thiolester **17** responsible for both the higher rate of hydrolysis than **6b** and the lower limit plateau of its pH/rate profile is the nucleophilic attack of the secondary anilino nitrogen of **17** on the thiolester carbonyl to displace thiolimidazole **7b** and re-form amide **2**, which may then undergo hydrolysis as shown in **Scheme 23**. If this is so, then from **Scheme 23** it is apparent that the observed rate of disappearance of thiolester is a composition of the rates of hydrolysis, ring opening and ring closure with subsequent hydrolysis. The fact that **17** and **13b** follow pH/rate profiles which display essentially the same features suggests that they hydrolyze to give carboxylic acid **19** (see Experimental) by similar mechanisms. It should be noted that the hydrolysis of other dimethylaminoethane thiolesters has been proposed[83] to proceed through a "loosening" of the carbonyl through the nucleophilic involvement of the pendant tertiary amine; however, the nature of this "loosening" was not rigorously described.[83]

Scheme 23

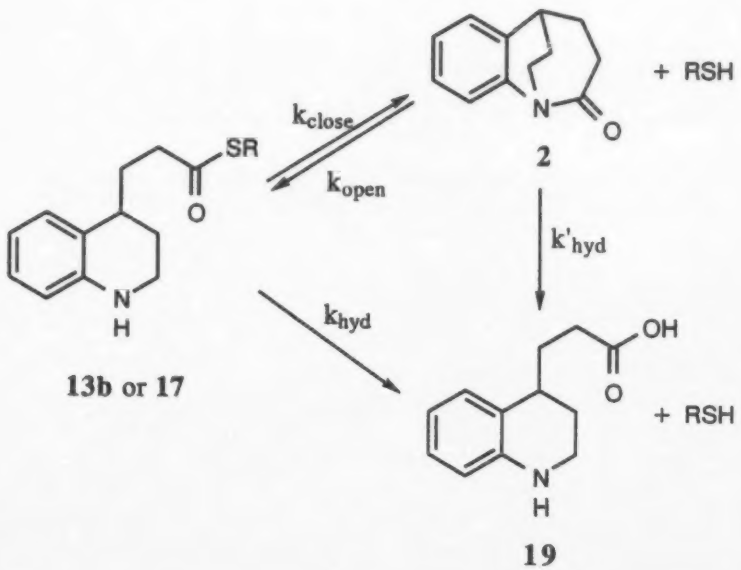

The fact that the observed rate of decomposition of thiolesters **13b** and **17** is significantly greater than that reported for thiolester **6b** suggests that it is possible that the open thiolesters are in equilibrium with the closed amide and thiolamines. Inspection of **Scheme 23** suggests that if that equilibrium exists, then the importance of the ring closure reaction of the thiolesters could be suppressed by the addition of excess thiolamine, as the equilibrium position would be shifted further to the side of open thiolester.

In order to test this hypothesis, the hydrolysis of **13b** at pH 10.10 was followed in solutions to which up to 23 equivalents of **10b** had been added. (The observation of the rate of disappearance of **17** in the presence of added **7b** was logistically impossible since the disappearance of **17** was followed by the appearance of **7b** - see Experimental). If thiolamine were able to assist in the breakdown of thiolester in a general acid or general base manner, the rate of disappearance of thiolester would be expected to *increase* with free thiol concentration. However, the observed rate of disappearance of thiolester *decreased* sharply with added equivalents of **10b**, (see Appendix 2) asymptotically approaching a limiting value as shown in **Figure 6**. At pH 10.10 the pseudo-first order rate constant for the hydrolysis of amide **2** (k'_{hyd} from **Scheme 23**) has previously been shown[56] to be ~ 6×10^{-3} s^{-1}. Under these conditions, any amide re-formed from thiolester **13b** would react with hydroxide at a rate greater than that observed for the disappearance of thiolester, so the rate determining step leading to decomposition of thiolester through this pathway would be represented by k_{close}. As the concentration of free thiol is increased, the equilibrium between the open and closed forms of the amide is shifted to the left, suppressing the intramolecular closure of the thiolester. The observed rate of disappearance of thiolester would therefore fall due to a transition from processes involving both k_{close} and k_{hyd} to the limiting case where it is represented by k_{hyd} alone. A limiting conditional value of k_{hyd} = 3.8×10^{-4} s^{-1} at pH 10.10 was thus determined from a fit of the rate suppression data to a standard exponential decay model.

Figure 6 : Plots of the rate of disappearance of thiolester **13b** as a function of added dimethylaminoethanethiol (**10b**); pH 10.10, T = 25 °C, μ = 1.0 (KCl). Solid line is the non-linear least squares fit of the data to an empirically chosen exponential decay model. Asymptotic $k_{hyd} = (3.8 \pm 0.7) \times 10^{-4}\ s^{-1}$.

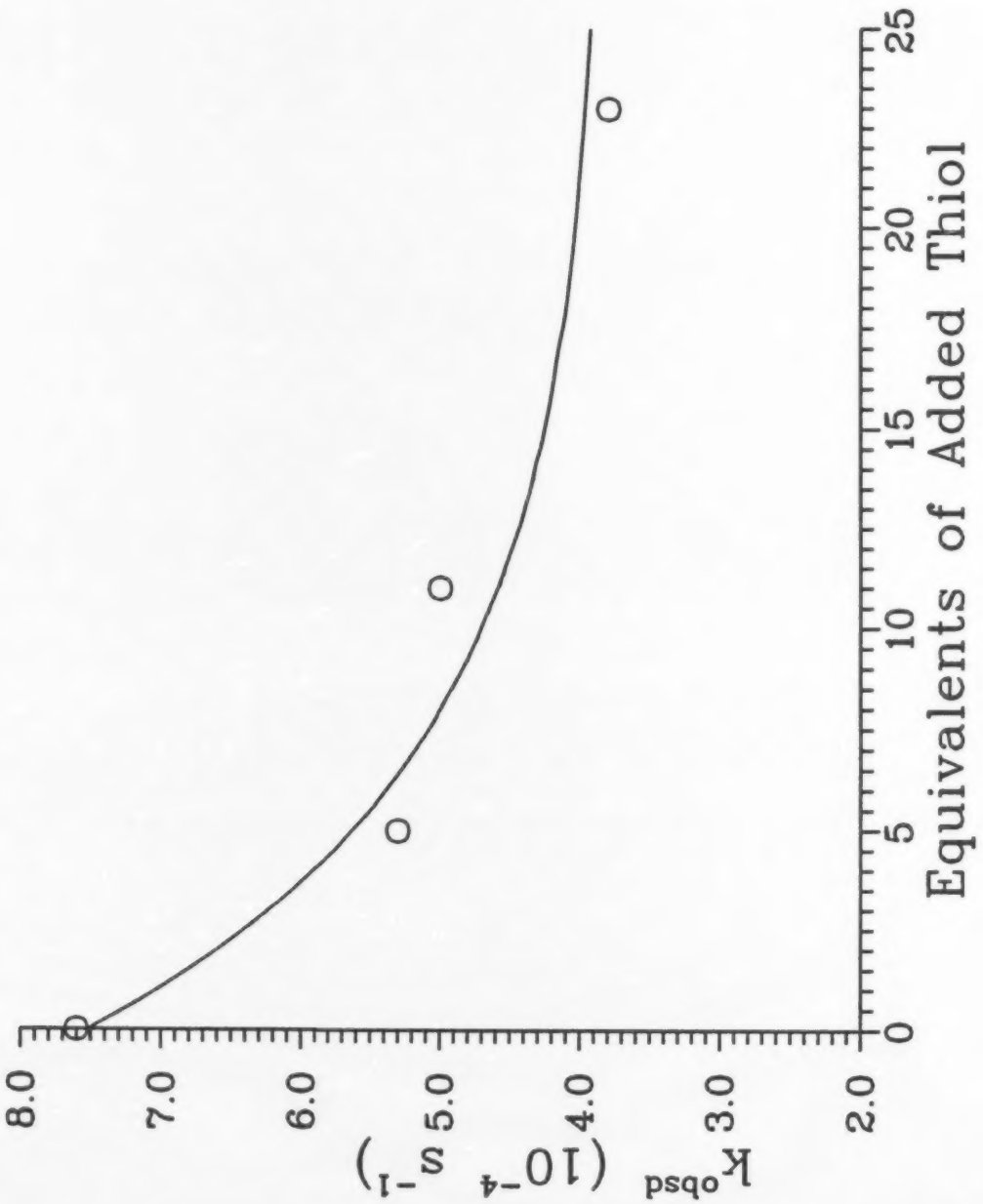

The value of $k_{hyd} = (3.8 \pm 0.7) \times 10^{-4}$ s^{-1} for thiolester **13b** at pH 10.10 is still an order of magnitude greater than the rate of intramolecular general base hydrolysis of thiolester **6b** at the same pH. This can be attributed partially to the greater basicity of the pendant dimethylamino group of **13b** ($pKa^{NH+} = 8.95 \pm 0.14$) over that of **6b** ($pKa^{NH+} = 6.58 \pm 0.4$), assuming a Brønsted relationship where the rate of amino catalyzed hydrolysis is dependent solely on the basicity of the amine involved.

When the rate suppression experiment was repeated for thiolester **13b** at pH 7.4, the observed rate of thiolester decomposition was not found to decrease as significantly. At this pH the added thiolamine exists predominantly as the ammonium thiol, and not as the zwitterionic thiolate which is required[54] to react with amide **2**. The amount of added thiolamine necessary in order to completely suppress the rate of amide formation through thiolester closure would therefore be over three times larger at pH 7.4 than at pH 10.10, as evidenced by the decreased effect.

It was shown in Chapter 1 that the rate of reaction of amide **2** with thiolamine is dependent on the concentration of only the zwitterionic form of the thiolamine, introducing a pH dependency of k_{open} upon the pKa^{SH} and pKa^{NH+} of the thiolamine. With the reasonable assumptions that the anilino nitrogen acts as a nucleophile in its neutral form and that the protonated ammonium thiolate is a better leaving group than the anionic amine thiolate, the observed rate of amide formation through thiolester closure can also be shown to be dependent on two pKa values. The intramolecular general base catalyzed hydrolysis of thiolesters **13b** and **17** is dependent on the neutral form of the pendant amino group, as shown[50b] for thiolester **6b** as well. Finally, the rate of the hydroxide catalyzed hydrolyses of amide **2** and thiolesters **13b** and **17** is also directly dependent on the pH of the kinetic solutions. The interpretation of the results of rate suppression experiments at other pH levels is extremely complex due to the pH dependence of the observed rate constants of each step of simplified **Scheme 23**, as is depicted in **Scheme 23a**. This complexity was deemed sufficient to discourage the determination of k_{hyd} at pH values other than 10.10.

Scheme 23a

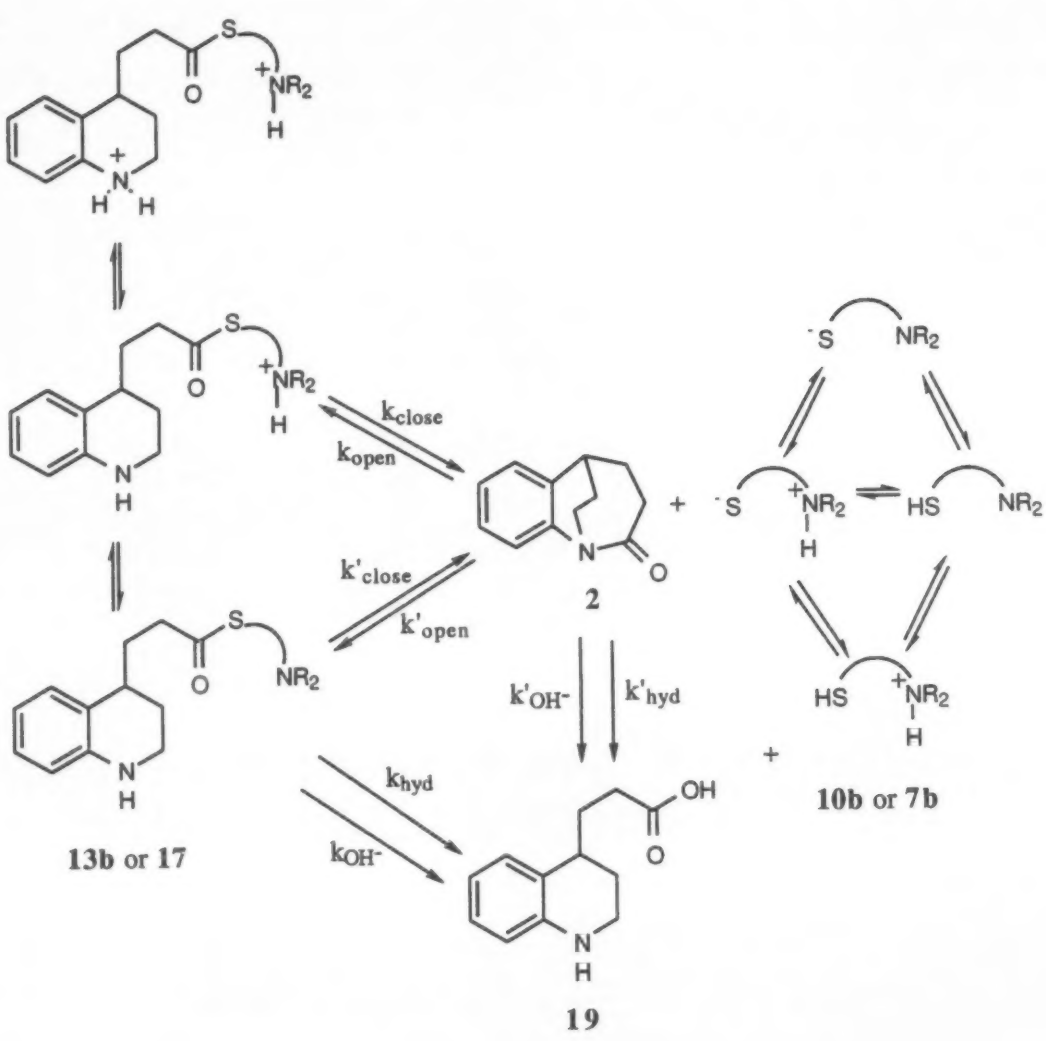

The skie for the disappearance of **13b** at pL 10.6 was found to be 0.9 ± 0.1 (see **Table 12S**, Appendix 2). However, because this disappearance has been shown to involve the closure, re-opening and hydrolysis of **13b**, an unambiguous interpretation of this result is not obvious.

E) Conclusions

Although the complex nature of the mechanism of the hydrolysis of thiolesters **13b** and **17** complicates a detailed interpretation of the results of this work, some conclusions may still be drawn:

1. Thiolesters **13b** and **17** do hydrolyze, with a pH/rate dependence indicative of the participation of the basic form of their pendant amino groups. The kinetics of their disappearance has been followed by UV spectrophotometry under conditions similar to those used previously[50b] for thiolester **6b**. The final products of the reactions of thiolesters **13b** and **17** in water were found to be the corresponding acid, **19**, and free thiols **10b** and **7b**, respectively (see Experimental). This regeneration of thiol in its active form, capable of reacting with amide **2** to form more thiolester (see Chapter 1), essentially constitutes a slow turnover step. The possible role of thiolamines as true turnover catalysts in the hydrolysis of amides is explored further in the following chapter.

2. The phenomenological similarity of this turnover to the deacylation of cysteine protease acyl-enzymes suggests the possibility that, like those studied earlier,[50b] this system could be taken as simple model for the deacylation step. The pendant amino groups of the thiolesters studied here appear to participate in a manner similar to those studied[50b] earlier in this research group (i.e. **5** and **6a,b**) in a role consistent with general base catalysis, such as is thought to occur in the deacylation step of the cysteine proteases.[33i,35a,36b,40]

3. The reaction of amide **2** with thiolamines is reversible, since thiolesters **13b** and **17** react intramolecularly to re-form amide **2**. Evidence for this "back reaction" was found in the suppression of the observed rate of disappearance of the thiolesters with the addition of free corresponding thiol to the reaction mixture. This observed reversibility suggests that if a thiolamine is a true turnover catalyst for the hydrolysis of an amide (k_{hyd} from **Scheme 24**) then, from the law of microscopic reversibility, it should also be able to catalyze the

formation of that amide from its constituent acid and amine (k_{form} from **Scheme 24**). The pursuit of this possibility is described in Chapter 3.

Scheme 24

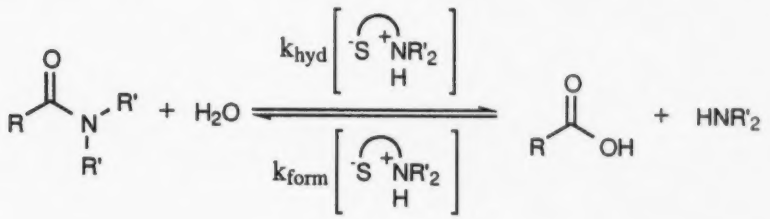

CHAPTER 3

A) Introduction

As discussed in Chapters 1 and 2, previous work in this laboratory[50b,54] has shown that the zwitterionic form of **7b** reacts rapidly with pNPA and with distorted anilide **2** to yield the corresponding thiolesters. These thiolesters then hydrolyze in aqueous solution with the assistance of the pendant imidazole to produce the respective carboxylic acids thereby regenerating the thiolate in its active form. Described in this chapter is the use of 2-mercaptomethyl-N-methylimidazole (**7b**) as a catalyst for the hydrolysis of the non-activated amides formamide, dimethylformamide (DMF), and N-formylmorpholine (NFM), amides **20a-c**. Also reported herein is the use of **7b** as a catalyst for the microscopic reverse reaction, namely the re-formation of **20c** from its constituent acid and amine in D_2O at near neutral pD values.[55]

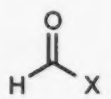

20a X = NH_2

b X = $N(CH_3)_2$

c X = N O

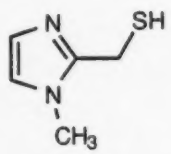

7b

B) Experimental

a) General: High field NMR spectra were recorded on a Bruker WH-200 (200 MHz) spectrometer.

b) Materials: Formamide (**20a**), N,N-dimethylformamide (DMF, **20b**), N-formylmorpholine (NFM, **20c**) and sodium 3-trimethylsilylpropane sulfonate (DSS) were commercially available (Aldrich) and were used without further purification. Phosphate buffer (KH_2PO_4 / K_2HPO_4) was reagent grade (Sigma) and used as supplied. Deuterium oxide (99.9 %, Aldrich) was purged of O_2 by passing a stream of Ar through it for several hours. 2-Mercaptomethyl-N-methylimidazole (**7b**) was prepared as reported.[50b]

c) Kinetics: In a typical kinetics experiment, a solution 100 mM (for DMF or formamide) or 200 mM (for NFM) in amide, 0 - 150 mM in **7b**, and 35 mM in sodium 3-trimethylsilylpropane sulfonate (DSS) as a ^1H NMR standard was prepared in 6 - 10 mL of D_2O at pD 7.8 - 8.0 (buffered by **7b** itself) with the ionic strength controlled by KCl such that μ=1.0. Aliquots of this solution 0.6 mL in volume were then transferred into each of 8 argon-purged 5 mm NMR tubes, which were flame-sealed. ^1H NMR spectroscopy was performed on two of the tubes for the "zero time" spectra. All of the tubes were then heated to 98 °C (refluxing water vapour) and at various times, duplicate tubes were removed and frozen. The ^1H NMR spectra of all eight tubes were subsequently recorded, and the ^1H NMR signals due to the formate-H (δ 8.5) and formyl-H (δ 8.0) were integrated relative to DSS to determine the progress of the hydrolysis reaction. The solution pD was measured before and after the reactions with a Radiometer VIT90 Titrator equipped with a GK2401C Combination Electrode and did not change by more than 0.05 units.

For formamide, the hydrolysis was sufficiently fast so that a non-linear least squares (NLLSQ) fit of the exponential decay of formamide concentration with time was possible, giving a pseudo-first order rate constant for each concentration of **7b**. However,

for the slower hydrolyses of DMF and NFM, the initial rates of the reactions were determined by measuring the linear least squares slope of the first 6 - 10 points on the plots of amide concentration versus time for the initial 3 - 10% of the reaction (up to 14 days required for the blank runs) and dividing by the initial amide concentration. This was necessary, as the catalyst appeared to begin to decompose after ~24 hours, to what is believed to be a product of oxidation, such as the corresponding disulfide.

d) Formation Reactions: The formation of NFM was similarly followed by ^{1}H NMR in D_2O, pD 8.0, μ = 1.0 (KCl), using solutions 0 or 100 mM in **7b**, or 200 mM in phosphate, and 200 or 400 mM in both formic acid and morpholine. The observed pseudo-first order rate constants were determined by dividing the initial slope (3 - 5 points, in duplicate) of the plot of [NFM] vs time by the initial concentration of formic acid (200 mM). For the blank reaction, 7 days were required to generate 5% reaction. The second order rate constant was determined by measuring the slope of the plot of the pseudo-first order rate constants of formation of NFM versus the concentration of **7b** (0 - 100 mM, with an additional point at 100 mM [**7b**] derived from half the rate observed at 400 mM formic acid).

e) Equilibrium Endpoint Determination: Two sealed NMR tubes 200 mM in each of formic acid, morpholine, and phosphate (pD 7.6, μ = 1.0 (KCl)) were heated for 20 days at 98 °C. Periodically, the tubes were removed from heating, cooled, and examined by ^{1}H NMR. Non-linear least squares analysis of the 8 data points of [NFM] vs time so collected gave a pseudo-first order rate constant for formation of NFM with phosphate catalysis. The hydrolysis of 200 mM NFM in the presence of 100 mM phosphate was monitored in an identical manner to give a pseudo-first order rate constant for the hydrolysis of NFM with phosphate catalysis. The final, asymptotic value of [NFM] from the exponential fit for both of these experiments was identical within experimental error.

C) Results and Discussion

a) Hydrolysis: The kinetics of the reactions of the various amides with **7b** were followed at pD 7.8 - 8.0 at 98 °C and μ = 1.0 (KCl). At these pD values, it has been shown that at 25 °C thiolimidazole **7b** exists predominantly as a zwitterion[50b] in an aqueous environment. Although the pKa values of both the thiol and imidazolium groups are anticipated to drop by about 0.6 units (according to pKa = ΔG° / (2.303 RT)) on the change in temperature from 25 to 98 °C, the zwitterionic form of thiolimidazole **7b** is still expected to be the dominant form in solution, and as such is in its most catalytically active form.[50b,54] ^{1}H NMR signals due to the formate-H (δ 8.5) and formyl-H (δ 8.0) of substituted formamides **3a-c** were integrated relative to sodium 3-trimethylsilylpropane-sulfonate (DSS) to determine the progress of the hydrolysis reaction. The pseudo-first order rate constants (see Appendix 3) were then plotted against catalyst concentration for each amide, giving the observed second order rate constants reported in **Table 4**. The observed pseudo-first order rate constants for the blank, or uncatalyzed reactions for these amides at the indicated pD are also given in **Table 4**. In no case is the blank reaction negligible. No accumulation of thiolester **21** was observed in any case, indicating its concentration must be in a steady state, and that **7b** is acting as a true turnover catalyst. There seems to be no justifiable reason to invoke a mechanism for this catalytic hydrolysis other than the one outlined in the preceding chapters, represented in **Scheme 25**.

b) Amide Formation: There is literature precedence (both theoretical[84] and experimental[84,85]) to suggest that at neutral pH, an amide can exist in equilibrium with its hydrolysis products. For most alkyl amine amides, the position of this equilibrium - the endpoint of the hydrolysis reaction - lies so far to the hydrolysis products that the existence of such an equilibrium becomes difficult to detect. However, Fersht has indirectly determined[85] an equilibrium constant[87] for the formation of N-formylmorpholine (see

equation (**10**)) of 1.35 M^{-1} (at pD 7.7), a value that indicates a significant amount of acid, amine and amide would be present at the endpoint under conditions employed herein.

Table 4 : Rate Constants for the Hydrolysis (and Formation) of Various Formamides Mediated by Thiolimidazole **7b** in D_2O Solution (T = 98 °C, μ = 1.0 (KCl))

Amide	$k_2^{obsd} \times 10^5$ ($M^{-1}s^{-1}$)[a]	$k_0^{obsd} \times 10^8$ (s^{-1})[f]
20a	13 ± 1[b]	36.4 ± 4.2[g]
20b	1.6 ± 0.2[c]	2.8 ± 0.6[g]
20c	1.1 ± 0.1[d]	3.0 ± 0.1[c]
(**20c** formation)	$((3.9 \pm 2.3) \times 10^{-2})$[e]	

[a] The second order rate constants are the slopes of the linear least squares fits of the plots of the pseudo-first order rate constants for hydrolysis vs four concentrations of **7b**, determined in duplicate. The reported errors are the standard deviations of the linear least squares treatment. Due to the inherent difficulties in obtaining kinetic rate constants from NMR data, real errors are estimated to be ± 10%.

[b] pD 7.8.

[c] pD 8.0.

[d] k_{cat} of **Scheme 26**, pD 8.0.

[e] k_{dehyd} of **Scheme 26** was determined as the slope of the linear least squares fit of the plot of k^{obsd} for the formation of NFM vs [**7b**] at 200 mM [formic acid] (pD 7.7, see **Table 18S**, Appendix 3).

[f] Observed pseudo-first order rate constants measured for hydrolysis with no added catalyst. Determined by the initial rate method over more than two weeks.

[g] pD 7.9.

Scheme 25

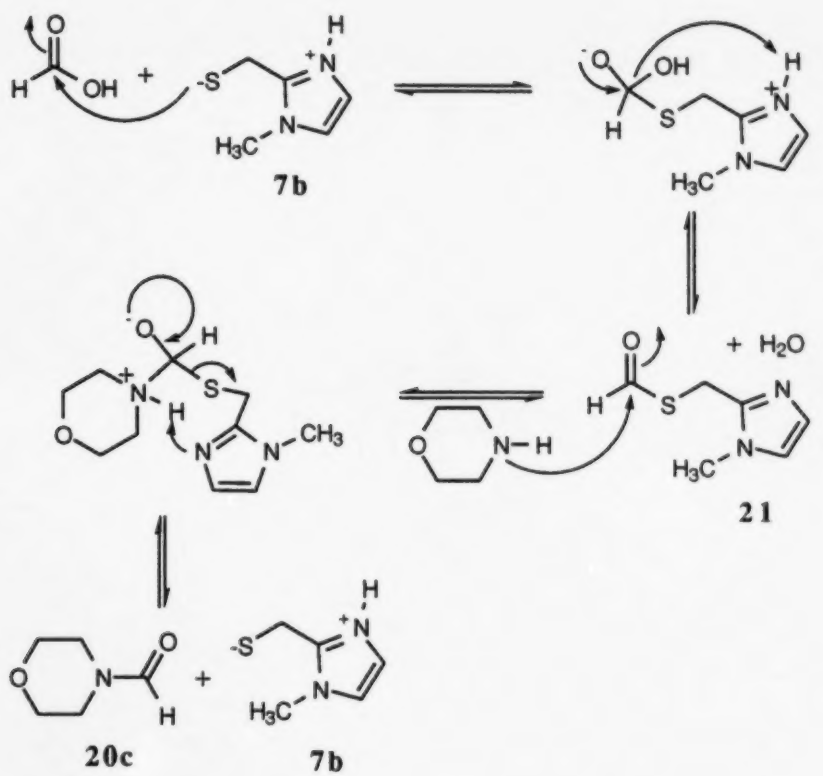

The formation of NFM from formic acid and morpholine was similarly followed by ^1H NMR in D_2O, using **7b** or phosphate as a buffer and catalyst.[88] From the observed pseudo-first order rate constants obtained using 0 - 100 mM **7b** as a catalyst (see Appendix 3), it was possible to determine a value for the observed second order rate constant for the catalyzed formation of NFM of $(3.9 \pm 2.3) \times 10^{-7}$ $M^{-1}s^{-1}$. Thiolester **21** (see **Scheme 25**) was not observed to accumulate in the formation of NFM under the conditions employed, indicating the concentration of thiolester was again in a steady state. When the concentrations of formic acid and morpholine were both doubled, the rate approximately doubled (within experimental error) but did not quadruple, indicating that only formic acid is involved in the rate determining step, which is probably the formation of the intermediate

thiolester. A catalytic cycle consistent with all of the observed data is shown in **Scheme 26**.

Scheme 26

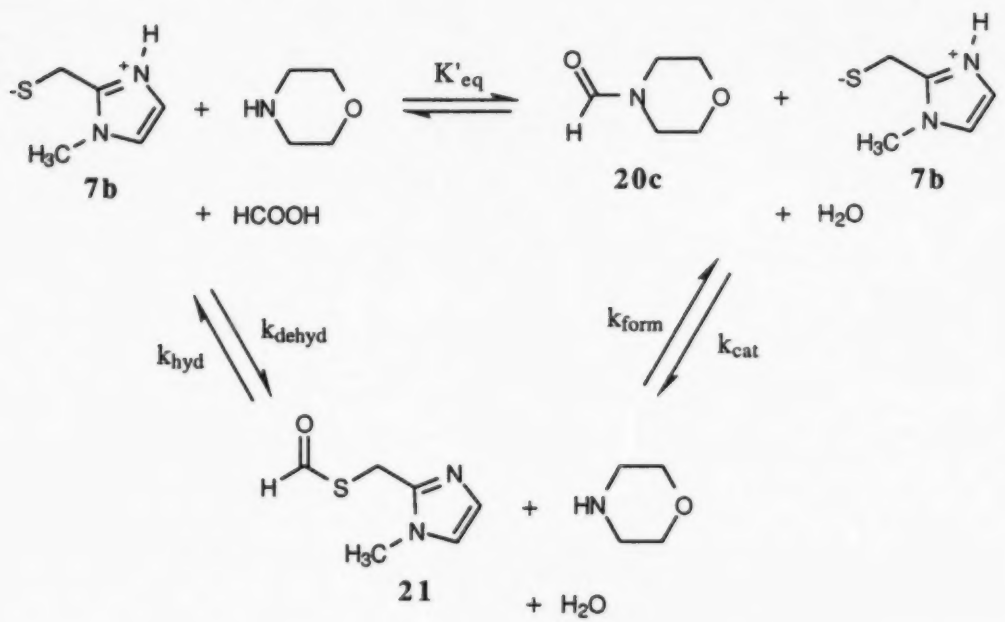

$$K'_{eq} = \frac{k_{dehyd}}{k_{hyd}} \times \frac{k_{form}}{k_{cat}} = \frac{k_{dehyd}}{k_{cat}} \times \frac{k_{form}}{k_{hyd}} = 1.2 \pm 0.2\ M^{-1}$$

The detailed mechanism for this thiolester formation is believed to be simply the microscopic reverse of the mechanism for thiolester hydrolysis described in Chapter 2. That is (see **Scheme 25**), attack of **7b** on formic acid is followed by intramolecular imidazolium general acid catalyzed breakdown of the tetrahedral intermediate with loss of a water molecule to give the formyl thiolester. Rapid intermolecular aminolysis of this thiolester through nucleophilic attack of the morpholine nitrogen then produces a second

tetrahedral intermediate, from which the imidazolium thiolate is ejected as an excellent leaving group, in its catalytically active form.

Using the steady state approximation, (steady state in [thiolester **21**]) the rate of amide formation can be expressed by equation (**6**) (see Appendix 3 for derivation). Since the rate of amide formation was found to be roughly independent[89] of morpholine concentration, the partitioning of the thiolester intermediate of **Scheme 26** must be such that, under the conditions of this study, $k_{form}[amine] > k_{hyd}$. As is shown in equation (**7**), the observed rate constant for amide formation is therefore k_{dehyd}.

$$V_f = \frac{k_{dehyd}\, k_{form}[acid][cat][amine]}{k_{form}[amine] + k_{hyd}} \qquad (6)$$

$$V_f = k_{dehyd}[acid][cat] \qquad (7)$$

Similarly, an expression for the rate of the hydrolysis reaction can be derived (see Appendix 3) and is given in equation (**8**). Under the conditions employed here, the concentration of amine present during the hydrolysis of amide is vanishingly small, so that equation (**8**) reduces to equation (**9**) and the observed rate constant of hydrolysis is k_{cat}.

$$V_r = \frac{k_{hyd}\, k_{cat}[amide][cat]}{k_{form}[amine] + k_{hyd}} \qquad (8)$$

$$V_r = k_{cat}[amide][cat] \qquad (9)$$

c) Equilibrium Endpoint: When the reactions of NFM hydrolysis and formation were allowed to proceed to "completion" as shown in **Figure 7**, (~6 half-lives, using phosphate as a catalyst[88]) the equilibrium position for the formation of NFM from formic acid and morpholine was determined by the endpoint of the reaction (33 mM NFM, 167 mM formic acid, 167 mM morpholine). This allowed calculation of K'_{eq}, as defined in

equation (**10**). Our so determined experimental value for K'_{eq} of 1.2 ± 0.2 M^{-1} compares favourably to the value of 1.35 M^{-1} reported by Fersht.[85,87]

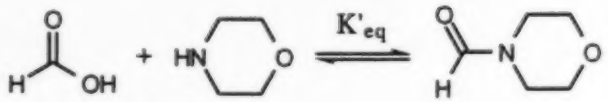

(**10**)

$$K'_{eq} = [NFM] / ([HCOOH]_{tot}\,[morpholine]_{tot})$$

Finally, since the thermodynamic cycle can be drawn as in **Scheme 26**, and the values of K'_{eq}, k_{cat} and k_{dehyd} can be measured (see **Table 4**, footnotes d and e for k_{cat} and k_{dehyd}, respectively) a value can be determined for the ratio of k_{hyd} to k_{form}. This partitioning ratio of the intermediate thiolester between acyl transfer to amine (k_{form} for the reaction with morpholine) and hydrolysis (k_{hyd} for the reaction with water) was determined to be $k_{hyd}/k_{form} = (3.0 \pm 1.5) \times 10^{-2}$ M. This ratio corresponds to the concentration of free morpholine that must be present for the thiolester intermediate to partition equally between hydrolysis and aminolysis.

Figure 7 : Establishment of equilibrium endpoint between NFM hydrolysis (circles, $k^{obsd} = (2.5 \pm 0.2) \times 10^{-6}\ s^{-1}$) and formation (squares, $k^{obsd} = (2.2 \pm 0.1) \times 10^{-6} s^{-1}$) in D_2O; T = 98 °C, pD 7.6, μ=1.0 (KCl), [phosphate] = 200 mM (see reference 88). Solid line is the non-linear least squares fit of the data. $[NFM]_{eq}$ was found to be 33 ± 2 mM.

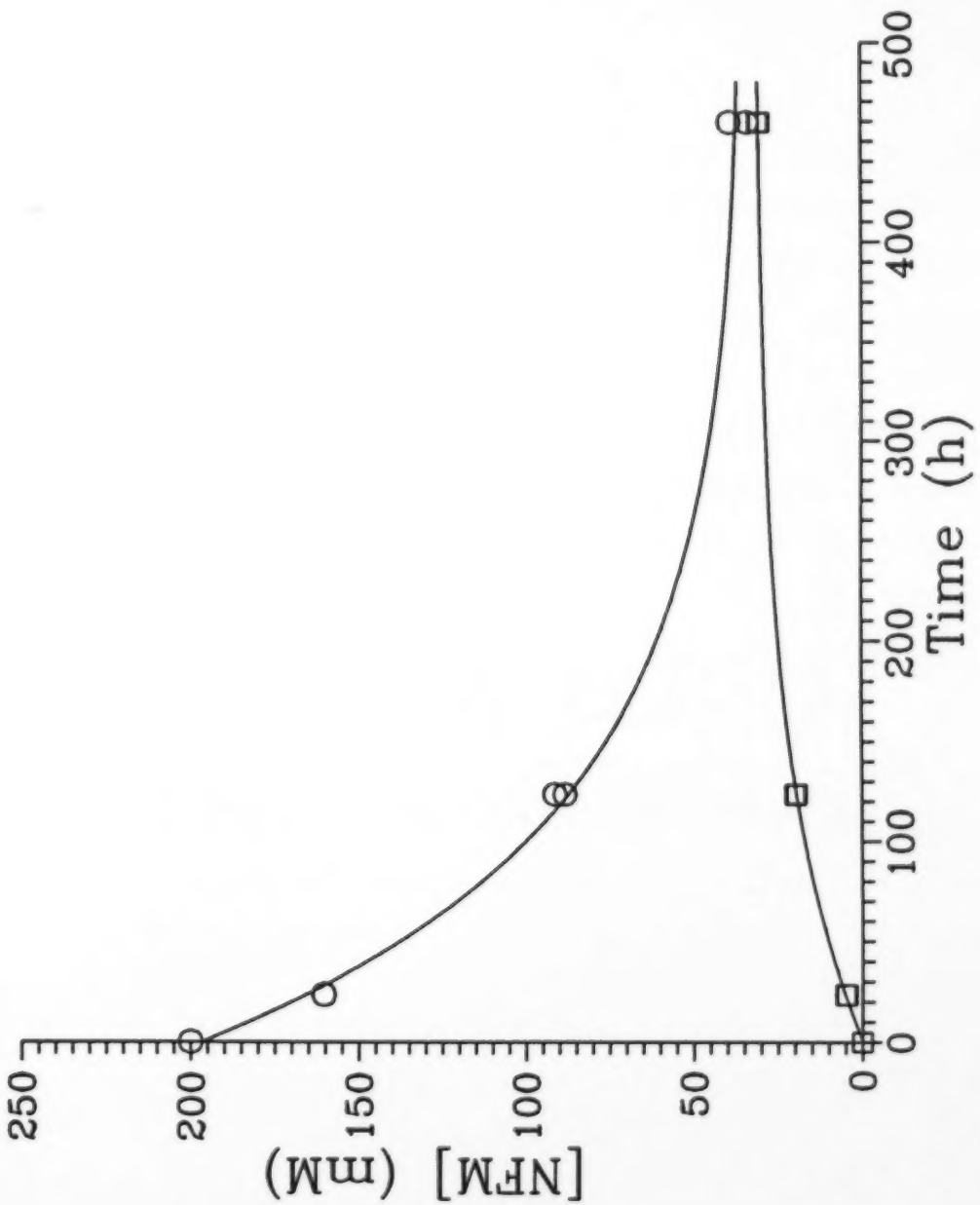

D) Conclusions

There are three salient points suggested by this work:

1. It has been clearly shown that under the reaction conditions employed, the hydrolysis of N-formylmorpholine is reversible (see equation (**10**)) and does not proceed to completion but rather to an equilibrium position. This equilibrium position has also been approached from the reverse direction in the formation of the amide from its constituent acid and amine. This modest catalysis by thiolimidazole **7b** of the formation of an unstrained amide from its constituent carboxylic acid and alkyl amine serves as a phenomenological model for peptide formation mediated by the cysteine proteases.

2. 2-Mercaptomethyl-N-methylimidazole (**7b**) is one of the first man-made non-metal-containing turnover catalysts of the hydrolysis of unactivated amides at physiological pH and elevated temperature. By way of comparison, the second order rate constants reported herein are within an order of magnitude of those reported recently by Chin[90] for a metal-containing catalyst. However, since this simple model system lacks the obvious catalytic advantages enjoyed by the cysteine proteases attributable to the correct orientation of the catalytically essential residues and the desolvation of substrates within the active site, this enzyme model is not as effective a catalyst as the enzyme itself.

3. There is an observable blank amide hydrolysis reaction (independent of catalyst) active in the neutral pH region that makes a non-negligible contribution to the rate of hydrolysis of amides mediated by poor catalysts. This reaction is slow, but several times faster than expected from extrapolation of the second order acid and base hydrolysis terms[91] to neutral pH, indicating the presence of an additional significant water term.[92]

CONCLUSION

A) Relevance to the Cysteine Proteases

a) Structure: The small bifunctional nucleophile, 2-mercaptomethyl-N-methylimidazole (**7b**) is incapable of modeling the binding site of an enzyme, but by incorporating an imidazole ring and an adjacent thiol group intramolecularly it approximately models the essential histidine and cysteine residues[32] in the active site of the cysteine proteases. At pH levels near neutrality, at which the enzymes display maximum activity, **7b** has previously been shown[50] to exist in aqueous solution predominantly as a zwitterion. In this way, **7b** may approximate the zwitterionic ion pair believed[37,38] to exist in the active site of the enzyme at physiological pH.

b) Acylation: During the enzyme mediated hydrolysis of amides, the acylation of the active site thiolate of many cysteine proteases appears to be rate limiting.[34] For typical amide substrates this acylation step follows a bell-shaped pH/rate profile consistent with the kinetic competence of a neutral or more probably the zwitterionic form of the active site, in which an essential sulfhydryl residue is ionized (pKa ~ 3.9 - 4.3) and an essential imidazole residue is protonated (pKa ~ 8.2 - 8.5).[35] The reaction of **7b** with strained amide **2** displays an analogous bell-shaped pH/rate profile, demonstrating herein the essentiality of the pendant imidazolium ion to the acylation of the thiolate. Furthermore, this model system has revealed (Chapter 1) the role of this imidazolium to be that of an intramolecular general acid trap of the unstable tetrahedral intermediate formed through the nucleophilic attack of thiolate on the anilide carbonyl. In the acylation of papain with amides,[35c] the poorness of the amino leaving group causes the breakdown of a similar tetrahedral intermediate to become rate limiting, and to require general acid assistance. The model system presented here provides chemical precedence for the involvement of the histidine imidazolium as this general acid trap, as shown in the Introduction in **Scheme 7**.

c) Deacylation: The deacylation step of the cysteine proteases is thought to proceed through general base assisted hydrolysis of the acyl-enzyme thiolester. The observed apparent pKa[31a,35a] and skie values[35a,39] for this process are consistent with the histidine imidazole acting as the general base.[33i,40] Earlier model systems of pendant amino thiolester hydrolysis (wherein the amino and thiol groups were retained intramolecularly[50]) clearly demonstrated the general base role of the pendant amino group. As shown in Chapter 2, the hydrolysis of thiolesters **13b** and **17** is believed to proceed through a similar involvement of the amino groups but there are structural components to these that introduce significant competing processes. Although the clarity of a mechanism showing the nature of the general base process was clouded by intramolecular aminolysis of these thiolesters, a general base role is consistent with the evidence herein. On the basis of this model study and those conducted earlier in this laboratory,[50] the deacylation step of the cysteine proteases involves general base catalysis and requires no S→N acyl transfer. This deacylation mechanism is also represented in **Scheme 7** in the introduction.

d) Catalysis: The system examined herein is able to model both the acylation and deacylation of the cysteine proteases by amides through its intramolecular incorporation of a thiolate and imidazolium group. As the zwitterionic thiolate **7b** attacks the amidic carbonyl of **2**, the adjacent imidazolium is able to act as a general acid trap of the tetrahedral intermediate, preventing the expulsion of the thiolate and taking the intermediate on to thiolester formation (see **Scheme 18** of Chapter 1). This thiolester (**17**) is generated with a pendant imidazole that can now act as a general base in the assistance of the hydrolysis of the thiolester. A product of this hydrolysis is the imidazolium thiolate **7b**, regenerated in its active form. As mentioned in the Introduction, the appeal of the application of these model mechanisms to cysteine protease catalyzed amide hydrolysis is found in the elegance with which each successive step is accomplished. Each step generates as a product of that step the form of the catalyst/enzyme required to mediate the next transformation.

B) Future Considerations

Although the reaction of thiolamines with a strained amide has served as a good model for the acylation and deacylation steps of the cysteine proteases, the portion of this work that holds the most promise for intriguing future studies is the catalytic hydrolysis and formation of unstrained amides, discussed in Chapter 3. Generally speaking, a catalyst of amide hydrolysis must contain both a nucleophile and an intramolecular proton source (general acid trap). Evidence for this is found in the mechanism of amide hydrolysis followed by all three classes of proteolytic enzymes and several model systems discussed in the Introduction. Catalysis of the microscopic reverse reaction - the formation of an amide from its constituent carboxylic acid and amine - must hold the same requirements.

In this study, the best catalyst of both of these processes was found to be thiolamine **7b**. As a zwitterion in solution, it contains a nucleophilic thiolate and an acidic imidazolium in close proximity to each other. The hydrolysis of strained amide **2** and unstrained amides **20a-c** as well as the formation of amide **20c** were accelerated by the presence of **7b**. While these results are encouraging for further investigation, the oxidative and thermal instability of the model compound have been noted as an obstacle to more widespread use of **7b** as a general catalyst for these transformations.

One possibility for future stabilization of this thiol which is currently being investigated in this laboratory is the covalent attachment of **7b** to a solid support, as shown in **Scheme 27**. If the distance between thiolate groups is sufficiently large to prevent oxidative disulfide formation, then the lifetime of the catalyst in its active form may be extended. Another advantage to the construction of this catalyst is the ease of handling associated with the use of polystyrene beads as the solid support. It is envisioned that these beads could be added to a solution of amide, the solution heated to reflux, and the amide hydrolysed. After the reaction was complete, the beads could simply be filtered away from the solution, ready to use again.

Scheme 27

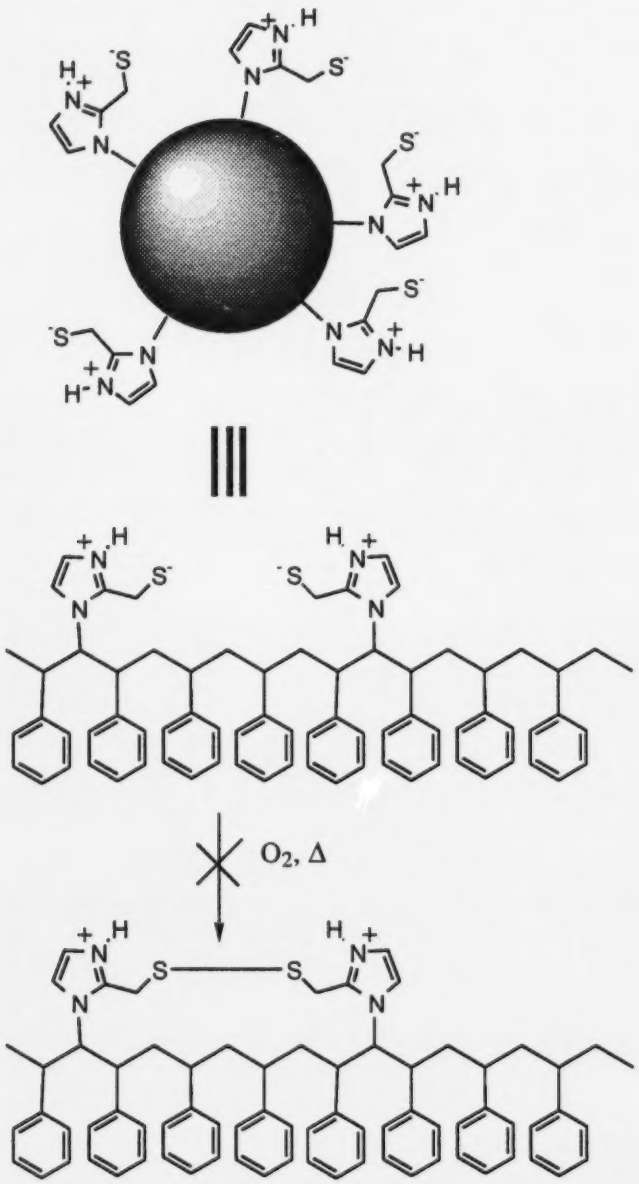

Another catalyst of both amide hydrolysis and formation that was discovered through this study is phosphate (KH_2PO_4 / K_2HPO_4). Although phosphate is not as active a catalyst as **7b** under the conditions employed in this work, it has been demonstrated that phosphate shows an advantage over **7b** in its geater stability to heating for prolonged times. This ability of a common, naturally occurring inorganic molecule to catalyze the formation of amides (possibly including peptides) is of great interest. Currently, work is underway in this laboratory to attempt the catalytic formation of small dipeptides and to investigate the mechanism of catalysis by phosphate. Two possible mechanisms envisioned for the observed catalysis of amide formation by phosphate are the general base / general acid catalysis pathway and the bifunctional catalysis pathway. Bifunctional catalysis has been invoked to account for the accelerated rate of amide[93] and imidate ester[94] hydrolysis as well as amide thiolysis[73] by buffers such as phosphate, acetate, carbonate and arsenate. These buffers are able to mediate acyl transfer reactions through concerted proton addition and removal in the formation and breakdown of tetrahedral intermediates. The mechanism of bifunctional catalysis of amide hydrolysis by phosphate is presented hypothetically in **Scheme 28**.

Scheme 28

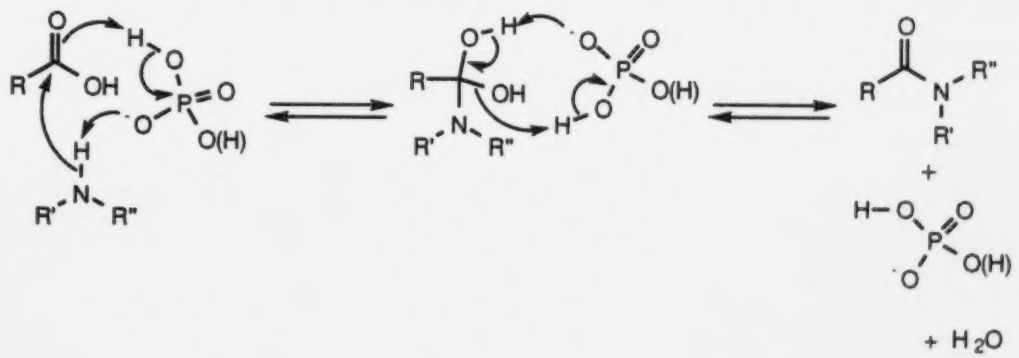

REFERENCES

1. For a summary of the current understanding of acid- and base-catalyzed amide hydrolysis reactions, see the following :

   (a) Lowry, T.H.; Richardson, K.S. In *Mechanism and Theory in Organic Chemistry*, 3rd ed.; Harper and Row Inc.: New York, NY, 1987; pp 714-717.

   (b) Jencks, W.P. In *Catalysis in Chemistry and Enzymology*; Dover Publications, Inc.: New York, NY, 1987; pp 523-527.

   (c) Isaacs, N.S. In *Physical Organic Chemistry*; Longman Scientific and Technical and J. Wiley and Sons: New York, NY, 1987; pp 484-486.

   (d) March, J. In *Advanced Organic Chemistry*, 3rd ed.; J. Wiley and Sons: New York, NY, 1985; pp 338-341.

   (e) Deslongchamps, P. In *Stereoelectronic Effects in Organic Chemistry*; Pergamon Press: Oxford, 1983; pp 101-162.

   (f) O'Connor, C.J. *Q. Rev. Chem. Soc.* **1971**, *24*, 553-564.

   (g) Bender, M.L. *Chem. Rev.* **1960**, *60*, 53-113.

2. Brown, R.S.; Bennet, A.J.; Slebocka-Tilk, H. *Acc. Chem. Res.* **1992**, *25*, 481-488.

3. The derivation leading to the kinetic expressions is straightforward. If k_1 is redefined to include the protonation, and k_2 is redefined as including the equilibrium between T^o and T_N+ and the subsequent breakdown step, then the rate constants can be defined as

   $$k_{hyd} = k_1k_2/(k_{-1} + k_2)$$

   and $$k_{ex} = k_1k_{-1}/2(k_{-1} + k_2)$$

   such that $$k_{ex}/k_{hyd} = k_{-1}/2k_2.$$

4. Bender, M.L.; Thomas, R.J. *J. Am. Chem. Soc.* **1961**, *83*, 4183-4189 and references therein.

5. Bunton, C.A.; Farber, S.J.; Millbank, A.J.G.; O'Connor, C.J.; Turney, T.A. *J. Chem. Soc., Perkin Trans. 2* **1972**, 1869-1875 and references therein.

6. Smith, C.R.; Yates, K. *J. Am. Chem. Soc.* **1972**, *94*, 8811-8817.

7. McClelland, R.A. *J. Am. Chem. Soc.* **1975**, *97*, 5281-5282.

8. Bennet, A.J.; Slebocka-Tilk, H.; Brown, R.S.; Guthrie, J.P.; Jodhan, A.J. *J. Am. Chem. Soc.* **1990**, *112*, 8497-8506.

9. (a) DeWolfe, R.H.; Newcomb, R.C. *J. Org. Chem.* **1971**, *36*, 3870-3878.

(b) Young, J.K.; Pazhanisamy, S.; Schowen, R.L. *J. Org. Chem.* **1984**, *49*, 4148-4152.

(c) Eriksson, S.O. *Acta Chem. Scand.* **1968**, *22*, 892-906.

(d) Pollack, R.M.; Dumsha, T.C. *J. Am. Chem. Soc.* **1973**, *95*, 4463-4465.

(e) Biechler, S.; Taft, R.W. *J. Am. Chem. Soc.* **1957**, *79*, 4927-4935.

(f) Menger, F.M.; Donohue, J.A. *J. Am. Chem. Soc.* **1973**, *95*, 432-437.

(g) Cipiciani, A.; Linda, P.; Savelli, G. *J. Heterocycl. Chem.* **1979**, *16*, 673-675.

10. (a) Bender, M.L.; Ginger, R.D.; Kemp, K.C. *J. Am. Chem. Soc.* **1954**, *76*, 3350-3351.

(b) Bender, M.L.; Ginger, R.D.; Unik, J.P. *J. Am. Chem. Soc.* **1958**, *80*, 1044-1048.

11. (a) Bunton, C.A.; Nayak, B.; O'Connor, C.J. *J. Org. Chem.* **1968**, *33*, 572-575.

(b) Bunton, C.A.; Lewis, T.A.; Llewellyn, D.R. *Chem. Ind. (London)* **1954**, 1154-1155.

12. (a) Slebocka-Tilk, H.; Bennet, A.J.; Keillor, J.W.; Brown, R.S.; Guthrie, J.P.; Jodhan, A.J. *J. Am. Chem. Soc.* **1990**, *112*, 8507-8514.

(b) Slebocka-Tilk, H.; Bennet, A.J.; Hogg, H.J.; Brown, R.S. *J. Am. Chem. Soc.* **1991**, *113*, 1288-1294 and references therein.

13. (a) DeRoo, M.; Bruylants, A. *Bull. Soc. Chim. Belg.* **1954**, *63*, 140-157.

(b) Calvet, E. *J. Chim. Phys.* **1933**, *30*, 140-166.

14. (a) Deslongchamps, P.; Cheriyan, U.O.; Guida, A.; Taillefer, R.J. *Nouv. J. Chim.* **1977**, *1*, 235-241.

(b) Deslongchamps, P.; Gerval, P.; Chiryan, U.O.; Guida, A.; Taillefer, R.J. *Nouv. J. Chim.* **1978**, *2*, 631-636.

(c) Deslongchamps, P.; Barlet, R.; Taillefer, R.J. *Can. J. Chem.* **1980**, *58*, 2167-2172.

15. In a manner analogous for **Scheme 1**, found in reference 3, the following expression can be derived from an evaluation of **Scheme 2** :

$$k_{hyd} = k_1k_2[OH^-] / (k_{-1} + k_2)$$

and $$k_{ex} = k_1k_{-1}[OH^-] / 2(k_{-1} + k_2).$$

When exchange is small relative to hydrolysis, $k_2 >> k_{-1}$, so

$$k_{hyd} = k_1[OH^-]$$

and $$k_{ex} = k_1k_{-1}[OH^-] / 2k_2$$

such that $$k_{ex}/k_{hyd} = k_{-1} / 2k_2.$$

Similarly, if hydrolysis is much slower than exchange, $k_2 << k_{-1}$ so that

$$k_{hyd} = k_1k_2[OH^-] / k_{-1}$$

and $$k_{ex} = k_1[OH^-] / 2$$

such that $k_{ex}/k_{hyd} = k_{-1} / 2k_2$, again.

16. For reviews of the structure and mechanism of action of the serine proteases see :

(a) Walsh, C. In *Enzymatic Reaction Mechanisms*; W.H. Freeman: San Francisco, 1979; pp 56-97.

(b) Fersht, A. In *Enzyme Structure and Mechanism*; 2nd ed.; W.H. Freeman: San Francisco, 1985; pp 405-413.

17. (a) Hubbard, C.D.; Shoupe, T.S. *J. Biol. Chem.* **1977**, *252*, 1633-1638.

(b) Quinn, D.M.; Elrod, J.P.; Ardis, R.; Friesen, P.; Schowen, R.L. *J. Am. Chem. Soc.* **1980**, *102*, 5358-5365.

18. (a) Stein, R.L.; Strimpler, A.M. *J. Am. Chem. Soc.* **1987**, *109*, 4387-4390.

(b) Kovach, I.M.; Larson, M.; Schowen, R.L. *J. Am. Chem. Soc.* **1986**, *108*, 5490-5495.

(c) Stein, R.L.; Strimpler, A.M. *Biochemistry* **1987**, *26*, 2238-2242.

(d) Stein, R.L.; Strimpler, A.M.; Hori, H.; Powers, J.C. *Biochemistry* **1987**, *26*, 1305-1314.

19. (a) Blow, D.M.; Birktoft, J.J.; Hartley, B.S. *Nature* **1969**, *221*, 337-340.

(b) Kraut, J. *Annu. Rev. Biochem.* **1977**, *46*, 331-358.

(c) Bachovichin, W.M. *Biochemistry* **1986**, *25*, 7751-7759.

20. Summaries of the arguments for both cases can be found in 17c, 19c and the following :

(a) Abeles, R.H.; Liang, T.-C. *Biochemistry* **1987**, *26*, 7603-7608.

(b) Sprang, S.; Standing, T.; Fletterick, R.J.; Stroud, R.M.; Finer-Moore, J.; Xuong, N.-H.; Hamlin, R.; Rutter, W.J.; Craik, C.S. *Science* **1987**, *237*, 905-909, and references therein.

(c) Craik, C.S.; Roczniak, S.; Largman, C.; Rutter, W.J. *Science* **1987**, *237*, 909-913.

(d) Bachovichin, W.M.; Roberts, J.D. *J. Am. Chem. Soc.* **1978**, *100*, 8041-8047.

(e) Satterthwait, A.C.; Jencks, W.P. *J. Am. Chem. Soc.* **1974**, *96*, 7018-7031.

(f) Kossiakoff, A.A.; Spencer, S.A. *Biochemistry* **1981**, *20*, 6462-6474.

21. (a) Walsh, C. In *Enzymatic Reaction Mechanisms*; W.H. Freeman: San Francisco, 1979; pp 98-104.

(b) Fersht, A. In *Enzyme Structure and Mechanism*; 2nd ed.; W.H. Freeman: San Francisco, 1985; pp 422-426.

(c) *Aspartic Proteinases and Their Inhibitors*; Proceedings of FEBS Advanced Course No. 84/07; Kosta, V., Ed.; Walter de Gruyer: Berlin, 1985.

(d) *Acid Proteases: Structure, Function, and Biology*; Tang, J., Ed.; Plenum: New York, 1977; p 95.

(e) Polgár, L. *FEBS Lett.* **1987**, *219*, 1-4.

22. For a review of the status of thinking on the mechanism, see the following :

(a) Hofmann, T.; Fink, A.L. *Biochemistry* **1984**, *23*, 5247-5256, and the Appendix therein.

(b) Dunn, B.M.; Fink, A.L. *Biochemistry* **1984**, *23*, 5241-5247.

23. Knowles, J.R. *Philos. Trans. R. Soc. London, B* **1970**, *257*, 135-146.

24. (a) Aldersley, M.F.; Kirby, A.J.; Lancaster, P.W.; McDonald, R.S.; Smith, C.R. *J. Chem. Soc., Perkin Trans. 2* **1974**, 1487-1495.

(b) Kirby, A.J.; McDonald, R.S.; Smith, C.R. *J. Chem. Soc., Perkin Trans. 2* **1974**, 1495-1504.

25. Kluger, R.; Chin, J. *J. Am. Chem. Soc.* **1982**, *104*, 2891-2897.

26. (a) Antonov, V.K.; Ginodman, L.M.; Kapitannikov, Yu.V.; Barshevskaya, T.N.; Gurova, A.G.; Rumsh, L.D. *FEBS Lett.* **1978**, *88*, 87-90.

(b) Holladay, M.W.; Salituro, F.G.; Schmidt, P.G.; Rich, D.H. *Biochem. Soc. Trans.* **1985**, *13*, 1046-1048.

27. (a) Blum, M.; Cunningham, A.; Bendiver, M.; Hofmann, T. *Biochem. Soc. Trans.* **1985**, *13*, 1044-1046.

(b) Takahashi, M.; Wang, T.T.; Hofmann, T. *Biochem. Biophys. Res. Commun.* **1974**, *57*, 39-46.

(c) Wang, T.T.; Hofmann, T. *Biochem. J.* **1976**, *153*, 691-699.

28. (a) Antonov, V.K.; Ginodman, L.M.; Rumsh, L.D.; Kapitannikov, Yu.V.; Barshevskaya, T.N.; Yavashev, L.B.; Gurova, A.G.; Volkova, L.I. *Bioorg. Khim.* **1980**, *6*, 436-446.

(b) Antonov, V.K. in reference 21c, pp 202-220.

(c) Antonov, V.K.; Ginodman, L.M.; Rumsh, L.D.; Kapitannikov, Yu.V.; Barshevskaya, T.N.; Yavashev, L.B.; Gurova, A.G.; Volkova, L.I. *Eur. J. Biochem.* **1981**, *117*, 195-200.

29. (a) Somayaji, V.; Keillor J.W.; Brown, R.S. *J. Am. Chem. Soc.* **1988**, *110*, 2625-2629.

(b) Hofmann, T.; Fink, A.L. *Biochemistry* **1984**, *23*, 5247-5256.

30. (a) Veerapandian, B.; Cooper, J.B.; Sali, A.; Blundell, T.L.; Rosati, R.L.; Dominy, B.W.; Damon, D.B.; Hoover, D.R. *Protein Sci.* **1992**, *1*, 322-328.

(b) Blundell, T.L.; Cooper, J.B.; Sali, A.; Zhu, Z.-Y. In *Structure and Function of the Aspartic Proteinases*, Dunn, B.M., Ed.; Plenum (New York): New York, 1991, pp 443-453.

(c) Hyland, L.J.; Tomaszek, T.A.; Meek, T.D. *Biochemistry* **1991**, *30*, 8454-8463.

(d) Davies, D.R. *Annu. Rev. Biophys. Biophys. Chem.* **1990**, *19*, 189-215.

(e) Suguna, K.; Padlan, E.A.; Smith, C.W.; Carlson, W.D.; Davies, D.R. *Proc. Natl. Acad. Sci. U.S.A.* **1987**, *84*, 7009-7013.

31. (a) Glazer, A.N.; Smith, E.L. In *The Enzymes*; Boyer, P.D., Ed.; Academic Press: New York, 1971, Vol. 3, pp 501-546.

(b) Drenth, J.; Jansonius, J.N.; Koekoek, R.; Wolthers, B.G. In *The Enzymes*; Boyer, P.D., Ed.; Academic Press: New York, 1971, Vol. 3, pp 485-499.

(c) Liu, T.-Y.; Elliott, S.D. In *The Enzymes*; Boyer, P.D., Ed.; Academic Press: New York, 1971, Vol. 3, pp 609-647.

(d) Mitchell, W.M.; Harrington, W.F. In *The Enzymes*; Boyer, P.D., Ed.; Academic Press: New York, 1971, Vol. 3, pp 699-719.

(e) Brocklehurst, K. *Methods Enzymol.* **1982**, *87c*, 427-469.

(f) Polgár, L.; Halász, P. *Biochem. J.* **1982**, *207*, 1-10.

(g) Drenth, J.; Kalk, K.H.; Swen, H.M. *Biochemistry* **1976**, *15*, 3731-3738.

(h) Baker, E.N.; Drenth, J. *Biol. Macromol. Assem.* **1987**, *3*, 313-368.

(i) Magrath, J.; Abeles, R.H. *J. Med. Chem.* **1992**, *35*, 4279-4283 and references therein.

32. (a) Boland, M.J.; Hardman, M.J. *FEBS Lett.* **1972**, *27*, 282-284.

(b) Boland, M.J.; Hardman, M.J. *Eur. J. Biochem.* **1973**, *36*, 575-582.

(c) Hussain, S.S.; Lowe, G. *Biochem. J.* **1968**, 855-859.

33. (a) Wilson, I.B.; Bergmann, F.; Nachmansohn, D. *J. Biol. Chem.* **1950**, *186*, 781-790.

(b) Lowe, G.; Williams, A. *Biochem. J.* **1965**, *96*, 199-204.

(c) Storer, A.C.; Murphy, W.F.; Carey, P.R. *J. Biol. Chem.* **1979**, *254*, 3163-3165.

(d) Brocklehurst, K.; Cook, E.M.; Wharton, C.W. *J. Chem. Soc., Chem. Commun.* **1967**, 1185-1187.

(e) Brubacher, L.J.; Bender, M.L. *J. Am. Chem. Soc.* **1964**, *86*, 5333-5334.

(f) Smolarsky, M. *Isr. J. Chem.* **1974**, *12*, 615-629.

(g) Malthouse, J.P.G.; Gamcsik, M.P.; Boyd, A.S.F.; Mackenzie, N.E.; Scott, A.I. *J. Am. Chem. Soc.* **1982**, *104*, 6811-6813.

(h) Williams, D.C.; Whitaker, J.R. *Biochemistry* **1967**, *6*, 3711-3717.

(i) Lowe, G. *Tetrahedron* **1976**, *32*, 291-302.

34. Stevens, F.C.; Glazer, A.N.; Smith, E.L. *J. Biol. Chem.* **1967**, *242*, 2764-2779.

35. (a) Whitaker, J.R.; Bender, M.L. *J. Am. Chem. Soc.* **1965**, *87*, 2728-2737.

(b) Smith, E.L.; Parker, M.J. *J. Biol. Chem.* **1958**, *233*, 1387-1391.

(c) Lowe, G.; Yuthavong, Y. *Biochem. J.* **1971**, *124*, 117-122.

36. (a) Lucas, E.C.; Williams, A. *Biochemistry* **1969**, *8*, 5125-5135.

(b) Lowe, G. *Phil. Trans. R. Soc. London Ser. B* **1970**, *257*, 237-248.

37. (a) Lewis, S.D.; Johnson, F.A.; Shafer, J.A. *Biochemistry* **1976**, *15*, 5009-5017.

(b) Lewis, S.D.; Johnson, F.A.; Shafer, J.A. *Biochemistry* **1981**, *20*, 48-51.

(c) Johnson, F.A.; Lewis, S.D.; Shafer, J.A. *Biochemistry* **1981**, *20*, 52-58.

(d) Sluyterman, L.A.Æ.; Wijdenes, J. *Eur. J. Biochem.* **1976**, *71*, 383-391.

(e) Creighton, D.J.; Schamp, D.J. *FEBS Lett.* **1980**, *110*, 313-318.

(f) Creighton, D.J.; Gessouroun, M.S.; Heapes, J.M. *FEBS Lett.* **1980**, *110*, 319-322.

(g) Shipton, M.; Kierstan, M.P.J.; Malthouse, J.P.G.; Stuchbury, T.; Brocklehurst, K. *FEBS Lett.* **1975**, *50*, 365-368.

(h) Polgár, L. *Eur. J. Biochem.* **1976**, *71*, 563-569.

(i) Polgár, L. *Eur. J. Biochem.* **1976**, *71*, 571-575.

(j) Polgár, L. *FEBS Lett.* **1974**, *47*, 15-18.

(k) Polgár, L. *FEBS Lett.* **1974**, *38*, 187-190.

(l) Polgár, L. *Acta Biochim. Biophys. Hung.* **1988**, *23*, 207-213.

(m) Polgár, L. *Biol. Chem. Hoppe-Seyler (Suppl.)* **1990**, *371*, 327-331.

38. (a) Angelides, K.J.; Fink, A.L. *Biochemistry* **1978**, *17*, 2659-2668.

(b) Angelides, K.J.; Fink, A.L.*Biochemistry* **1979**, *18*, 2355-2363.

39. Brubacher, L.J.; Bender, M.L. *J. Am. Chem. Soc.* **1966**, *88*, 5871-5880.

40. (a) Johnson, F.A.; Lewis, S.D.; Shafer, J.A. *Biochemistry* **1981**, *20*, 44-48.

(b) Lowe,G.; Whitworth, A.S. *Biochem. J.* **1974**, *141*, 503-515.

(c) Sluyterman, L.A.Æ.; De Graaf, M.J.M. *Biochem. Biophys. Acta* **1972**, *258*, 554-561.

(d) Hinkle, P.M.; Kirsch, J.M. *Biochemistry* **1970**, *9*, 4633-4643.

(e) Szawelski, R.J.; Wharton, G.W. *Biochem. J.* **1981**, *199*, 681-692.

41. Several studies have reported this S→N acyl transfer in the hydrolysis of thiolesters as a model for this deacylation step in the cysteine proteases :

(a) Fife, T.H.; DeMark, B.R. *J. Am. Chem. Soc.* **1979**, *101*, 7379-7385.

(b) Bruice, T.C. *J. Am. Chem. Soc.* **1959**, *81*, 5444-5449.

(c) Heller, M.J.; Walder, J.A.; Klotz, I.M. *J. Am. Chem. Soc.* **1977**, *99*, 2780-2785.

(d) Bruice, T.C.; Fedor, L.R. *J. Am. Chem. Soc.* **1964**, *86*, 4880-4897.

(e) Bruice, T.C.; Fedor, L.R. *J. Am. Chem. Soc.* **1964**, *86*, 4117-4123.

(f) Bender, M.L.; Turnquest, B.W. *J. Am. Chem. Soc.* **1957**, *79*, 1656-1662.

(g) Noda, L.H.; Kuby, S.A.; Lardy, H.A. *J. Am. Chem. Soc.* **1953**, *75*, 913-917.

(h) Lowe, G.; Williams, A. *Biochem. J.* **1965**, *96*, 194-204.

42. Kirby, A.J. In *Enzyme Mechanisms*, Page, M.I., Williams, A., Eds.; The Royal Society of Chemistry: London, 1987; pp 67-77.

43. (a) Bruice, T.C.; Schmir, G.L. *J. Am. Chem. Soc.* **1958**, *80*, 148-156.

(b) Werber, M.M.; Shalitin, Y. *Bioorg. Chem.* **1973**, *2*, 202-220.

(c) Hine, J.; Khan, M.N. *J. Am. Chem. Soc.* **1977**, *99*, 3847-3850.

(d) Kitaura, Y.; Bender, M.L. *Bioorg. Chem.* **1975**, *4*, 237-249.

(e) Kunitake, T.; Okahata, Y.; Sakamoto, T. *Chem. Lett.* **1975**, 459-462.

(f) Sunamoto, J.; Kondo, H.; Okamoto, H.; Murakami, Y. *Tetrahedron Lett.* **1977**, 1329-1332.

(g) Moss, R.A.; Nahas, R.C.; Ramaswami, S. *J. Am. Chem. Soc.* **1977**, *99*, 627-629.

(h) Fife, T.H.; Benjamin, B. *J. Chem. Soc., Chem. Commun.* **1974**, 525-526.

(i) Bruice, T.C.; York, J.L. *J. Am. Chem. Soc.* **1961**, *83*, 1382-1387.

(j) Khan, M.N. *J. Org. Chem.* **1985**, *50*, 4851-4855.

(k) Kunitake, T.; Okahata, Y.; Tahara, T. *Bioorg. Chem.* **1976**, *5*, 155-167.

(l) Tonellato, U. *J. Chem. Soc., Perkin Trans. 2* **1977**, 821-827.

(m) Cram, D.J.; Lam, P.Y.-S.; Ho, S.P. *J. Am. Chem. Soc.* **1986**, *108*, 839-841.

(n) Cram, D.J.; Katz, H.E.; Dicker, I.B. *J. Am. Chem. Soc.* **1984**, *106*, 4987-5000.

(o) Menger, F.M.; Whitesell, L.G. *J. Am. Chem. Soc.* **1985**, *107*, 707-708.

44. (a) Page, M.I.; Jencks, W.P. *J. Am. Chem. Soc.* **1972**, *94*, 8818-8827.

(b) Somayaji, V.; Skorey, K.I.; Brown, R.S.; Ball, R.G. *J. Org. Chem.* **1986**, *51*, 4866-4872.

(c) Somayaji, V.; Skorey, K.I.; Brown, R.S. *J. Am. Chem. Soc.* **1988**, *110*, 5205-5206.

(d) Skorey, K.I.; Somayaji, V.; Brown, R.S. *J. Am. Chem. Soc.* **1989**, *111*, 1445-1452.

(e) Anoardi, L.; Tonellato, U. *J. Chem. Soc., Chem. Commun.* **1977**, 401-402.

45. (a) Komiyama, M.; Bender, M.L. *Bioorg. Chem.* **1977**, *6*, 13-20.

(b) Komiyama, M.; Bender, M.L.; Utaka, M.; Takeda, A. *Proc. Natl. Acad. Sci. U.S.A.* **1977**, *74*, 2634-2638.

(c) Mallick, I.M.; D'Souza, V.T.; Yamaguchi, M.; Lee, J.; Chalabi, P.; Gadwood, R.C.; Bender, M.L. *J. Am. Chem. Soc.* **1984**, *106*, 7252-7254.

(d) Rogers, G.A.; Bruice, T.C. *J. Am. Chem. Soc.* **1974**, *96*, 2473-2481.

(e) Komiyama, M.; Breaux, E.J.; Bender, M.L. *Bioorg. Chem.* **1977**, *6*, 127-136.

(f) Roberts, J.D.; Kanamori, K. *Proc. Natl. Acad. Sci. U.S.A.* **1980**, *77*, 3095-3097.

(g) Boudreau, J.A.; Farrar, C.R.; Williams, A. *J. Chem. Soc., Perkin Trans. 2*, **1978**, 46-51.

(h) Cramer, K.D.; Zimmerman, S.C. *J. Am. Chem. Soc.* **1990**, *112*, 3680-3682.

(i) Zimmerman, S.C.; Korthals, J.S.; Cramer, K.D. *Tetrahedron*, **1991**, *47*, 2649-2660.

46. (a) D'Souza, V.T.; Bender, M.L. *Acc. Chem. Res.* **1987**, *20*, 146-152.

(b) D'Souza, V.T.; Hanabusa, K.; O'Leary, T.; Gadwood, R.C.; Bender, M.L. *Biochem. Biophys. Res. Commun.* **1985**, *129*, 727-732.

(c) Cruickshank, P.A.; Sheehan, J.C. *J. Am. Chem. Soc.* **1964**, *86*, 2070-2071.

(d) Nishi, N.; Nakajima, B.; Mirishige, M.; Tokura, S. *Int. J. Pept. Protein Res.* **1986**, *27*, 261-268.

47. Somayaji, V.; Brown, R.S. *J. Am. Chem. Soc.* **1987**, *109*, 4738-4739.

48. Kirby, A.J. *Adv. Phys. Org. Chem.* **1980**, *17*, 183-278.

49. (a) Schonbaum, G.R.; Bender, M.L. *J. Am. Chem. Soc.* **1960**, *82*, 1900-1904.

(b) Rylander, P.N.; Tarbell, D.S. *J. Am. Chem. Soc.* **1950**, *72*, 3021-3025.

(c) Morse, B.K.; Tarbell, D.S. *J. Am. Chem. Soc.* **1952**, *74*, 416-419.

50. (a) Street, J.P.; Brown, R.S. *J. Am. Chem. Soc.* **1985**, *107*, 6084-6089.

(b) Street, J.P.; Skorey, K.I.; Brown, R.S.; Ball, R.G. *J. Am. Chem. Soc.* **1985**, *107*, 7669-7679.

51. (a) Schneider, F.; Wenck, H. *Z. Physiol. Chem.* **1969**, *350*, 1653-1661.

(b) Schneider, F.; Wenck, H. *Z. Physiol. Chem.* **1969**, *350*, 1521-1530.

(c) Schneider, F.; Schaich, E.; Wenck, H. *Z. Physiol. Chem.* **1968**, *349*, 1525-1528.

(d) Petz, D.; Schneider, F. *Z. Naturforsch. C.* **1976**, *31*, 534-543.

(e) Sluyterman, L.A.Æ.; De Graaf, M.J.M. *Biochem. Biophys. Acta* **1972**, *258*, 554-561.

(f) Lochon, P.; Schoenleber, J. *Tetrahedron* **1976**, *52*, 3023-3030.

(g) Krati, N.; Brembilla, A.; Lochon, P. *Tetrahedron Lett.* **1989**, *30*, 79-82.

(h) Lindley, H. *Biochem. J.* **1966**, *74*, 577-584.

(i) Whitaker, J.R. *J. Am. Chem. Soc.* **1960**, *84*, 1900-1904.

(j) Ogilvie, J.W.; Tildon, J.T., Strauch, B.S. *Biochemistry* **1964**, *3*, 754-758.

(k) Fersht, A.R. *J. Am. Chem. Soc.* **1971**, *93*, 3504-3515.

(l) Brembilla, A.; Roizard, D.; Schoenleber, J.; Lochon, P. *Can. J. Chem.* **1984**, *62*, 2330-2336.

52. Skorey, K.I.; Brown, R.S. *J. Am. Chem. Soc.* **1985**, *107*, 4070-4072.

53. (a) McDonald, R.S.; Patterson, P.; Rodwell, J.; Whalley, A. *Can. J. Chem.* **1992**, *70*, 62-67.

(b) McDonald, R.S.; Patterson, P.; Stevens-Whalley, A. *Can. J. Chem.* **1983**, *61*, 1846-1852.

(c) Jencks, W.P.; Carriuolo, J. *J. Biol. Chem.* **1958**, *234*, 1280-1285.

(d) Dafforn, G.A.; Koshland, D.E. *J. Am. Chem. Soc.* **1977**, *99*, 7246-7257.

(e) Nakken, K.F.; Eldjarn, L.; Pihl, A. *Biochem. Pharmacol.* **1960**, *3*, 89-100.

54. (a) A preliminary account of a portion of this work has appeared : Keillor, J.W.; Brown, R.S. *J. Am. Chem. Soc.* **1991**, *113*, 5114-5116.

(b) This work has also been published in its entirety : Keillor, J.W.; Brown, R.S. *J. Am. Chem. Soc.* **1992**, *114*, 7983-7989.

55. An account of this work has been submitted to the Journal of the American Chemical Society for publication.

56. Somayaji, V.; Brown, R.S. *J. Org. Chem.* **1986**, *51*, 2676-2686.

57. (a) Vanin, E.F.; Ji, T.H. *Biochemistry* **1981**, *20*, 6754-6760.

(b) Traut, R.R.; Bollen, A.; Sun, T.-T.; Hershey, J.W.B.; Sundberg, J. Pierce, R. *Biochemistry* **1973**, *12*, 3266-3273.

58. Owen, T.C. *J. Chem. Soc. C.* **1967**, 1373-1376.

59. Brown, R.S.; Ulan, J.G. *J. Am. Chem. Soc.* **1983**, *105*, 2382-2388.

60. Fife, T.H.; Bruice, T.C. *J. Phys. Chem.* **1961**, *65*, 1079-1080.

61. Scott, A.I. *Pure Applied Chem.* **1986**, *58*, 753-766 reports that thiolesters generally exhibit $^{13}C{=}O$ resonances in the range of 195 - 200 ppm ~ 20 ppm downfield from their corresponding carboxylic acids. In the case of the authentic

amino acid of **2**, the $^{13}C{=}O$ peak is at 176.6 ppm (CD_3CN containing 13 vol. % H_2O).

62. Benesch, R.E.; Benesch, R. *J. Am. Chem. Soc.* **1955**, *77*, 5877-5881.

63. (a) Kostyukovskii, Ya. L.; Bruk, Yu. A.; Pavlova, L.V.; Slavachevskaya, N.M.; Kokushkina, A.V.; Mirkin, B.S.; Belen'kaya, I.A. *Zh. Obshch. Khim.* **1972**, *42*, 662-665.

(b) Kostyukovskii, Ya. L.; Bruk, Yu. A.; Kokushkina, A.V.; Mirkin, B.S.; Slavachevskaya, N.M.; Pavlova, L.V.; Belen'kaya, I.A. *Zh. Obshch. Khim.* **1972**, *42*, 2104-2106.

64. Bagiyan, G.A.; Koroleva, I.K.; Soroka, N.V. *Zh. Neorgan. Khim.* **1977**, *22*, 3078-3085.

65. Jencks, W.P.; Salvesen, K. *J. Am. Chem. Soc.* **1971**, *93*, 4433-4436.

66. Bagiyan, G.A.; Koroleva, I.K.; Grachev, S.A.; Soroka, N.v. *Akad. Nauk SSSR. Bulletin, Div. Chem. Sci.* **1976**, *25*, 966-971 gives pKa^{SH} values of 9.39 (20 °C) and 9.14 (30 °C): value at 25 °C taken as the average.

67. Nenasheva, T.N.; Salinkova, G.A. *Zh. Org. Khim.* **1979**, *15*, 835-839.

68. The pKa values quoted in **Scheme 17** are the correct ones - those reported in reference 50b, Table IV for 2-thiomethylimidazole, and N-methyl-2-thiomethyl-imidazole should be interchanged.

69. The actual equation fit was:

$$k_2^{obsd} = (k_2 K_{ZW}) [H^+] / (([H^+]^2 / Ka^{Im}) + (1 + K_{ZW}) [H^+] + Ka^{SH})$$

70. The macroscopic Ka values are defined as:

$$Ka^1 = Ka^{Im} + K_1 \text{ and } 1/K_a^2 = 1/Ka^{SH} + 1/K_3$$

71. Alvarez, F.J.; Schowen, R.L. In *Isotopes in Organic Chemistry*, Vol. 7, "Secondary and Solvent Isotope Effects", Buncel, E.; Lee, C.C., Eds.; Elsevier: Amsterdam, 1987; pp 1-60.

72. Estimated on the basis of values given for N-H^+ ionization of the zwitterionic form of the $HOCH_3$ addition product of dehydroquinolone:
(a) Kirby, A.J.; Mujahid, T.G.; Camilleri, P. *J. Chem. Soc., Perkin Trans. 2* **1979**, 1610-1616.
(b) Fox, J.P.; Jencks, W.P. *J. Am. Chem. Soc.* **1974**, *96*, 1436-1449.

73. (a) Barnett, R.E.; Jencks, W.P. *J. Am. Chem. Soc.* **1969**, *91*, 2358-2369.
(b) Barnett, R.E.; Jencks, W.P. *J. Am. Chem. Soc.* **1968**, *90*, 4199-4200.

74. Keillor, J.W.; Brown, R.S. unpublished observations CAPS = 3-(N-cyclohexyl-amino)-propanesulfonic acid; CHES = 2-(N-cyclohexylamino)ethanesulfonic acid; EPPS = N-(2-hydroxyethyl)piperazine-N'-3-propanesulfonic acid.

75. Hupe, D.J.; Jencks, W.P. *J. Am. Chem. Soc.* **1977**, *99*, 451-464.

76. Jencks, W.P. In *Catalysis in Chemistry and Enzymology*; Dover Publications, Inc.: New York, NY, 1987; pp 243-281.

77. (a) Melander, L.; Saunders, W.H., Jr. In *Reaction Rates of Isotopic Molecules*; Wiley-Interscience: New York, 1980; pp 202-224 and 42.
(b) Schowen, R.L. *Prog. Phys. Org. Chem.* **1972**, *9*, 275-332.
(c) More-O'Ferrall, R.A. In *Proton-transfer Reactions*; Calden, E.F.; Gold, V., Eds.; Wiley: New York, 1975; pp 201-261.

78. (a) Swain, C.G.; Thornton, E.R. *J. Am. Chem. Soc.* **1962**, *84*, 817-821.
(b) Thornton, E.R. *J. Am. Chem. Soc.* **1967**, *89*, 2915-2927.

79. (a) Schowen, K.B.J. In *Transition States of Biochemical Processes*; Gandour, R.D.; Schowen, R.L., Eds.; Plenum Press: New York, 1978; pp 225-283.
(b) Schowen, R.L. In *Isotope Effects on Enzyme Catalyzed Reactions*; Cleland, W.W.; O'Leary, M.H.; Northrup, D.B., Eds.; University Park Press: Baltimore, 1977; pp 64-99.

80. Bergman, N.A.; Chiang, Y.; Kresge, A.J. *J. Am. Chem. Soc.* **1978**, *100*, 5954-5956.

81. Cox, M.M.; Jencks, W.P. *J. Am. Chem. Soc.* **1981**, *103*, 572-580.

82. Tammelin, L.E. *Acta. Chem. Scand.* **1957**, *11*, 487-490.

83. (a) Green, C.L.; Houghton, R.P.; Phipps, D.A. *J. Chem. Soc., Perkin Trans. 1* **1974**, 2623-2629.

(b) Wieland, T.; Hornig, H. *Annalen* **1956**, *600*, 12-22.

84. Guthrie, J.P. *J. Am. Chem. Soc.* **1974**, *96*, 3608-3615.

85. Fersht, A.R.; Requena, Y. *J. Am. Chem. Soc.* **1971**, *93*, 3499-3504.

86. Morawetz, H.; Otaki, P.S. *J. Am. Chem. Soc.* **1963**, *85*, 463-468.

87. This apparent equilibrium constant takes into account the amount of formic acid and morpholine that would exist as their neutral species at pH levels between the pKa values of formic acid and morpholinium ion, so that the total concentrations of formic acid and morpholine may be used in the equilibrium expression :

$K_{eq} = 2.24 \times 10^5\ M^{-1} = [NFM] / [HCOOH]\ [morpholine]$;

$K'_{eq} = 1.35\ M^{-1} = [NFM] / [HCOOH]_{tot}\ [morpholine]_{tot}$.

See Appendix 3 for derivation.

88. Phosphate buffer (i.e. KH_2PO_4 / K_2HPO_4) was serendipitously found to have a modest catalytic effect on the hydrolysis of the three amides studied, with the advantage over **7b** of being more thermally stable over long periods of heating.

89. On doubling the concentration of both morpholine and formic acid, the observed rate of amide formation actually increased by ~ 240%. The partitioning ratio of k_{hyd}/k_{form} was determined to be 30 mM (*vide infra*). Using this value, the ratio of $(k_{form}[amine])/k_{hyd}$ can be calculated to be 6.6 at 200 mM [morpholine] and 13.2 at 400 mM [morpholine]. The approximation that $k_{form}[amine] + k_{hyd} \approx k_{form}[amine]$ may partially account for the additional 40% rate increase. However, we believe the assumption that the rate of formation of NFM is independent of morpholine concentration under these conditions to be justified in this approximate treatment of the data.

90. Chin, J.; Mrejen, K. *J. Chem. Soc., Chem. Commun.* **1990**, 1326-1328.

91. (a) Hine, J.; King, R.S.-M.; Midden, W.R.; Sinha, A. *J. Org. Chem.* **1981**, *46*, 3186-3189.

(b) Langlois, S.; Broche, A. *Bull. Chem. Soc. Fr.* **1964**, 812-816.

(c) Takasaki, B.K.; Kim, J.H.; Rubin, E.; Chin, J. *J. Am. Chem. Soc.* **1993**, *115*, 1157-1159.

92. (a) Wang, Q.P.; Bennet, A.J.; Brown, R.S.; Santarsiero, B.D. *J. Am. Chem. Soc.* **1991**, *113*, 5757-5765.

(b) Wang, Q.; Bennet, A.J.; Brown, R.S. *Can. J. Chem.* **1990**, *68*, 1732-1739.

(c) Kahne, D.; Still, W.C. *J. Am. Chem. Soc.* **1988**, *110*, 7529-7534.

(d) Somayaji, V.; Brown, R.S. *J. Org. Chem.* **1986**, *51*, 2676-2686.

(e) Hine, J.; King, R.S.-M.; Midden, W.R.; Sinha, A. *J. Org. Chem.* **1981**, *46*, 3186-3189.

(f) Komiyama, M.; Bender, M.L. *Bioorg. Chem.* **1978**, *7*, 133-139.

93. (a) Schepartz, A.; Breslow, R. *J. Am. Chem. Soc.* **1987**, *109*, 1814-1826.

(b) Boreham, C.J.; Buckingham, D.A.; Keene, F.R. *J. Am. Chem. Soc.* **1979**, *101*, 1409-1421.

94. (a) Lee, Y.-N.; Schmir, G.L. *J. Am. Chem. Soc.* **1979**, *101*, 3026-3035.

(b) Cunningham, B.A.; Schmir, G.L. *J. Am. Chem. Soc.* **1966**, *88*, 551-558.

APPENDIX 1

Supplementary Material to Chapter 1

Preparation of Amide **14a**:

0.6 g (3 mmol) of [2-(benzylthio)ethyl]amine-HCl was dissolved in 2.5 equivalents (0.7 g, 1 mL) of triethylamine and 25 mL $CHCl_3$. Into this solution was dripped, with stirring, a $CHCl_3$ solution of 1 equivalent of the respective N-tosylated acid chloride of **2**. Stirring was continued for two hours, followed by extraction of the $CHCl_3$ once with 0.5 M HCl and twice with H_2O. The aqueous layers were extracted once again with $CHCl_3$, the organic layers combined, dried over $MgSO_4$, and stripped of solvent. A syrup was obtained in 95% yield and was characterized by 80 MHz NMR, FTIR, and EI mass spectroscopy. The syrup was purified through silica gel column chromatography (20/80 EtOAc/pet. ether) and 0.45 g of the material was added to a flask fitted with a dry ice condenser and dissolved in 7 mL freshly distilled THF. The flask was cooled to -50 °C in a dry ice/acetone bath and 80 mL of $NH_{3(l)}$ was condensed inside. Sodium metal was added until a blue colour persisted, stirring was continued for 15 minutes, and ammonium chloride was added until the solution turned yellow. The condenser and bath were removed and the ammonia was allowed to evaporate under gentle Ar flow. The remaining powder was dissolved in Ar-purged EtOH, and the solution filtered of salts. Bubbling HCl gas through the solution precipitated out some more salts, which were also removed through filtration. The solvent was then removed, leaving behind a yellow residue, which was dissolved in Ar-purged H_2O, adjusted to pH 7 (with 1 M NaOH) and extracted with Ar-purged $CHCl_3$. The organic layers were combined, dried over $MgSO_4$, and removed. The waxy solid (**14a**) was purified through preparative reversed-phase TLC (14/86 H_2O/MeOH) and characterized : ^1H NMR (300 MHz, $CDCl_3$) δ 6.95 (m, 2H), 6.60 (d of t, 1H), 6.45 (d of d, 1H), 6.34 (s), 3.8 (s, 1H), 3.54 (q, 2H), 3.28 (q, 2H), 2.97 (t, <

1H), 2.76 (t, 2H), 2.30 (m, 1H), 2.25 (m, 2H), 2.09-1.84 (br m, 2H), 1.84-1.67 (br m, 2H), 1.4-1.0 (br s, 1H); ^{13}C NMR (75 MHz, $CDCl_3$) 173.54, 4° C; 144.22, 4° C; 129.13; 3° C, 127.05, 3° C; 124.04, 3° C; 116.54, 3° C; 114.16, 3° C; 77.47, 77.04, 76.62, ($CDCl_3$ triplet); 38.43, 2° C; 38.27, 2° C; 37.76, 2° C; 35.08, 3° C; 33.89, 2° C; 31.90, 2° C; 26.22, 2° C; FTIR ($CHCl_3$, cm^{-1}) 3307, 3002, 2936, 1647, 1605; MS (NH_4^+ positive ionization) m/z (relative intensity) 265 ($M-H^+$, 100); 261 (15.5); 247 (10.5); 234 (15.9); 188 (4.5).

Tables of Observed Second-order Rate Constants:

Table 1S : Second Order Rate Constants at Various pH Values for the Reaction of Cysteamine (**10a**) with Distorted Amide **2** (T = 25 °C, μ = 1.0 (KCl))

pH	k_2^{obsd} ($M^{-1}s^{-1}$)[a]
6.15	0.962 ± 0.044
7.25	7.03 ± 0.23
8.05	34.2 ± 1.5
8.65	62.7 ± 1.8
9.35	90.8 ± 0.8

[a] Relative error calculated from the standard deviation of the fit of k_{obsd} vs $[RSH]_{total}$ at the given pH level.

Table 2S : Second Order Rate Constants at Various pH Values for the Reaction of N,N-Dimethylaminoethanethiol (**10b**) with Distorted Amide **2** (T = 25 °C, μ = 1.0 (KCl))

pH	k_2^{obsd} ($M^{-1}s^{-1}$)[a]
6.25	0.929 ± 0.013
7.15	5.17 ± 0.05
7.98	20.3 ± 0.5
8.39	25.3 ± 0.7
9.33	29.3 ± 1.0

[a] Relative error calculated from the standard deviation of the fit of k_{obsd} vs $[RSH]_{total}$ at the given pH level.

Table 3S : Second Order Rate Constants at Various pH Values for the Reaction of 4-(2-Mercaptoethyl)morpholine (**10c**) with Distorted Amide **2** (T = 25 °C, μ = 1.0 (KCl))

pH	k_2^{obsd} ($M^{-1}s^{-1}$)[a]
6.28	0.626 ± 0.008
7.23	1.22 ± 0.02
8.26	1.48 ± 0.04

[a] Relative error calculated from the standard deviation of the fit of k_{obsd} vs $[RSH]_{total}$ at the given pH level.

Table 4S : Second Order Rate Constants at Various pH Values for the Reaction of 2-Mercaptomethyl-N-methylimidazole (**7b**) with Distorted Amide **2** (T = 25 °C, μ = 1.0 (KCl))

pH	k_2^{obsd} ($M^{-1}s^{-1}$)[a]
5.39	8.25 ± 0.24
5.99	19.2 ± 0.2
6.29	22.1 ± 0.6
6.85	48.2 ± 1.1
7.92	71.7 ± 2.7
8.35	70.1 ± 2.7
8.60	63.7 ± 2.8
8.95	50.4 ± 0.9
9.74	17.7 ± 0.6
10.32	5.65 ± 0.25

[a] Relative error calculated from the standard deviation of the fit of k_{obsd} vs $[RSH]_{total}$ at the given pH level.

Table 5S : Second Order Rate Constants at Various pH Values for the Reaction of 3-Mercaptopropylamine (**10d**) with Distorted Amide **2** (T = 25 °C, μ = 1.0 (KCl))

pH	k_2^{obsd} ($M^{-1}s^{-1}$)[a]
7.27	0.22 ± 0.05
8.46	2.12 ± 0.02
9.33	8.44 ± 0.30
10.55	14.8 ± 0.3

[a] Relative error calculated from the standard deviation of the fit of k_{obsd} vs $[RSH]_{total}$ at the given pH level.

Table 6S : Second Order Rate Constants at Various pH Values for the Reaction of 3-Mercaptopropylamine (**10d**) with Distorted Amide **2** in D_2O (T = 25 °C, μ = 1.0 (KCl))

pD	k_2^{obsd} ($M^{-1}s^{-1}$)[a]
9.08	3.25 ± 0.13
9.75	9.66 ± 0.08
10.9	14.9 ± 0.2

[a] Relative error calculated from the standard deviation of the fit of k_{obsd} vs $[RSH]_{total}$ at the given pH level.

Table 7S : Second Order Rate Constants[a] at Various Concentrations of N-Methyl-imidazole Buffer for the Reaction of 4-(2-Mercaptoethyl)morpholine (**10c**) with Distorted Amide **2** (pH 7.4, T = 25 °C, μ = 1.0 (KCl))

[Buffer] (M)	k_2^{obsd} ($M^{-1}s^{-1}$)
0.05	3.33 ± 0.17
0.1	4.80 ± 0.24
0.2	8.14 ± 0.41
0.3	13.6 ± 0.7
0.5	19.2 ± 1.0
1.0	37.7 ± 1.9
2.0	82.4 ± 9.4

[a] Calculated from the observed pseudo first-order rate constant, at 1.02 mM thiol concentration. Relative error from buffer concentration, thiol concentration, pH measurement and standard deviation of kinetic fit estimated at about 5 %.

Table 8S : Second Order Rate Constants[a] at Various Concentrations of N-Methyl-imidazole Buffer for the Reaction of 4-(2-Mercaptoethyl)morpholine (**10c**) with Distorted Amide **2** (pH 8.4, T = 25 °C, μ = 1.0 (KCl))

[Buffer] (M)	k_2^{obsd} ($M^{-1}s^{-1}$)
0.1	1.65 ± 0.09
0.2	2.55 ± 0.13
0.5	5.12 ± 0.26
1.0	10.8 ± 0.5

[a] Calculated from the observed pseudo first-order rate constant, at 1.02 mM thiol concentration. Relative error from buffer concentration, thiol concentration, pH measurement and standard deviation of kinetic fit estimated at about 5 %.

Table 9S : Second Order Rate Constants[a] at Various Concentrations of N-Methyl-imidazole Buffer for the Reaction of 4-(2-Mercaptoethyl)morpholine (**10c**) with Distorted Amide **2** in D_2O (pD 7.9, T = 25 °C, μ = 1.0 (KCl))

[Buffer] (M)	k_2^{obsd} ($M^{-1}s^{-1}$)
0.1	5.70 ± 0.46
0.2	10.8 ± 0.9
0.5	24.1 ± 1.9
1.0	48.0 ± 3.8

[a] Calculated from the observed pseudo first-order rate constant, at 1.02 mM thiol concentration. Relative error from buffer concentration, thiol concentration, pH measurement and standard deviation of kinetic fit estimated at about 8 %.

Table 10S : Second-order Rate Constants[a] at Various Concentrations of N-Methyl-imidazole Buffer for the Reaction of 2-Mercaptomethyl-N-methylimidazole (**7b**) with Distorted Amide **2** (pH 7.3, T = 25 °C, μ = 1.0 (KCl))

[Buffer] (M)	k_2^{obsd} ($M^{-1}s^{-1}$)
0.1	72 ± 7
0.2	76 ± 7
0.5	68 ± 7

[a] Calculated from the observed pseudo first-order rate constant, at 1.03 mM thiol concentration. Relative error from buffer concentration, thiol concentration, pH measurement and standard deviation of kinetic fit estimated at about 10 %.

Table 11S : Second-order Rate Constants[a] at Various Concentrations of N-Methyl-imidazole Buffer for the Reaction of Cysteamine (**10a**) with Distorted Amide **2** (pH 7.8, T = 25 °C, μ = 1.0 (KCl))

[Buffer] (M)	k_2^{obsd} ($M^{-1}s^{-1}$)
0.1	15.7 ± 1.1
0.2	21.4 ± 1.5
0.5	27.9 ± 2.0

[a] Calculated from the observed pseudo first-order rate constant, at 1.01 mM thiol concentration. Relative error from buffer concentration, thiol concentration, pH measurement and standard deviation of kinetic fit estimated at about 7 %.

Derivation of Equation (2):

$$\text{Rate} = \frac{dP}{dt} = k_2 [RS^-] [2]$$

$$Ka^{SH} = \frac{[RS^-] [H^+]}{[RSH]} \; ; \; [RSH] = \frac{[RS^-] [H^+]}{Ka^{SH}}$$

$$[RSH]_{tot} = [RS^-] + [RSH] \; ; \; f_{RS^-} = \frac{[RS^-]}{[RSH]_{tot}} = \frac{[RS^-]}{[RS^-] + [RSH]}$$

$$= \frac{[RS^-]}{\frac{[RS^-] [H^+]}{Ka^{SH}} + [RS^-]} = \frac{Ka^{SH}}{[H^+] + Ka^{SH}}$$

$$\text{Rate} = k_2 (f_{RS^-} [RSH]_{tot}) [2] \; ; \; k_2^{obsd} = \frac{k_2 Ka^{SH}}{[H^+] + Ka^{SH}}$$

Derivation of Equation (3):

$$\text{Rate} = \frac{dP}{dt} = (k_2' [ZW] + k_2'' [ImS^-])\,[pNPA] \quad \text{(Let "ImSH" represent compound 7b.)}$$

$$Ka^{Im} = \frac{[N]\,[H^+]}{[HIm^+SH]} \; ; \; Ka^{SH} = \frac{[ImS^-]\,[H^+]}{[N]} \; ; \; K_{ZW} = \frac{[ZW]}{[N]} \quad \text{(from Scheme 17)}$$

$$[N] = \frac{Ka^{Im}\,[HIm^+SH]}{[H^+]} \; ; \; [ImS^-] = \frac{Ka^{SH}\,[N]}{[H^+]} = \frac{Ka^{SH}\,Ka^{Im}\,[HIm^+SH]}{[H^+]^2}$$

$$[ZW] = K_{ZW}\,[N] = \frac{K_{ZW}\,Ka^{Im}\,[HIm^+SH]}{[H^+]}$$

$$[ImSH]_{tot} = [HIm^+SH] + [N] + [ZW] + [ImS^-]$$

$$f_{ZW} = \frac{[ZW]}{[HIm^+SH] + [N] + [ZW] + [ImS^-]}$$

$$f_{ZW} = \frac{\dfrac{K_{ZW}\,Ka^{Im}\,[HIm^+SH]}{[H^+]}}{[HIm^+SH] + \dfrac{Ka^{Im}\,[HIm^+SH]}{[H^+]} + \dfrac{K_{ZW}\,Ka^{Im}\,[HIm^+SH]}{[H^+]} + \dfrac{Ka^{SH}\,Ka^{Im}\,[HIm^+SH]}{[H^+]^2}}$$

$$= \frac{K_{ZW}\,Ka^{Im}\,[H^+]}{[H^+]^2 + Ka^{Im}\,[H^+] + K_{ZW}\,Ka^{Im}\,[H^+] + Ka^{SH}\,Ka^{Im}}$$

Likewise,

$$f_{ImS^-} = \frac{[ImS^-]}{[HIm^+SH] + [N] + [ZW] + [ImS^-]}$$

$$f_{ImS^-} = \frac{\dfrac{Ka^{SH}\,Ka^{Im}\,[HIm^+SH]}{[H^+]^2}}{[HIm^+SH] + \dfrac{Ka^{Im}\,[HIm^+SH]}{[H^+]} + \dfrac{K_{ZW}\,Ka^{Im}\,[HIm^+SH]}{[H^+]} + \dfrac{Ka^{SH}\,Ka^{Im}\,[HIm^+SH]}{[H^+]^2}}$$

$$= \frac{Ka^{SH}\,Ka^{Im}}{[H^+]^2 + Ka^{Im}\,[H^+] + K_{ZW}\,Ka^{Im}\,[H^+] + Ka^{SH}\,Ka^{Im}}$$

$$\text{Rate} = \frac{dP}{dt} = (k_2'\,f_{ZW} + k_2''\,f_{ImS^-})\,[ImSH]_{tot}[pNPA]\,;$$

$$k_2^{obsd} = \frac{k_2'\,K_{ZW}\,Ka^{Im}\,[H^+] + k_2''\,Ka^{SH}\,Ka^{Im}}{[H^+]^2 + (\,Ka^{Im} + K_{ZW}\,Ka^{Im}\,)\,[H^+] + Ka^{SH}\,Ka^{Im}}$$

Derivation of Equation (4):

$$\text{Rate} = \frac{dP}{dt} = k_2 [ZW] [\mathbf{2}]$$

$[ZW] = f_{ZW} [ImSH]_{tot}$, derived as for equation (3).

$$\text{Rate} = (k_2 f_{ZW}) [ImSH]_{tot} [\mathbf{2}] ;$$

$$k_2^{obsd} = \frac{k_2 K_{ZW} Ka^{Im} [H^+]}{[H^+]^2 + (Ka^{Im} + K_{ZW} Ka^{Im}) [H^+] + Ka^{SH} Ka^{Im}}$$

APPENDIX 2

Supplementary Material to Chapter 2

Table 12S : Observed Pseudo-First Order Rate Constants vs pH for the Disappearance of **13b** (μ = 1.0 (KCl), T = 25 °C)

pH	$k^{obsd} \times 10^4$ (s^{-1})[a]
6.21[b]	1.94 ± 0.07
7.38[b]	2.15 ± 0.03
9.25[c]	6.13 ± 0.47
10.10[c]	7.15 ± 1.05
10.60[d]	8.50 ± 1.13
10.93[c]	8.14 ± 0.41
12.39[e]	8.25 ± 0.83

[a] Reported values are the averages of duplicate or triplicate runs; relative errors reported are the standard deviations of the average values.

[b] Phosphate buffer.

[c] Carbonate buffer.

[d] Carbonate buffer, D_2O.

[e] Sodium hydroxide.

Table 13S : Observed Pseudo-First Order Rate Constants vs pH for the Disappearance of **17** (μ = 1.0 (KCl), T = 25 °C)

pH	$k^{obsd} \times 10^4$ (s^{-1})[a]
6.21[b]	0.63 ± 0.13
7.38[b]	1.34 ± 0.06
9.25[c]	2.61 ± 0.04
10.10[c]	2.69 ± 1.72

[a] Reported values are the averages of at least duplicate runs; relative errors reported are the standard deviations of the average values.

[b] Phosphate buffer.

[c] Carbonate buffer.

Derivation of Equation (5):

Let $TE\text{-}NR_2$ represent a thiolester with a pendant amino group.

$$\text{Rate} = \frac{dP}{dt} = k_0 [TE\text{-}NR_2]_{tot} + k_{cat} [TE\text{-}NR_2]$$

$$Ka^{NH+} = \frac{[TE\text{-}NR_2]\,[H^+]}{[TE\text{-}^+NHR_2]}\ ;\ [TE\text{-}NR_2] = \frac{[TE\text{-}^+NHR_2]\,Ka^{NH+}}{[H^+]}$$

$$[TE\text{-}NR_2]_{tot} = [TE\text{-}NR_2] + [TE\text{-}^+NHR_2]$$

$$f_{TE\text{-}NR2} = \frac{[TE\text{-}NR_2]}{[TE\text{-}NR_2]_{tot}} = \frac{[TE\text{-}NR_2]}{[TE\text{-}NR_2] + [TE\text{-}^+NHR_2]}$$

$$= \frac{\dfrac{[TE\text{-}^+NHR_2]\,Ka^{NH+}}{[H^+]}}{\dfrac{[TE\text{-}^+NHR_2]\,Ka^{NH+}}{[H^+]} + [TE\text{-}^+NHR_2]} = \frac{1}{1 + \dfrac{[H^+]}{Ka^{NH+}}}$$

$$\text{Rate} = k_0 [TE\text{-}NR_2]_{tot} + k_{cat}\, f_{TE\text{-}NR2}\, [TE\text{-}NR_2]_{tot}$$

$$= (k_0 + k_{cat}\, f_{TE\text{-}NR2})\, [TE\text{-}NR_2]_{tot}$$

$$k^{obsd} = k_0 + \frac{k_{cat}}{1 + \dfrac{[H^+]}{Ka^{NH+}}}$$

Table 14S : Observed Pseudo-First Order Rate Constants vs Equivalents of Added Dimethylamioethanethiol (**10b**) for the Disappearance of **13b**[a] (pH 10.10,[b] μ = 1.0 (KCl), T = 25 °C)

Equivalents of **10b**	$k^{obsd} \times 10^4$ (s^{-1})[c]
0	7.6 ± 0.8
5	5.3 ± 0.5
11	5.0 ± 0.5
23	3.8 ± 0.4

[a] **[13b]** = 4.1×10^{-4} M.

[b] Carbonate buffer.

[c] Relative error estimated at 10%.

APPENDIX 3

Supplementary Material to Chapter 3

Table 15S : Observed Pseudo-First Order Rate Constants for the Reaction of **7b** with 100 mM DMF (pD 8.0, T = 98 °C, μ = 1.0 (KCl))

[**7b**] (mM)	$k^{obsd} \times 10^6$ (s^{-1})[a]
0	0.030 ± 0.003
20	0.50 ± 0.05
50	1.13 ± 0.11
100	1.80 ± 0.18
150	2.61 ± 0.26

[a] Relative error in the rate constants is estimated at 10%.

Table 16S : Observed Pseudo-First Order Rate Constants for the Reaction of **7b** with 100 mM Formamide (pD 7.8, T = 98 °C, μ = 1.0 (KCl))

[**7b**] (mM)	$k^{obsd} \times 10^6$ (s^{-1})[a]
0	0.36 ± 0.04
50	6.17 ± 0.36
100	12.2 ± 0.6
150	19.5 ± 1.8

[a] Error shown is standard deviation from non-linear least squares fit of the data.

Table 17S : Observed Pseudo-First Order Rate Constants for the Reaction of **7b** with 200 mM N-Formylmorpholine (pD 8.0, T = 98 °C, μ = 1.0 (KCl))

[**7b**] (mM)	$k^{obsd} \times 10^6$ (s^{-1})[a]
0	0.030 ± 0.001
100	1.13 ± 0.08
150	1.63 ± 0.13

[a] Error shown is standard deviation of linear least squares analysis of [NFM] vs time data. Rate constants were calculated by dividing the initial slopes by the initial concentration of amide (200 mM).

Table 18S : Observed Pseudo-First Order Rate Constants for the Formation of NFM by the Reaction of **7b** with Formic Acid and Morpholine (T = 98 °C, μ = 1.0 (KCl))

[**7b**] (mM)	[HCOOH] (mM)	$k^{obsd} \times 10^7$ (s^{-1})[a]
0	200	0.95 ± 0.04[b]
100	200	1.21 ± 0.06[b]
100	400	2.94 ± 0.24[c]

[a] Pseudo-first order rate constants were calculated by dividing the initial slope of [NFM] vs time by the initial concentration of formic acid (initial rates method). Relative error shown is the standard deviation of the linear least squares fit of the initial rate data.

[b] pD 7.6, 200 mM morpholine.

[c] pD 7.7, 400 mM morpholine. Note that the observed pseudo-first order rate constant approximately doubled on doubling the concentrations of both formic acid and morpholine. (The fact that the observed rate did **not** *quadruple*, and that no build-up of thiolester was observed under any conditions indicates that only formic acid is involved, with the catalyst, in the rate-determining step.)

Derivation of Equation (6):

Let "TE" represent the intermediate thiolester.

If [TE] is in a steady state, then from **Scheme 26**,

$$\frac{d[TE]}{dt} = k_{dehyd}[acid][cat] - k_{hyd}[TE] - k_{form}[TE][amine] = 0$$

$$[TE] = \frac{k_{dehyd}[acid][cat]}{k_{form}[amine] + k_{hyd}}$$

Let the rate of amide production be given by V_f.

$$V_f = k_{form}[TE][amine] = \frac{k_{dehyd}\,k_{form}[acid][cat][amine]}{k_{form}[amine] + k_{hyd}}$$

Derivation of Equation (8):

If [TE] is in a steady state in the reverse direction of **Scheme 26**,

$$\frac{d[TE]}{dt} = k_{cat}[amide][cat] - k_{hyd}[TE] - k_{form}[TE][amine] = 0$$

$$[TE] = \frac{k_{cat}[amide][cat]}{k_{form}[amine] + k_{hyd}}$$

Let the rate of acid production be given by V_r.

$$V_r = k_{hyd}[TE] = \frac{k_{hyd}\,k_{cat}[amide][cat]}{k_{form}[amine] + k_{hyd}}$$

Derivation of Equation (10):

$$Ka^{FA} = \frac{[HCOO^-]\,[H_3O^+]}{[HCOOH]} \qquad [HCOOH] = \frac{[HCOO^-]\,[H_3O^+]}{Ka^{FA}}$$

$$Ka^{NH+} = \frac{[morph]\,[H_3O^+]}{[morph\text{-}H^+]} \qquad [morph] = \frac{Ka^{NH+}\,[morph\text{-}H^+]}{[H_3O^+]}$$

$$[HCOOH] = f_{FA}\,[HCOOH]_{tot} \qquad f_{FA} = \frac{[HCOOH]}{[HCOOH] + [HCOO^-]}$$

$$f_{FA} = \frac{\dfrac{[HCOO^-]\,[H_3O^+]}{Ka^{FA}}}{\dfrac{[HCOO^-]\,[H_3O^+]}{Ka^{FA}} + [HCOO^-]} = \frac{[H_3O^+]}{[H_3O^+] + Ka^{FA}}$$

$$[morph] = f_{morph}\,[morph]_{tot} \qquad f_{morph} = \frac{[morph]}{[morph] + [morph\text{-}H^+]}$$

$$f_{morph} = \frac{\dfrac{Ka^{NH+}\,[morph\text{-}H^+]}{[H_3O^+]}}{\dfrac{Ka^{NH+}\,[morph\text{-}H^+]}{[H_3O^+]} + [morph\text{-}H^+]} = \frac{Ka^{NH+}}{Ka^{NH+} + [H_3O^+]}$$

$$K_{eq} = \frac{[NFM]}{[HCOOH]\,[morph]}$$

$$= \frac{[NFM]}{\left(\dfrac{[H_3O^+]}{[H_3O^+] + Ka^{FA}}\right)[HCOOH]_{tot}\left(\dfrac{Ka^{NH+}}{Ka^{NH+} + [H_3O^+]}\right)[morph]_{tot}}$$

$$= \frac{K'_{eq}}{\text{"F"}} \;;\; K'_{eq} = \text{"F"}\,K_{eq}$$

From reference 86, $K_{eq} = 2.24 \times 10^5\ M^{-1}$, $pKa^{FA} = 3.66$, $pKa^{NH+} = 8.87$.

In D_2O, $pKa^{FA} = 4.06$, $pKa^{NH+} = 9.27$

(see reference 71).

At pD 7.6 (under conditions used herein), "F" $= 6.00 \times 10^{-6}$, and

$$K'_{eq} = \text{"F"}\ K_{eq} = (6.00 \times 10^{-6})\ (2.24 \times 10^5\ M^{-1}) = 1.35\ M^{-1}$$